FROM GATEKEEPER TO EFFECTOR: A STRUCTURAL AND FUNCTIONAL ANALYSIS OF THE MULTIFACETED *CHLAMYDIAL* PROTEIN, COPN.

By

Tara Lakshimi Archuleta

Dissertation

Submitted to the Faculty of the

Graduate School of Vanderbilt University

In partial fulfillment of the requirements

for the degree of

DOCTOR OF PHILOSOPHY

in

Chemical and Physical Biology

August, 2014

Nashville, Tennessee

Approved:

Tina M. Iverson, Ph.D.

Irina I. Kaverina, Ph.D.

Anne K. Kenworthy, Ph.D.

Timothy L. Cover, M.D.

Benjamin W. Spiller, Ph.D.

To my loving parents, my heroes.

ACKNOWLEDGEMENTS

First and foremost, I would like to thank my mentor Dr. Benjamin Spiller. I have had the opportunity to work closely with Ben throughout my time in his laboratory. It would be an understatement to say he always available to answer questions or help trouble-shoot technical problems. Ben has provided me with the support, enthusiasm, time, patience, and advice, which been instrumental in my journey through graduate school and my thesis project. He has always been there when things are going right or wrong to share his input. His enthusiasm and tenacity towards our projects has been pivotal to our successes as his graduate students. It has been a great privilege to work with Dr. Spiller, and I am forever thankful for the training I have received.

A special thank you to my thesis committee members: Drs. Tina Iverson, Anne Kenworthy, Irina Kaverina, Tim Cover, and Ben Spiller. Thank you for allowing me to share my work with you, and offering thoughtful advice to forwarding my project. I appreciate the time and constructive criticism that has allowed me to analyze my work on another level.

I would like to thank the amazing women of the Spiller Lab. This lab has been more than just a place of work for me, but a second home. Thank you for being my family here—I love you guys. Katie Germane was my mentor and guide to graduate school life—I am forever indebted to your kindness and the good times we had together. Thank you Michele LeNoue for being a wonderful friend and cell biology mentor. Thank you for answering all of my random cell culture, biochemical, and scientific questions throughout the years. Thank you to Katie Winarski for being a wonderful friend and mentee. I will always be thankful for the opportunities to show you the ropes—in lab and at the climbing gym. Most importantly, thank you Lisa. When I first started in lab you were the one to take time to teach me how to clone, and other useful lesson around lab. You will always be the great cloning master. And thank you for being my sister—always being there for me to

share the joys and sorrows during these years. Additionally, I have had the pleasure of working with the Lacy Lab. Specifically, Dr. Borden Lacy has given me support, enthusiasm, and critical advice throughout my graduate career.

I would like to thank my wonderful family. Their love, support, and encouragement enabled me to strive towards my dreams, and for that I am greatly indebted. My parents are and will always be my heroes. You have shown me that hard work and perseverance will lead me to my goals. Thank you to my sister, my life-long best friend—the weirdness/silliness we share brings joy to my life. Thank you to Joseph—you are my angel. You have provided me with love, encouragement, and laughter. Thank you for spending countless hours talking with me about science and other nerdy things. I am excited to see where our journey takes us next. I would like to thank my friends—these wonderful people are a part of my family, and have always. Thank you to my wonderful chemistry family from college who showed me that science is about having fun and learning at the same time. Thank you to my family here at Vanderbilt. You have brought joy and comfort to my life as a graduate student, providing me with the support I would be lost without.

I would like to thank the administrative staff, my various funding sources, and facilities that have allowed my research in the Spiller Lab. Thank you to the administrative staff here at Vanderbilt. In particular, thank you Lindsay Meyers for being our friend and guide in the Chemical and Physical Biology Program—we would all be lost without you. A special thank you to Angela Reese for always helping us with the tedious task of grant applications. Thank you to the rest of the Pharmacology and Microbiology Departments for giving me a second home. Lastly, I would like to thank the Center for Structural Biology. The CSB has given graduate students and faculty the opportunity to utilize core facilities, and enables us to discuss and share our work. This project was supported by institutional funds to BWS and Public Health Service grant R01 AI072453 from the National Institutes of

Health. I was supported by the Integrative Training in Therapeutic Discovery Training Grant, DA022873, and an American Heart Association Predoctoral Fellowship, 12PRE11750031. Use of the Advanced Photon Source, an Office of Science User Facility operated for the U.S. Department of Energy (DOE) Office of Science by Argonne National Laboratory, was supported by the U.S. DOE under Contract No. DE-AC02-06CH11357. Use of the LS-CAT Sector 21 was supported by the Michigan Economic Development Corporation and the Michigan Technology Tri-Corridor (Grant 085P1000817). Core services performed through Vanderbilt University Medical Center's Digestive Disease Research Center were supported by NIH grant P30DK058404.

TABLE OF CONTENTS

LIST OF TABLES

LIST OF FIGURES

LIST OF ABREVIATIONS

MDR	Multidrug resistance
CDC	The Centers for Disease Control and Prevention
UTI	Urinary tract infection
CRE	Carbapenem-resistant Enterobacteriaceae
HAI	Healthcare-associated infection
ESBL	Extended-spectrum β-lactamase producing Enterobacteriaceae
T1SS	Type I secretion system
T2SS	Type II secretion system
T3SS	Type III secretion system
T4SS	Type IV secretion system
T5SS	Type V secretion system
T6SS	Type VI secretion system
T7SS	Type VII secretion system
IM	Inner membrane
OM	Outer membrane
Tat	Twin-arginine translocation
MFP	Membrane fusion protein
OMF	Outer membrane protein factor
ABC	ATP-binding cassette
inv	Invasion gene
T4CP	Type IV coupling protein
IMC	Inner membrane complex
OMC	Outer membrane complex
CAP	Community-acquired pneumonia

EB	Elementary body
RB	Reticulate body
MT	Microtubule
MAP	Microtubule associated protein
+TIP	Plus-end binding protein
MTOC	Microtubule organizing center
TBR	Tubulin binding repeat
TPR	Tetratricopeptide repeat
+TIP	Plus-end binding protein
GBR	Gatekeeper-binding region

CHAPTER I

Introduction

Gram negative-bacteria

Bacteria can be divided into Gram-negative and Gram-positive groups based on their ability to be stained by crystal violet or a counterstain, like safranin (1). Subsequent to this functional classification, it has been shown that bacteria that stain with crystal violet contain a single membrane and a thick peptidoglycan layer. Conversely, Gram-negative bacteria have a characteristic double membrane composed of an inner membrane, a thin peptidoglycan layer within the intervening (periplasmic) space, and an outer membrane.

Bacterial infection remains a major cause of death worldwide (2) with Gram-negative bacteria predicted to become the major cause of death from bacterial infection in the near future (3). Gram-negative bacteria are significant public health threats, responsible for pneumonia, blood stream infections, wound or surgical site infections, and meningitis (4). Additionally, antibiotic resistance among Gram-negative bacteria is a significant and growing concern (4-6). The additional membrane renders Gram-negative bacteria inherently less sensitive to antibiotics than Gram-positives (4), and the prevalence of acquired resistance multiple drugs (multidrug resistance, MDR) is increasing, especially to frequently used antibiotics (4-6). The Centers for Disease Control and Prevention (CDC) indicate that there are more than two million people infected every year, and at least 23,000 deaths result from antibiotic resistant infections per year in the United States (5). Recent data implicate gram-negative bacteria in over 30% of nosocomial infections, including 47% of pneumonia cases, and 45% of urinary tract infections (UTIs) alone (7). In U.S. intensive care units, gram-negative bacteria account for nearly 70% pneumonia and UTIs (8). Domestic healthcare costs associated with and resulting from antibiotic resistance are estimated to be at least $20 billion per year (9,10).

Major Gram-Negative pathogens and antibiotic resistance threats

Aside from the double membrane, gram-negative bacteria have acquired specialized features that allow for increased antibiotic resistance. These traits include acquisition of novel proteins (via horizontal gene transfer) and adaptations in the regulation of existing proteins (4). Examples include: the reduced expression of porins, which reduce drug influx; acquisition or enhanced expression of efflux pumps; acquisition of β-lactamases and other antibiotic detoxifying enzymes; alteration of bacterial ribosomes such that ribosome-targeted antibiotics are ineffective; point mutations in antibiotic targets that reduce antibiotic binding; acquisition of alternative metabolic enzymes bypassing metabolism-targeted antibiotics; and mutations in the lipopolysaccharide. Examples of these resistance strategies are shown in Figure 1-1 (4,6).

The 2013 CDC report on antibiotic resistance lists carbapenem-resistant Enterobacteriaceae (encompassing *Salmonella*, *Escherichia*, *Yersinia*, *Klebsiella*, *Shigella*, *etc.*) and drug-resistant *Neisseria gonorrhoeae* as urgent threats to human health (5). These bacteria are poised to rapidly become global threats unless action is taken in the sphere of public health to alter their prevalence. The CDC's recent analysis also highlights the following gram-negative bacteria as the most serious threats: multidrug-resistant *Acinetobacter*, drug-resistant *Campylobacter*, extended spectrum β-lactamase producing Enterobacteriaceae (which includes *Salmonella*, *Escherichia coli*, *Yersinia pestis*, *Klebsiella*, *Shigella*, *Proteus*, *Enterobacter*, *Serratia*, and *Citrobacter*), multidrug-resistant *Pseudomonas aeruginosa*, drug-resistant non-typhoidal *Salmonella*, drug resistant *Salmonella* typhi, and drug resistant *Shigella spp.* (5). Table 1-1 summarizes the number of infections and deaths caused by these gram-negative bacteria. From these data, it is clear that the most serious gram-negative infections are health-care associated from Enterobacteriaceae, *Pseudomonas aeruginosa*, and *Acinetobacter*.

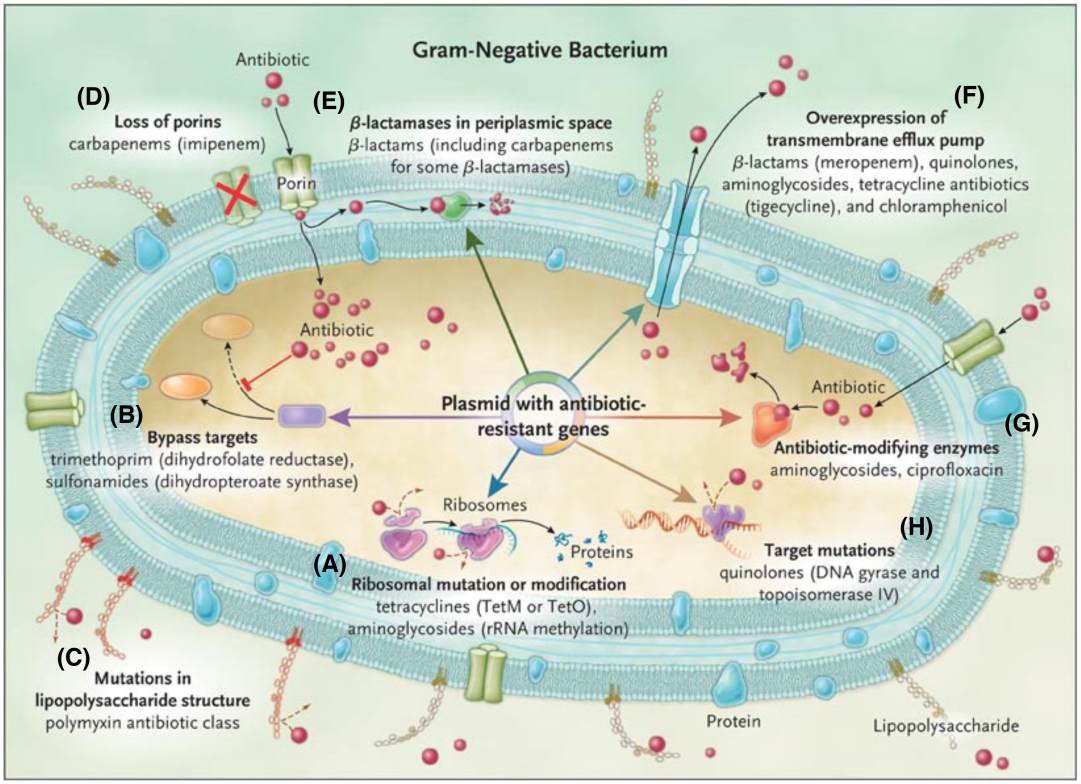

Figure 1-1: Mechanisms of antibiotic resistance in gram-negative bacteria. (A) Ribosomal mutations/modification; **(B)** Bypass targets; **(C)** mutations in lipopolysaccharide structure; **(D)** loss of porins; **(E)** β-lactamases in periplasm; **(F)** Over-expression of transmembrane efflux pumps; **(G)** Antibiotic-modifying enzymes; **(H)** and targeted mutations. Adapted from Peleg *et al.* 2010 (4).

Table 1-1: Estimated morbidity and mortality from antibiotic-resistance. Adapted from Center for Disease Control and Prevention's 'Antibiotic Resistance Threats in the United States, 2013.' (5)

Antibiotic Resistant Gram-negative Bacteria	Infections Included in Case/Death Estimates	Infections Not Included	Antibiotic Resistance	Estimated Annual Number of Cases	Estimated Annual Number of Deaths
Carbapenem-resistant Enterobacteriaceae (CRE)	Healthcare-associated infections (HAIs) caused by *Klebsiella* and *E. coli* with onset in hospitalized patients	Infections occurring outside of acute care hospitals (e.g., nursing homes) Infections acquired in acute care hospitals but not diagnosed until after discharge Infections caused by Enterobacteriaceae other than *Klebsiella* and *E. coli* (e.g., *Enterobacter spp.)*	Some of these bacteria are resistant to: - Nearly all antibiotics, including carbapenems	9,300	610
Drug-resistant *Neisseria gonorrhoeae* (any drug)	All infections	Not applicable	Strains show resistance to: - Cefixime (oral cephalosporin - Ceftriaxone (injectable cephalosporin) - Azithromycin - Tetracycline	246,000	< 5
Multidrug-resistant *Acinetobacter* (three or more drug classes)	HAIs with onset in hospitalized patients	Infections occurring outside of acute care hospitals (e.g., nursing homes) Infections acquired in acute care hospitals but not diagnosed until after discharge	Some strains are resistant to: - All antibiotics including carbapenems	7,300	500
Drug-resistant *Campylobacter* (azithromycin or ciprofloxacin)	All infections	Not applicable	Strains show resistance to: - Ciprofloxacin - Azithromycin	310,000	220
Extended-spectrum β-lactamase producing Enterobacteriaceae (ESBLs)	HAIs caused by *Klebsiella* and *E. coli* with onset in hospitalized patients	Infections occurring outside of acute care hospitals (e.g., nursing homes) Infections acquired	Some strains are resistant to nearly all: - Penicillins - Cephalosporins	26,000	1,700

		in acute care hospitals but not diagnosed until after discharge Infections caused by Enterobacteriaceae other than *Klebsiella* and *E. coli* (e.g., *Enterobacter spp.)*			
Multidrug-resistant *Pseudomonas aeruginosa* (three or more drug classes)	HAIs with onset in hospitalized patients	Infections occurring outside of acute care hospitals (e.g., nursing homes) Infections acquired in acute care hospitals but not diagnosed until after discharge	Some strains have been found to be resistant to: - Most antibiotics - Aminoglycosides - Cephalosporins - Fluoroquinolones - Carbapenems	6,700	440
Drug-resistant non-typhoidal *Salmonella* (ceftriaxone, ciprofloxacin, or 5 or more drug classes)	All infections	Not applicable	Strains are showing resistance to: - Ceftriaxone - Ciprofloxacin - Multiple classes of drugs	100,000	40
Drug-resistant *Salmonella* Typhi (ciprofloxacin)	All infections	Not applicable	Showing resistance to: - Ceftriaxone - Azithromycin - Ciprofloxacin (resistance is so common that this drug is not routinely used)	3,800	< 5
Drug-resistant *Shigella* (azithromycin ciprofloxacin)	All infections	Not applicable	Strains are resistant to: - Ampicillin (high resistance levels) - Trimethoprim-sulfamethoxazole (high resistance levels) - Ciprofloxacin - Azithromycin		

Secretion systems of Gram-negative bacteria

Bacterial infection requires the establishment of hospitable niches for replication and dissemination. Many bacteria secrete protein effectors to aid in infection. Protein secretion is essential for both prokaryotes and eukaryotes, as a key mechanism through which they interact with and adapt to their environments. In particular, bacteria utilize secretion systems to make their environment more hospitable. Secreted proteases are used to obtain nutrients, and toxins expand the pathogen's niche by targeting competing bacteria or a eukaryotic host. Infection by Gram-negative bacteria involves secretion of effector proteins from bacteria into host cells. These effectors aid infection by blunting host defenses and co-opting host process (11-13). In order to direct secreted effector proteins across the inner and outer membranes, gram-negative bacteria utilize specialized secretion systems. There are now, at least, seven known secretion systems that gram negative bacteria utilize, named sequentially from the type I secretion system (T1SS) to the type VII secretion system (T7SS) (14-18). Effectors traverse the inner membrane (IM) and outer membrane (OM) either by a one-step transport process (T1SS, T3SS, T4SS, T6SS, and T7SS) that leads the unfolded substrate into the extracellular space without assistance from periplasmic intermediates, or by a two-step process (T2SS, T4SS, T5SS) where substrates are transported to the periplasm, where they fold, and are subsequently transported across the OM (19-21). The T2SS, T4SS, and T5SS are dependent on the Sec and Tat pathways—the major pathways used to secrete proteins across the inner membrane and into the periplasm (19-22).

The Sec Secretion Pathway

The Sec pathway was originally identified by genetic studies in conditional lethal mutants exhibiting secretion defects (23). The Sec system consists of protein-targeting components, a motor protein, and a membrane integrated protein conducting channel (24).

The bacterial Sec translocase is composed of a membrane-embedded, protein-conducting channel that consists of three integral membrane proteins, SecY, SecE, and Sec G, and a peripheral associated ATPase, SecA, that functions as a molecular motor to drive the translocation of secretory proteins across the IM (24-26). In many Gram-negative bacteria, secretory proteins are guided to the Sec-translocase by the secretion specific chaperone, SecB, that maintains these proteins in a translocation-competent, unfolded state (27). Once at the membrane they are translocated by the heterotrimeric protein complex, Sec YEG, which is embedded in the IM of gram-negative bacteria (28).

The Twin-Arginine Translocation (Tat) Pathway

The second general secretion system that translocates proteins across the inner membrane is the Twin-Arginine Translocation (Tat) pathway (29,30). The Tat translocases consist of two or three membrane-integrated subunits, (TatA and TatC, or TatA, TatB and TatC), which together from a receptor and protein conducting machinery for substrates. The Tat system recognizes a conserved amino acid sequence (polar-Arg-Arg-hydrophobic-hydrophobic) on substrates, and directs proteins displaying this sequence for secretion (29). A key functional difference between the Sec and Tat systems is that many of the Tat substrates assemble with cofactors prior to translocation, and are thought to be fully folded when secreted (30-32). Perhaps for this reason, the Tat system is necessary for multiple redox pathways (32-35). Another important difference between the Tat and Sec pathways is that unlike the Sec system, which has a specialized ATPase and uses ATP as an energy source, the Tat system uses the proton motive force as an energy source.

Type I secretion system

The T1SS is a Sec/TAT-independent system that consists of a three proteins, which assemble into a tunnel-like structure (Figure 1-2) that delivers substrates directly

from the cytosol to the extracellular space (36,37). Essential T1SS components include an ABC transporter, a membrane fusion protein (MFP), and an outer membrane protein factor (OMF) (38). T1SS substrates contain a secretion sequence located on either the N- or C-terminus that is recognized by the T1SS (38). The ABC transporter uses energy released from ATP hydrolysis to translocate substrates across the IM (39). The inner membrane anchored MFP forms a conduit between the ABC transporter and the OMF by spanning the periplasm and connects ABC transporter to the OMF pore (40). The OMF protein forms the pore on the OM through which, substrates traverse into the extracellular space (38).

The ABC transporter consists of two transmembrane domains and two nucleotide-binding domains, which can be independent polypeptides, (41,42). The transmembrane helices form the conduit that substrates use to traverse the IM (43), while the nucleotide binding domains supply the energy required for substrate translocation via ATP hydrolysis (44). The nucleotide binding domains face each other in a head-to-tail orientation that sandwiches the nucleotide for an efficient transport of the substrate across the ABC transporter (39,45,46). Within T1SS systems, nucleotide-binding domains exhibit high sequence conservation, indicating an essential function (38). Conversely, the transmembrane domains are highly variable because these domains are responsible for disparate and species-specific substrates binding and transport (38).

Many T1SS ABC transporters deviate from the previously mentioned classical arrangement and have additional domains located on the cytosolic N-terminus of the transporter (38). These T1SS ABC transporter variations are divided into three distinct groups. The first group encompasses C39-containing transporters responsible for the secretion of small (<10 kDa) Class II microcins, which exhibit Ca^{2+}-dependent C39 peptidase-like activity, (common to the papain superfamily) (47-50). These C39-containing transporters recognize double glycine motifs present in Class II microcins, and cleave the N-terminal secretion signal I (49,50). The second group of transporters is the CLD-

containing ABC transporters. These transporters structurally resemble C39-containing transporters but lack protease activity (51,52). The CLD-containing transporters are responsible for the secretion of hemolysin (36,52). The third class of ABC transporters also contains the ABC/C39-like domains described above; however, their substrates are more diverse hydrolytic proteins, including proteases and lipases.

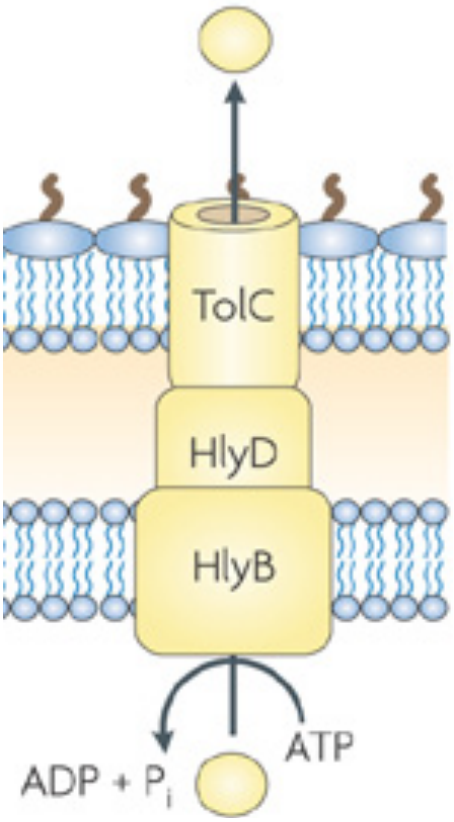

Figure 1-2: A model of type I secretion system. Type I secretion systems are simple, three-part systems facilitating the passage of proteins of various sizes across the cell envelope of Gram-negative bacteria. They consist of an ATP-binding cassette (ABC) transporter or a proton-antiporter, an adaptor protein that bridges the inner membrane (IM) and outer membrane (OM), and an outer membrane pore. They secrete substrates in a single step without a stable periplasmic intermediate. Adapted from Fronzes *et. al.* 2009 (18).

Type II secretion system

The type II secretion pathway uses a two-step process to secrete folded or oligomeric proteins into the extracellular space, where the substrates may be covalently bonded to the bacterial cell. These secreted proteins are often either involved in nutrient acquisition, such as hydrolytic enzymes that degrade biopolymers, or are toxins, that invade potential hosts (53-57). T2SS substrates that become chemically linked to the cell wall are often adhesins, cytochromes, motility proteins, or involved in biofilm formation (53-57). In *Chlamydia*, the T2SS is used to secrete proteins involved in host glycogen degradation (58). These substrates contain N-terminal signal sequences that target them to the Sec or Tat protein export systems. Substrates exported by the Sec system are unfolded until they reach the periplasm where chaperones and the periplasmic environment facilitate proper folding before exiting the OM (59-63). It is clear from genomic studies that hundreds of bacterial species contain T2SS proteins in their genomes (64-68).

The T2SS in Gram-negative bacteria contain between 12 and 16 genes designated for the general secretory pathway, which are denoted as *gsp* (68). The current model for T2S is summarized in Figure 1-3. In the cytosol, the ATPase GspE couples to the full apparatus through interactions with bitopic protein, GspL (69-72). The first sub-complex is the inner membrane platform, composed of five inner membrane proteins (GspC, GspF, GspL, and GspM) that form a pilus-like structure that might act as a piston, pushing the substrate through a protein complex termed the secretin (71). The T2SS relies on the Sec or Tat systems to deliver substrates to the periplasm, where the T2SS then exports the substrate into the extracellular space (73). The secretin, is a cylindrical GspD oligomer that forms a channel for substrates to exit into extracellular environment (74-78). In the periplasm, proteins called pseudopilins are thought to form a piston-like structure (75-82). The current model for secreton operation involves a piston like structure and ATP hydrolysis (83,84), pumping the substrates into the extracellular space (85-87).

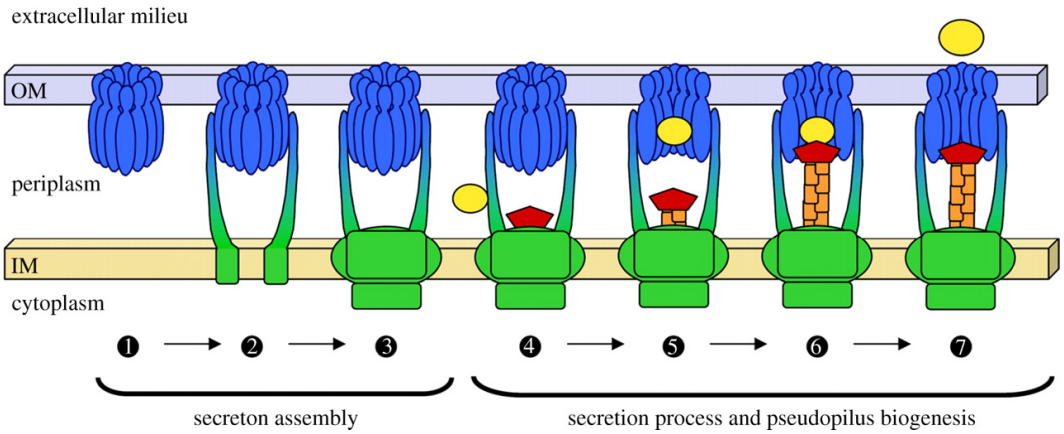

Figure 1-3: Model of secreton assembly and operation of the type II secretion system. 1) First, secretin assembles at the OM. **2)** The next step is successive recruitment of the trans-periplasmic protein $GspC_P$ **3)** tethering to the inner membrane surface. **4)** Substrate recognition by the T2SS takes place in the periplasm, which may involve a peripheral element of the secreton, $GspC_P$. 5) The substrate transferred to the secretin **6)** where it contacts the pseudopilus tip complex that is emerging from the inner membrane surface. **7)** The exoprotein is then released in the extracellular medium through the secretin pore. The secretin and $GspC_P$ are shown in blue, the components of the inner membrane are shown in green, the pseudopilus and the secreted proteins are shown in orange/red and yellow, respectively. Adapted from Douzi *et al.* 2012 (19).

Type III secretion system

Research in the late 1980's and early 1990's yielded evidence for a third secretory system in gram-negative bacteria. This secretory system, termed the Type III secretion system, is often contained in the invasion (*inv)* gene locus in T3SS-containing bacteria. The T3SS is a large syringe-like apparatus (88-92). This system is sequentially constructed from inside the cell, where secreted proteins first extend through the inner membrane, then the periplasm, spanning the bacterial outer membrane, and finally forming a pore in the host plasma membrane (93). The base of this complex contains an ATPase that generates energy for the secretion system (94-99). The substrates targeted for secretion into host cells are presented to the T3SS apparatus by specific T3S chaperones (100-105). These chaperones bind N-terminal signal sequences, which mark bacterial effector proteins for secretion. Once at the T3SS apparatus, the N-terminus of the effector is fed through the syringe and the apparatus unfolds effectors and passes them directly through the T3SS needle and into target cells (106,107).

The T3SS apparatus, shown in Figure 1-4, is built of six main assemblies: the export scaffold, the basal body, the needle, the needle tip, the translocon (which is formed by a subset of secreted proteins termed translocators), and accessory proteins. The export scaffold consists of an ATPase, a central stalk, a peripheral stalk, a C-ring, a gate, gatekeeper, autoprotease, and three inner membrane components (93). The basal body consists of two inner membrane rings, an outer membrane ring, pilotin, and an inner rod (108-114). The needle consists of a multimeric filament, made up of a single, species-specific protein (115-117). The translocation tip is comprised of a major and minor subunit (118-120). Accessory proteins include effectors and needle length regulators (121,122).

There are two models for export scaffold and basal body assembly of the T3SS: the *Salmonella* "inside-out" (123) and *Yersinia* "outside-in" (124,125) models. In the "inside-out" *Salmonella* model, the export scaffold initiates assembly at the IM, the general

order of assembly is as follows: first, the basal body rings and export scaffold must assemble; second, the formation of the inner rod and needle filament; third, the needle tip and the translocator major/minor units oligomerize; and finally, the secretion of bacterial effectors into the host cell occurs (123). Once the export apparatus is assembled at the IM, the basal body assembles adjacent to the export apparatus inside the cell. In the *Yersinia* "outside-in" model, the first basal body IM ring and export apparatus assemble in parallel. Next, the second basal body IM ring forms, followed by the final ATPase domain and C-ring assembly components. After the assembly of the export apparatus and basal body, the inner rod and hollow needle filament form sequentially.

Fully assembled T3SSs are capable of secretion, but do not begin secretion until an external signal triggers secretion of a protein termed the "gatekeeper" (126-131). Before secretion these gatekeepers are localized to the bacterial membrane via interactions with other components of the T3SS (109,129,130,132). These gatekeepers have conserved 4-helix bundle domains with the third C-terminal domain (133). The inner rod, needle, and secreted proteins all employ ATP hydrolysis to pump substrates from the bacteria to the host (134).

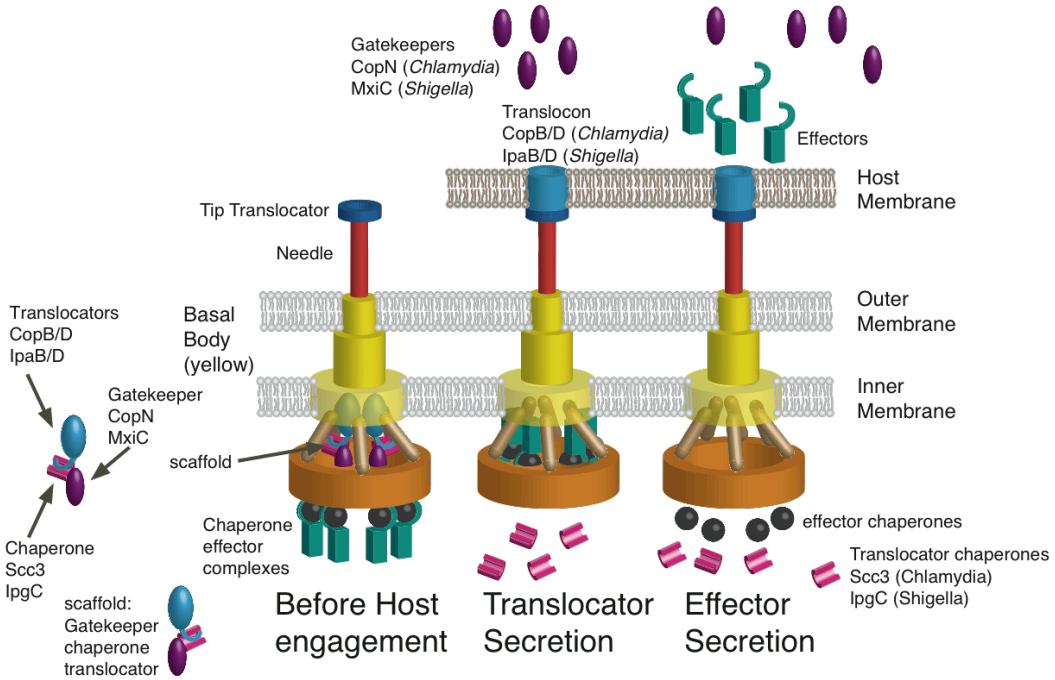

Figure 1-4: A model for type III secretion system. Before host engagement gatekeeper-chaperone-translocator complexes are bound to the apparatus and prevent secretion of effectors. Upon binding of the apparatus to target membranes the, gatekeeper and pore forming translocators are secreted. The pore forming translocators assemble within the target membrane to form the translocon. After translocator and gatekeeper secretion, the apparatus is able to efficiently secrete effectors, which are secreted through the translocon directly into the host cytosol. Adapted from Archuleta *et al.* 2014 (in revision).

Type IV secretion system

The T4SS is present in most Gram-negative bacteria, and can be divided into two subgroups: the conjugation system and the effector translocation system, which translocate DNA and protein respectively into other cells (135). The conjugation systems are responsible for DNA transfer between bacteria, which allows for genetic diversity in, and transfer of bacterial antibiotic resistance and bacterial virulence determinants (136,137). The effector secretion system subgroup utilizes the T4SS machinery to deliver protein substrates into eukaryotic hosts through a one or two-step process. In the one-step process, the type IV coupling protein (T4CP), a hexameric ATPase, drives protein secretion (20). Whereas the two-step process, substrates are delivered to the periplasm by SecYeG machinery, where substrates engage with the T4S machine for translocation across the outer membrane (18,20). *Helicobacter pylori, Legionella pneumophila, Brucella spp., Bartonella spp*., and *Rickettsial spp*. all utilize the T4SS for infecting their eukaryotic hosts (136,138-142).

The T4SS is composed of four functionally distinct subassemblies. The first (T4CP), provides the energy to drive the substrate out of the cell (143). Next, the inner membrane complex (IMC), transfers substrates across the inner membrane (144). Then an envelope-spanning outer membrane complex (OMC) receives the substrate from the IMC and transfers them across the periplasm and outer membrane (20). Finally, a pilus initiates contact with a host cell, and the substrate is pushed into the host cell (145).

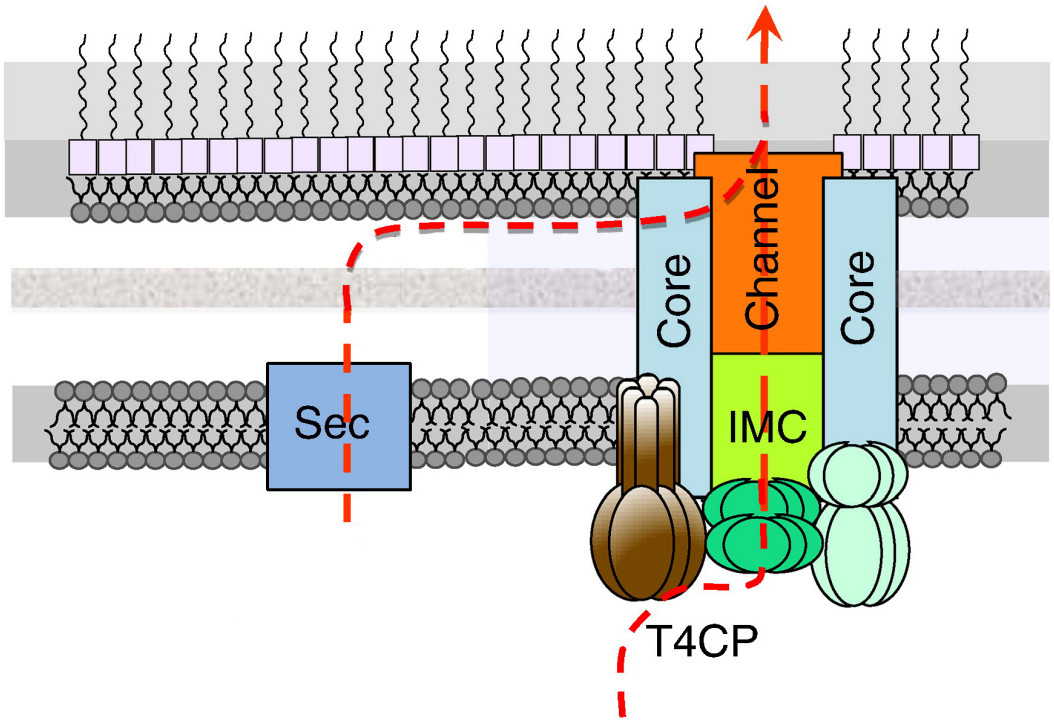

Figure 1-5: The one and two-step type IV secretion system. In the T4CP-independent pathway, The Sec system transfers the substrate from the cytoplasm to the periplasmic region of the T4CP. Once the substrate is transferred to the core/OM channel where it is translocated across the outer membrane. In the T4CP-dependant pathway, the substrates dock with the T4CP in the cytosol. Then the T4CP translocates the substrate across the inner membrane into the channel region, in the periplasm. Finally, the substrate is translocated across the OM channel. Adapted from Christie *et al.* 2014 (20).

Type V secretion system

The TVSSs includes five subgroups of auto transporters: type Va, type Vb, type Vc, type Vd, and type Ve.

Type Va subgroup is the considered the classical, monomeric auto-transporter system. These autotransporter polypeptides contain all functions needed for translocation across both membranes (146,147). Va autotransporters are synthesized by ribosomes attached to the *Sec* system (148). As the auto-transporter is threaded through the Sec machinery, its N-terminus remains attached to the Sec-system. In *E. coli*, chaperones keep the autotransporter unfolded in the periplasm (149-152). This monomeric autotransporter is then be inserted into the outer membrane (OM). Recently, it has been shown that β-barrel insertion into the OM requires a set of accessory proteins that form a β-barrel assembly complex (153). An example of one of these assembly complex chaperones is the *N. meningitides* protein BamA. The BamA complex catalyzes a fast and efficient insertion of the autotransporter β-barrel into the OM.

The T5SS type Vb is a two-partner system (TPS). In this system, the passenger and translocator functions of the autotransporter are located in two separate polypeptide chains: the passenger polypeptide (TpsA), and the β-barrel transport protein (TpsB). Typically, each TpsB transporter is dedicated to transporting a single TpsA substrate protein (154). However, there has been one case where a single TpsB transporter transports two different passengers, FhaC in *Bordetella bronchiseptica* (155). It is presumed that this class also contains periplasmic type Va-like chaperones (15).

The type Vc system is a trimeric autotransporter, where three discrete monomers translocate through a single pore, and typically form OM-linked trimeric adhesions (156). These proteins contain no enzymatic activity and remain tethered to the cell surface. These trimeric autotransporter adhesins (TAAs) have a modular and repetitive architecture. The modular arrangement of the TAAs allows pathogens to frequently and easily

recombine their adhesins, facilitating adaptation to host environments (157). As with type Va and Vb, type Vc similarly requires periplasmic chaperones to help fold and quickly insert into the membrane (15).

Type Vd systems are autotransporters with patatin-like lipase activity. The best-described example of this class is PlpD, from *Pseudomonas aeruginosa*. The passenger protein's N-terminus contains four conserved domains necessary for its lipase activity. These particular autotransporters contain 16-stranded β-barrels, similar to the type Vb system (158).

The type Ve sub family system is similar to the type Va, the classical autotransporters, but is inverted. In this case, the N-terminus of the protein encodes the β-barrel domain, and the C-terminus encodes the protein substrate component (159).

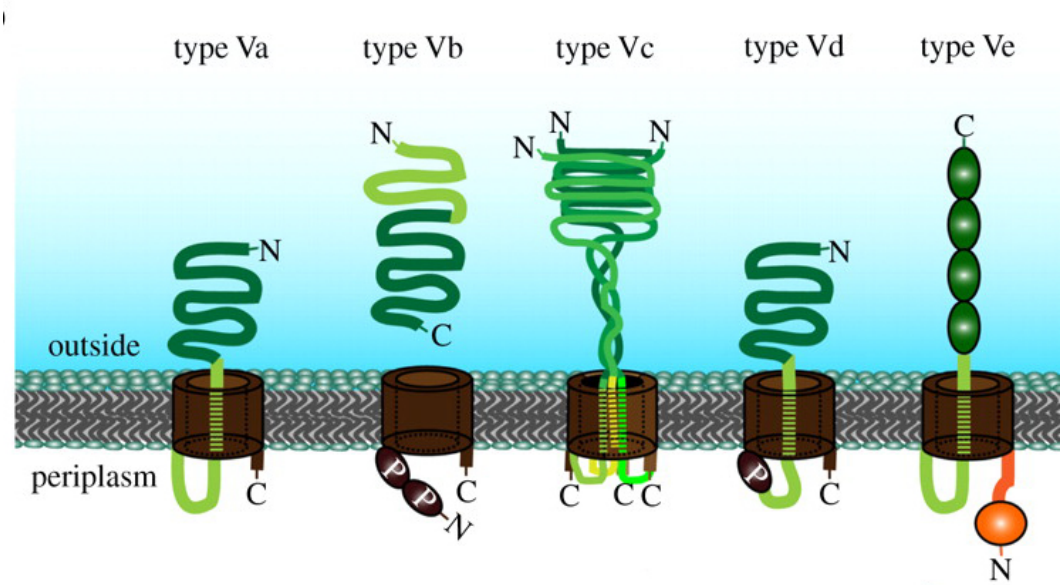

Figure 1-6: Topology models of the five, type V secretion systems. T5SS's Va-Ve are displayed above with the translocation domain displayed in brown, linker/Tps regions in light green, passenger domains in dark green, and periplasmic domains in orange. Adapted from Leo *et al.* 2012 (15).

Type VI secretion system

Type VI secretion system (T6SS) is a membrane-puncturing syringe assembly that injects effector proteins directly into the host (160-163). The T6SS is structurally similar to the bacteriophage tail and baseplate (164-166). T6SS can be separated into four categories based on their observed functions: bacterial cell targeting, eukaryotic cell targeting, bacterial and eukaryotic cell targeting, and conjugation/gene-regulation/cellular adhesion (167-170). The T6SS is a syringe-like assembly composed of at least 13 different core subunits (171,172) that form a base plate, a contractile sheath, a non-contractile tube within the contractile sheath, and a tail spike complex (173,174). This system cycles from needle polymerization, to contraction, and disassembly. The best characterized example of this rapid turnover can be seen in *V. cholera* (174). There are also gene clusters that encode accessory proteins required for proper assembly and function of the apparatus, however, their exact functions are not fully understood (16,175).

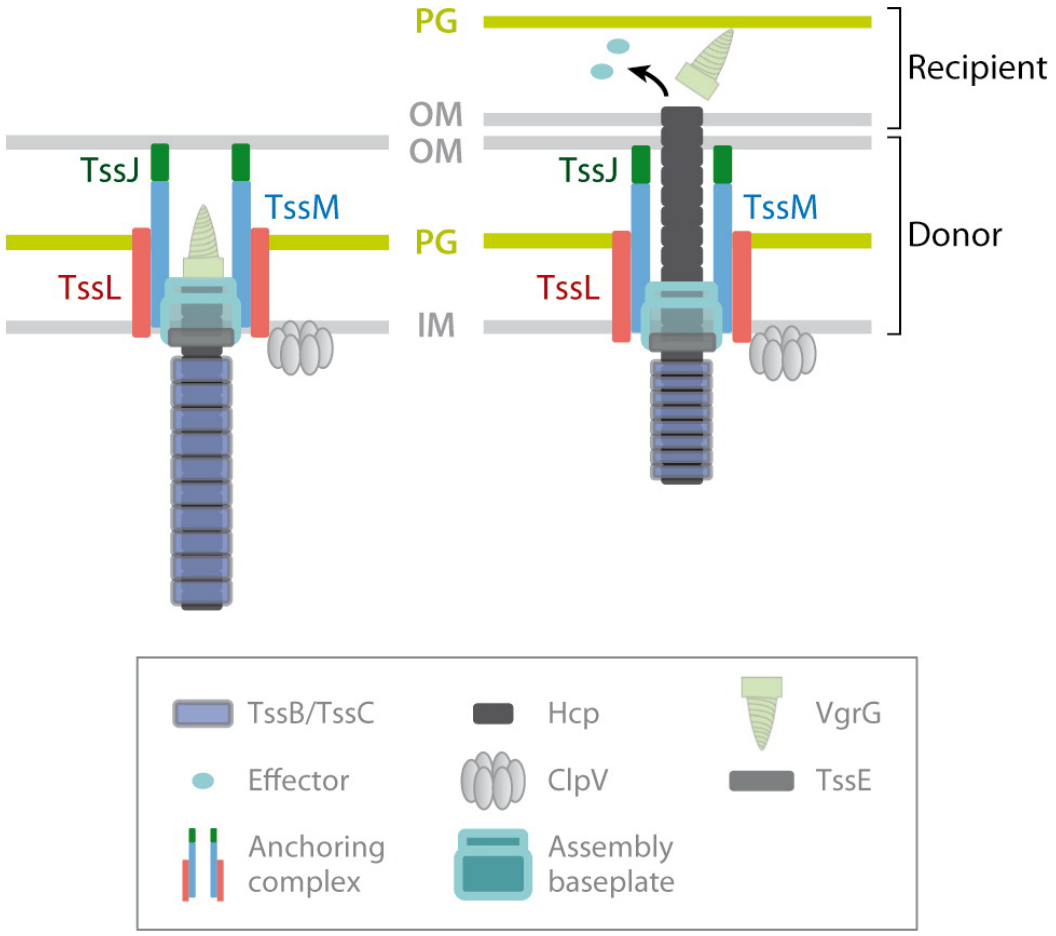

Figure 1-7: Models of inactivated to the activated state of the type VI secretion system. The three membrane-associated proteins TssL, TssM, and TssJ form a complex channel bound to the peptidoglycan layer via TssL. The pilus filament, Hcp, and the VgrG trimer are anchored to the system via interactions to the membrane bound proteins. Activation of the T6SS results in effector delivery to a target cell through the Hcp tube. Adapted from Silverman *et al.* 2011 (16).

Type VII secretion system

The final known secretion system is the T7SS utilized by pathogenic mycobacteria. In mycobacteria, T7SSs are also known as the ESX system. In the T7SS there can be up to five different loci found in a single species of *Mycobacterium*, however, most species only contain one to two loci (176,177). The substrates for mycobacteria T7SSs contain no signal sequence for Sec or Tat secretory systems. However, all T7SS subunits have predicted α-helical transmembrane domains, suggesting that these proteins are inserted into the inner membrane. There is also evidence that one of these membrane proteins, EccE, spans both membranes (178). Additional components seem necessary to complete the secretion across the outer membrane. Current data fail to clarify what type of structure is involved in performing this role in the mycomembrane/OM. The only well-studied mycomembrane protein is MspA from *Mycobacterium smegmatis*, which forms pores in this non-pathogenic mycobacterium. The crystal structure of MspA reveals an atypical octomeric β-barrel (179). So far, there is no evidence for mycobacteria utilizing β-barrel structures, because the channel can be formed by a ring of amphipathic α-helices, similar to the initial steps of T4SS assembly (180).

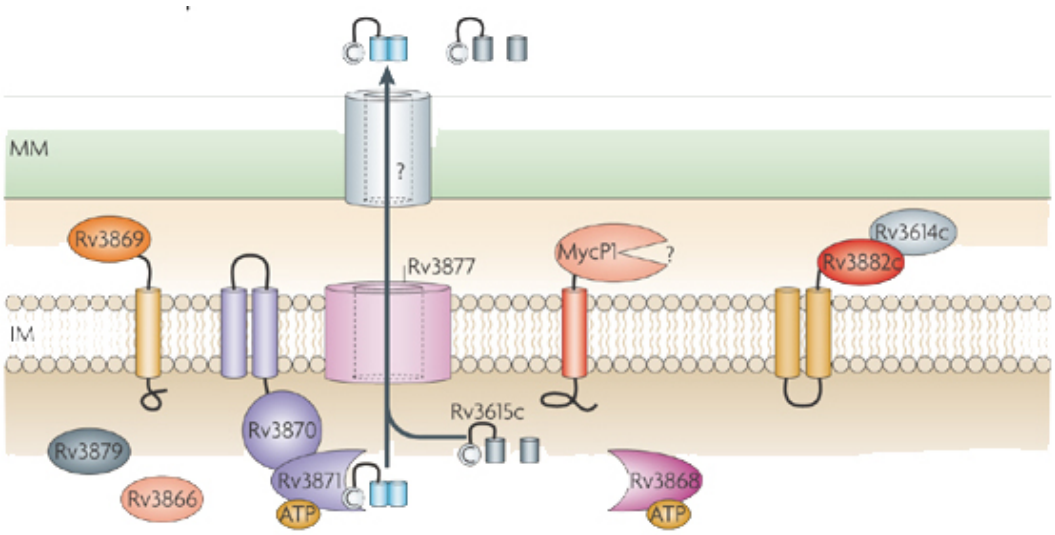

Figure 1-8: Model of the type VII secretion system. In this model, the substrate is transported from the inner membrane to the extracellular space, denoted in light blue and light grey. First, the substrate dimer is targeted for secretion through the recognition of the carboxy-terminal signal sequence by the cytoplasmic protein Rv3871. Rv3871 interacts with Rv3870 at the cell membrane to form an active ATPase. The Rv3781–Rv3780 complex could form a hexameric ring structure with a central cavity that propels ESX-1 substrates through the secretion channel. Adapted from Abdallah *et al.* 2007 (17).

Gatekeeper proteins

As noted above, the T3SS requires a group of proteins called gatekeepers to regulate T3SS activity (126-131). Gatekeeper-null strains display severely dysregulated secretion assembly, effector secretion, and overall reduced virulence (131,181). Gatekeepers can be subdivided into the YopN-TyeA family and the MxiC family(133). The difference between the two sub-families is whether the gatekeeper is two proteins (i.e., YopN-TyeA) or one protein (MxiC) (133). Both of these sub-families of proteins are known to control the secretion of effector proteins from the T3SS (127,128,131,133,181,182).

The mechanism by which gatekeepers regulate secretion is unclear, but a common deletion phenotype is constitutive effector secretion and poor translocator secretion (131). Gatekeeper mutants that lack an amino-terminal secretion signal are not secreted, which also prevents translocator secretion (131). From mutational studies, it has become evident that functional gatekeepers are needed for effective translocator secretion and subsequent formation of the translocon in the host cell. This translocation pore is essential for effector secretion into the host cell and thus T3SS function(183).

Gatekeepers are essential, and if absent or altered, the T3SS cannot properly release its effectors. In addition to this important role, gatekeepers can also acquire effector functions, as has been seen in two cases. The *Pseudomonas syringae* HrpJ protein acts as a virulence factor inside plant cells and suppresses PAMP-triggered immunity (184), and in *Chlamydia pneumoniae,* CopN, which is the focus of this thesis, causes mitotic arrest by sequestering αβ tubulin and preventing microtubule assembly in eukaryotic host cells (185,186).

Chlamydia background

Chlamydiae are gram-negative, obligate eukaryotic parasitic bacteria that have been implicated in the etiology of a wide range of human diseases. Three notable *Chlamydia* species are pathogenic to humans: *C. trachomatis*, *C. psittaci*, and *C. pneumoniae* (187-189). *C. trachomatis* infections result in pelvic inflammatory disease, infertility, and are major causes of preventable blindness in infants (187-190). *C. psittaci* causes acute respiratory disease (psittacosis). *C. pneumoniae* causes community-acquired pneumonia (CAP), bronchitis, asthma, contributes to atherosclerosis, and perhaps central nervous system disorders as well (187-189). All *Chlamydia* use a similar mode of infection, shown in Figure 1-9, including phases of phagocytosis to endosomes, entry, spread, and proliferation (187). *Chlamydiae* have a biphasic life cycle consisting of metabolically inactive elementary bodies (EBs) and metabolically active reticulate bodies (RBs) (191). Infection involves attachment and cellular uptake of EBs and subsequent differentiation into RBs. The RBs remain in endosome-derived membrane vacuoles termed 'inclusions' which migrate to the microtubule, MT, organizing center (MTOC) in a dynein and MT-dependent process (192-194). After several replications, RBs re-differentiate into infectious EBs and spread to neighboring cells (191). The molecular mechanisms that *Chlamydiae* utilize to invade the host cell are not well understood. However, it is known that *Chlamydiae,* use a type III secretion system (T3SS) to translocate effector proteins into the host cell to modulate host cell function (188,195-199). *Chlamydiae* deliver effector proteins across inclusion membranes to direct host cell processes (200). After entry, *Chlamydiae* secrete inclusion membrane proteins (Inc) family effectors termed modify the inclusion. These modifications prevent degradation or trafficking of the inclusion to the Golgi complex (201-203). Once modified by Inc proteins, the inclusion is trafficked to the MTOC, where it associates with the host centrosome and alters the MT network (204,205).

Although the importance of a T3SS is established, the mechanisms by which effectors subvert host defenses and enable colonization are not fully understood. The focus of this proposal is the protein CopN from *C. pneumoniae*, which arrests cell growth in metaphase (185). This cell cycle arrest has been attributed to alterations in the microtubule cytoskeleton (185). While T3SS effectors are known to target the host actin cytoskeleton, to date no T3SS effector has been shown to target the tubulin cytoskeleton. CopN is novel in that it targets microtubules (MTs), but it is not known how CopN interacts with and disrupts the microtubule network. This thesis will describe experiments that establish a mechanism by which CopN disrupts MT structures as well as describing how CopN regulates T3S.

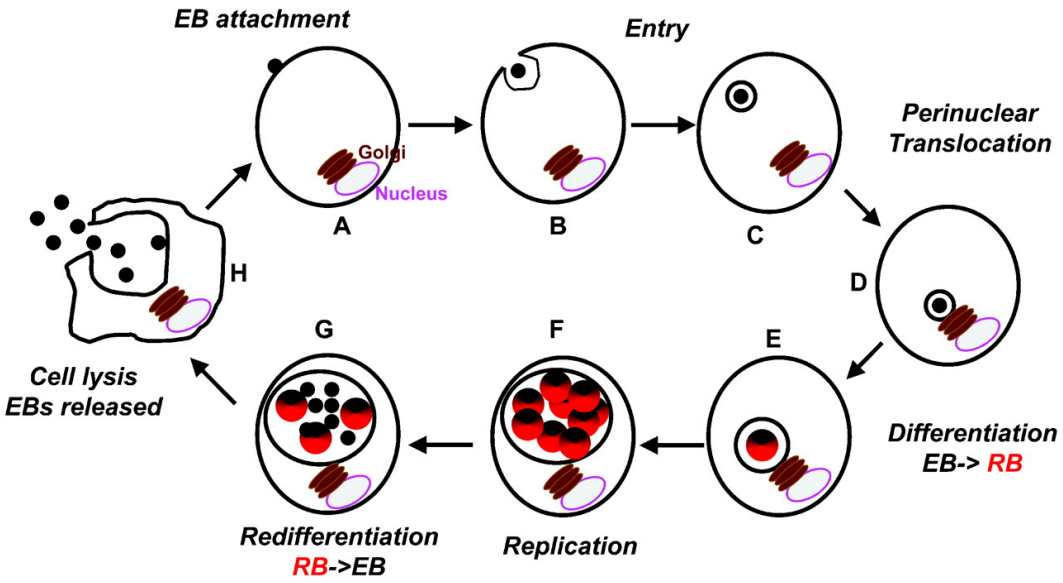

Figure 1-9: The *Chlamydia* life cycle. (A) Elementary bodies attach to the host cell; **(B, C) Elementary** body entry and formation of the inclusion; **(D)** modification and translocation of inclusion; **(E)** differentiation of elementary body to reticulate body; **(F)** replication of reticulate body; **(G)** redifferentiation of reticulate bodies to elementary bodies; **(H)** cell lysis and release of elementary bodies, which allow the pathogen to spread to other host cells. Adapted from Engel 2004 (187).

Microtubules

Microtubules are a component of the eukaryotic cytoskeleton, and are essential for moving cellular structures such as organelles, chromosomes, and other cargo throughout the cell (206). Microtubules are dynamic polymers composed of 13 protofilaments, each of which are built from αβ tubulin heterodimers (207). Microtubules are polar filaments, which grow and collapse rapidly at the plus end (207,208). The microtubule polymer is oriented in such a way that the αβ tubulin heterodimers are arranged by the α subunit oriented towards the minus end of the growing MT, towards the anchor point, and the β subunits are oriented in the growing or plus end of the MT (206). Thus, the MT is a polymer of αβ tubulin heterodimers that are aligned head-to-toe. In mammalian cells, the minus-end of the MTs are anchored centrosomes (209). In yeast, MTs are anchored to the spindle pole body (210). A growing microtubule is formed by GTP/GDP-bound αβ tubulin heterodimers: α-tubulin subunit has a bound molecule of GTP, that does not hydrolyze (206,207); and the β-tubulin subunit can bind either GTP or GDP, depending on whether the GTP is hydrolyzed or not. MTs polymerize via addition of GTP-bound tubulin subunits, which will hydrolyze once incorporated into the MT lattice (211). A semi stable GTP-tubulin cap is formed at the growing end of the MT, which suppresses a change in equilibrium towards disassembly, called catastrophe (211). *In vitro*, the GTP cap is estimated to be ~100-200 αβ tubulin heterodimers (212). However, in vivo, the GTP cap is measured to be composed of ~750 αβ tubulin heterodimers (211).

As mentioned above, microtubules have the ability to move cellular structures throughout the cytoplasm. By maintaining its attachment to a particular structure, the microtubules can move its cargo by growing and shrinking (213). Given this movement and force that is generated, MTs are molecular machines that converts chemical energy into mechanical force, which has been shown to be equivalent to motor proteins (206,214).

There are many proteins that are associated with microtubules. These proteins either aid in modulating microtubule dynamics, or utilize the MT as a means for transportation. Microtubule associated proteins, MAPs are one class of proteins that modulate microtubule dynamics by increasing stability of the MT causing increase growth rate by cross-linking adjacent protofilaments (215,216). Aside from MAPs, there are two classes of microtubule end binding proteins: mitotic centromere-associated kinesins, MKACs, which bind to microtubule ends and cause destabilization (217); and, plus end binding proteins, +TIPs, which bind and stabilize the growing end of the microtubule, and have a conserved tubulin binding TOG domain (218-221). Another modulatory protein, Op18/stathmin, sequesters two tubulin heterodimers, which promotes MT catastrophe by decreasing the free tubulin concentration in the cell (222-226). However, this function is dependent on the phosphorylation state of stathmin. Unphosphorylated stathmin destabilizes microtubules by reducing the concentration of tubulin in the cell needed to form MTs; and, phosphorylated stathmin cannot bind tubulin heterodimers, which allows MTs to grow (227-233).

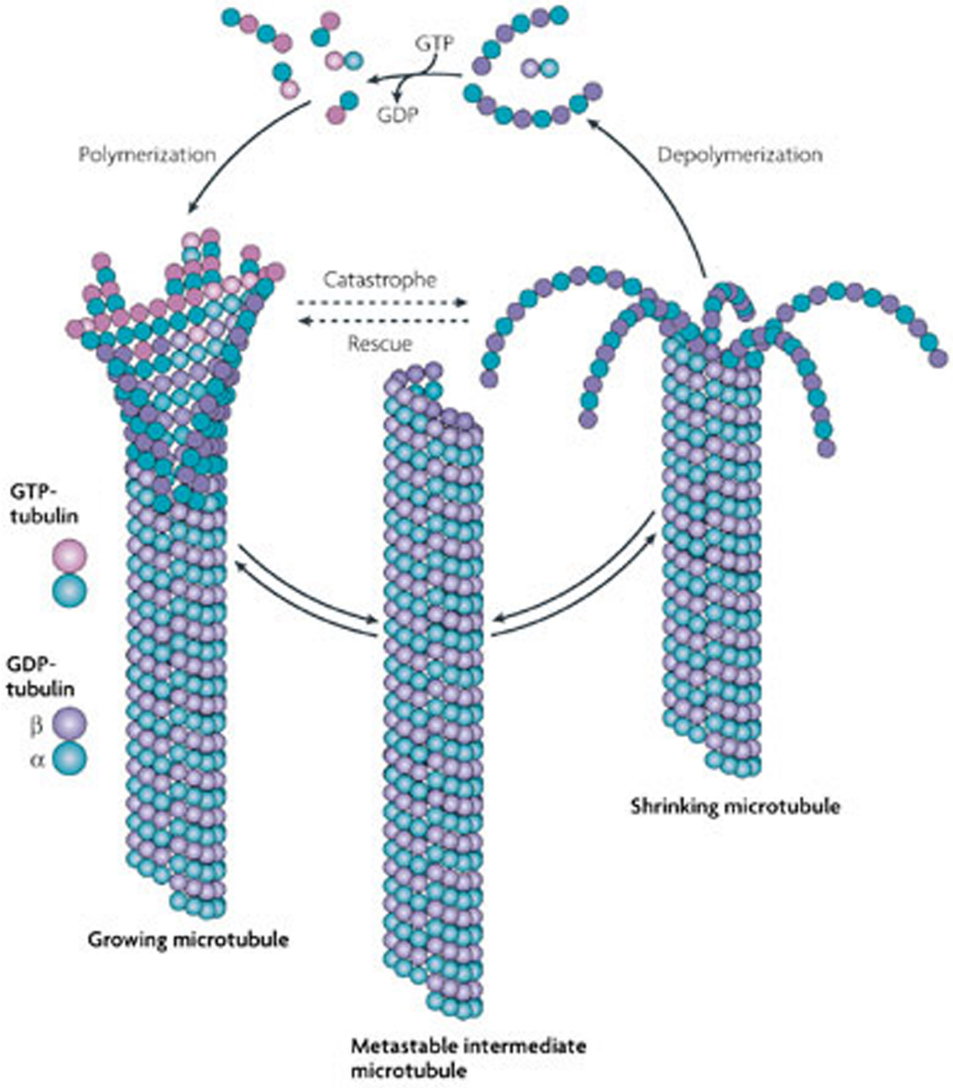

Figure 1-10: Microtubule dynamics. Microtubules are filamentous polymers, which switch between growth and shrinkage. Tubulin heterodimers are incorporated into the growing microtubules. In growing microtubules, GTP bound αβ tubulin heterodimers form GTP-caps at the plus end of the microtubule. The loss of the GTP-cap results in a switching from MT growth to MT shrinkage. Adapted from Conde & Cáceres 2009 (208).

Research objective

CopN is secreted by the T3SS (196,234) and shows sequence similarity to other T3SS gatekeepers (133,235). Heterologous expression of CopN in cells results in loss of microtubule spindles, disruption of metaphase plate formation, and causes mitotic arrest, leading to the classification of CopN as a secreted effector (185). By these criteria, CopN is deemed a T3SS gatekeeper protein and an effector (1,30). This combination of functions in a small protein motivated us to study CopN's biochemical activities and structure. Gatekeeper proteins typically block the T3SS pore; in anticipation of an unknown, extracellular signal which triggers gatekeeper release and effector export (31-33). The molecular mechanisms of microtubule networks disruption are not fully understood, but are known to include physical sequestration and chemical modification of tubulin (222,225,236-242). My objective in this project has been to understand how CopN performs these two functions--gatekeeper and MT-disrupting effector--as a compact, ~400 amino acid protein. I have combined structural biology, biochemistry, and microbiology in these endeavors.

I have shown that CopN directly binds αβ tubulin and inhibits tubulin polymerization into MTs. In addition to characterizing CopN's biochemical activity as an effector, I determined the structure of CopN bound to a translocator-specific chaperone, Scc3. The structure identifies a previously unknown interface between gatekeepers and translocator chaperones and reveals that in the gatekeeper-chaperone (CopN-Scc3) complex the translocator-binding groove is free to bind translocators. Structure-based mutagenesis of the homologous complex in Shigella reveals that the gatekeeper-chaperone-translocator complex is essential for translocator secretion and for the ordered secretion of translocators prior to effectors. Finally, I utilized the 2Å crystal structure of CopN and biochemical assays to elucidate the binding interface between CopN and tubulin. As suggested in my previous studies, CopN disrupts microtubules by sequestering

αβ tubulin, in a stathmin-like mode (225,236-239). This manuscript serves to demonstrate the unique dual-function of CopN: an effector protein and a general role as gatekeeper in the type 3 secretion system.

CHAPTER II

THE *CHLAMYDIA* EFFECTOR, *CHLAMYDIAL* OUTER PROTEIN N (COPN), SEQUESTERS TUBULIN AND PREVENTS MICROTUBULE ASSEMBLY.

Introduction

Chlamydia species, the causative agents of a range of human diseases including genital, ocular and respiratory infection (187-190), are obligate intracellular pathogens with a biphasic life cycle consisting of metabolically inactive elementary bodies (EBs) and metabolically active reticulate bodies (RBs) (191). Infection involves attachment and cellular uptake of EBs and subsequent differentiation into RBs. The RBs remain in endosome-derived membrane vacuoles termed 'inclusions,' which migrate to the microtubule-organizing center (MTOC) in a dynein dependent process (192,193,243). After multiple rounds of bacterial cell division, the RBs re-differentiate into infectious EBs and spread to neighboring cells (191). *Chlamydia* are intractable to genetic manipulation, complicating the task of assigning function to effector proteins, and hence, the development of a mechanistic understanding of interactions between *Chlamydia* and the host (188). As with other gram-negative bacteria, *Chlamydia* use a type three secretion system (T3SS) and T3SS effectors to subvert host defenses and reprogram cell processes (188,196,244).

Type three secretion is a complex pathway used by many gram-negative bacteria to deliver effector proteins to their hosts (for extensive reviews, please see (245,246). The T3SS is composed of a needle complex (or type three secretion apparatus), an ATPase, translocator molecules, effector molecules, and chaperones. The needle complex is a large multi-protein complex that spans both bacterial membranes and serves as a conduit

through which secreted proteins reach the target cell. Proteins are secreted through this pore in an ATP consuming process using specialized ATPases located in the bacterial cytosol, at the base of the needle complex. Secreted proteins include translocators, which are membrane proteins that form a pore in the host's membrane, and effectors, which are a diverse group of proteins that subvert host cell processes and orchestrate bacterial adhesion or engulfment (among other activities). Within the bacterial cytosol, effectors and translocators are often found in complex with specialized chaperones that keep them in a secretion competent state until secretion is initiated. External cues initiate secretion, at which time a gatekeeper protein that had been occluding the pore is secreted and the T3SS becomes active. A common target for T3SS effectors is the host's cytoskeleton, which is frequently remodeled during infection (188,245,247-250).

Bacterial pathogens typically secrete effectors that modulate the actin cytoskeleton, which enables remodeling of the membrane to promote uptake or adhesion of the bacteria. The tubulin cytoskeleton is less frequently the target of effectors, although there are some reports describing effectors that target tubulin or MTs (185,251). MTs are critical eukaryotic cytoskeletal structures (reviewed in (252)), composed principally of αβ tubulin and decorated with MT accessory proteins (MAPS). In non-dividing cells, they form a structural network used, in combination with microtubule-associated motor proteins, for vesicle trafficking and organelle localization. In motile cells they are essential components of cilia and flagella. During cell division MTs form the mitotic spindle and segregate the chromosomes to daughter cells.

A prominent feature of infection is that *Chlamydia* modulate the host's cell cycle, resulting in delayed cytokinesis and failure to properly segregate sister chromosomes (185,192,253). While the advantage afforded to the pathogen is not clear, two mechanistic strategies for affecting the cell cycle have been identified: regulation of the G2/M transition by cleavage of mitotic cyclin B1 (253) and a CopN-dependent mitotic arrest (185).

Expression of CopN in eukaryotic cells results in severe alterations in the MT network, including destruction of mitotic spindles (185). CopN is a putative T3SS gatekeeper protein (133,196). Gatekeeper proteins typically block the secretion pore allowing protein export only in the presence of an unknown extracellular signal (103,129,254). The discoveries that CopN was a T3SS effector (196) that destroyed MT networks (185,196), as well as a putative gatekeeper protein (133,235) motivated us to determine CopN's biochemical activity. This chapter shows that CopN directly binds αβ tubulin and inhibits tubulin polymerization into MTs.

Methods

Purification of His tagged proteins.

Gateway expression vectors for *CopN from C. pneumoniae, C. trachomatis, and C. psittaci B577 (C. abortus)* were previously described (185). *C. pneumoniae* CopN was subsequently cloned by standard PCR methods into pET28, thus incorporating an amino-terminal hexa-histadine tag, and all truncations were made in pET28 using PCR based mutagenesis. Scc2 and Scc3 were PCR amplified from genomic DNA (ATCC strain AR-39) and cloned into pET28, with an amino-terminal hexa-histadine tag. Human stathmin was sub-cloned from a pET15 vector into pET28 and fused to an amino-terminal hexa-histadine tag. Proteins were expressed in BL21 (DE3) cells grown in LB at 37˚C and induced with 0.1mM IPTG for 12 hours at 20 ˚C. Bacteria were harvested by centrifugation, lysed with a French Press, and proteins were purified by metal affinity chromatography and, for all proteins except stathmin, size exclusion chromatography. Proteins were snap-frozen in liquid nitrogen and stored at -80 ˚C until needed.

Tubulin purification.

Fresh bovine brains were obtained from a local slaughterhouse (C and F Meat Company, College Grove, TN) and tubulin was prepared as described (255), with the only modifications being that 600 g of bovine brains rather than 1 Kg of porcine brains were used (buffer volumes were adjusted accordingly) and that the rotors used were a JA-10, Ti-45, and Ti-70.1 rather than SLA 1500, Ti-45, and TLA 100.4 (rotor velocities were adjusted to achieve appropriate g forces). Tubulin was snap-frozen in BRB80 buffer (80mM PIPES, 1mM $MgCl_2$, 1mM EGTA, pH 6.8) in liquid nitrogen and stored at -80 C until needed.

Size exclusion chromatography.

Tubulin and chaperone binding assays were performed by size exclusion chromatography, using a 24 mL Superdex S200 column (GE Healthcare), equilibrated in S200 buffer (10mM Tris-HCl, 150mM NaCl, pH 7.5), run at 0.5 mL/min, and maintained at 4˚C. CopN and tubulin, or CopN and Scc3 were mixed, allowed to form complexes for 15 minutes, and applied to the column. For the stathmin-tubulin-CopN experiments, stathmin and tubulin were mixed first, allowed to equilibrate for 15 minutes, then CopN was added and allowed to equilibrate for an additional 15 minutes.

Microtubule pelleting assays.

MT pelleting assays were performed essentially as described (222,256). 10 mg/rxn of Taxol stabilized MTs, were incubated with 2, 6, 10, 20. 30, 40 mg/rxn of the CopNΔ84 for 15 minutes at 25˚C and spun through a 60% sucrose cushion (20 min at 140 K x g in a TLA 100.4 rotor). Fractions from the supernatant and pellet were analyzed by SDS PAGE. Human stathmin (5 mg/rxn) and rat microtubule associated protein 2c microtubule-binding domain (257) (MAP2c MTBD: used at 20 mg/rxn) were used as positive and negative

controls, for MT binding, respectively. MAP2c MTBD was a gift from Kevin Slep, University of North Carolina, Chapel Hill.

Tubulin turbidity assays.

Turbidity assays were performed in triplicate in a BioTek Synergy 4 plate reader in 96 well plates. Each assay well included 200 μg of tubulin, 3mM GTP, 80mM PIPES, 2mM $MgCl_2$, 0.5mM EGTA, and 30% glycerol in 300 μL total volume. Plates were setup on ice, mixed, and transferred to an incubated plate reader maintained at 37˚C, absorbance at 340 nm was measured at 45 s intervals, and the plates were shaken for 5 s before each measurement. Data presented are the average of three replicate wells.

Microtubule disassembly.

MT disassembly was assayed essentially as described (222,256,258). Surfaces of double-stick tape flow cells were coated with 1 mg/ml biotinylated BSA followed by 0.1mg/ml streptavidin, 1mM fluorescent (1:9 rhodamine-labeled:unlabeled), biotinylated (1:100 biotinylated:unmodified) GMPCPP-MTs were then bound to the flow cell surface, and washed with flow cell buffer (FCB; 80mM Pipes, pH 6.8, 0.5mM $MgCl_2$, 1mM EGTA containing 1mM MgATP, 500 mg/ml casein, 50mM KCl, and an oxygen scavenging mix (259). CopN was diluted to 2.8 μM in FCB and added to the flow cell. MT disassembly was monitored by time-lapse fluorescence microscopy using a Nikon 90i epifluorescence microscope with a 100X 1.4 NA Nikon objective and a CoolSNAP HQ2 cooled CCD camera. MT lengths were measured at 0 and 4 minutes. These experiments were performed simultaneously with experiments presented in Du *et al*. 2010 (256), therefore, the control experiments represent the same set of controls reported in that publication.

Electron microscopy.

GMPCPP stabilized MTs were prepared as described (260). Microtubules were mixed with either buffer alone (BRB80), MAP2c MTBD (a known MT bundling protein (257), or CopN and incubated for 5 minutes at room temperature before being prepared for imaging by conventional negative stain electron microscopy. Uranyl formate stained samples were prepared for EM as described (261). In brief, 3 ml of sample was absorbed to a glow discharged 200-mesh copper grid covered with carbon-coated collodion film. The grid was washed with two drops of water and then stained with two drops of uranyl formate (0.75%). Samples were imaged on a FEI Morgagni electron microscope operated at an acceleration voltage of 100 kV. Images were recorded at a magnification of either 11,000X or 36,000X and collected using a 1K x 1K CCD camera (ATM).

Competitive binding assay.

This assay was performed analogously to a competitive ELISA. Wells in a 96 well microtiter plate were coated with 1 mg/well tubulin in BRB80 for 10 hrs at 4˚C. The plate was subsequently washed 2 times with PBS, blocked for 2 hrs with PBS/3% BSA at 22˚C, and washed 4 times with PBS. Biotinylated stathmin, labeled with sulfo-NHS-Biotin (Thermo-Scientific) following the manufacturer's protocol and using a 40 fold molar excess of sulfo-NHS-Biotin, was added simultaneously with unlabeled CopN to each well. 100mL of 2.0mM biotin-stathmin was added to each well. This value was the EC50 of biotin-stathmin in experiments without CopN. 100mL CopN was added as a dilution series from 10mM to 0.020mM. To add these reagents simultaneously, and avoid order of addition kinetics, they were pre-mixed in a 96 well plate with very low protein binding in PBS/3%BSA/0.05% Tween 20. Binding was for 2 hrs at 22 ˚C followed by 4 PBS washes. The biotin signal was developed with alkaline phosphates linked streptavidin using reagents from Kikegaard and Perry Laboratories and read on a BioTek Synergy 4 plate

reader at 405nM. Control experiments included conditions without tubulin, without CopN, and without biotin-stathmin.

Results

Domain mapping experiments demonstrate that CopN encodes three domains.

CopN, which is found in all *Chlamydia* species, shows weak sequence homology to a family of bacterial proteins that function as gatekeeper proteins for the T3SS (133). This family includes YopN from *Yersinia pestis* and MxiC from *Shigella*. Gatekeeper proteins exist in two different organizational structures, a YopN-like form in which the gatekeeper and a regulator protein (TyeA in the case of YopN) exist as two separate polypeptides (103), and a single polypeptide form exemplified by MxiC, the T3SS gatekeeper protein from *Shigella* (254). In MxiC a TyeA-like domain is present in the carboxy terminal region of the protein (254). CopN is ~100 amino acids longer than YopN (399 versus 293 amino acids), ~50 amino acids longer than MxiC (399 versus 354), and has been proposed to be a MxiC-like gatekeeper protein (133).

As a first step in the biochemical characterization of CopN, I mapped its domain structure by limited proteolysis and mass spectrometry, using trypsin and chymotrypsin. This approach, in which unstructured regions are rapidly degraded, identifies domains based on protease resistance. My results, summarized in figure 2-1, indicate that CopN is composed of a flexible amino-terminus, a protease resistant central core, and a protease resistant carboxy terminal domain. Despite very low sequence identity (45 conserved residues between CopN and MxiC), this domain structure is similar to the domain organization of MxiC (254). This domain structure has two implications: First, that amino acids 85-268 form a gatekeeper domain that is structurally similar to YopN and the

gatekeeper region of MxiC. Second, that the carboxy terminal ~130 amino acids of CopN form a regulatory domain, perhaps similar to TyeA and the carboxy terminal domain or MxiC, which controls CopN secretion and hence activation of the T3SS. In the case of *Y. pestis*, TyeA binds the carboxy-terminus of YopN and prevents YopN's secretion until an unknown signal promotes the release of TyeA (103). In the case of CopN, and other MxiC-like gatekeeper proteins, secretion is likely triggered by a conformational change within the carboxy-terminal domain, rather than by release of a regulatory protein.

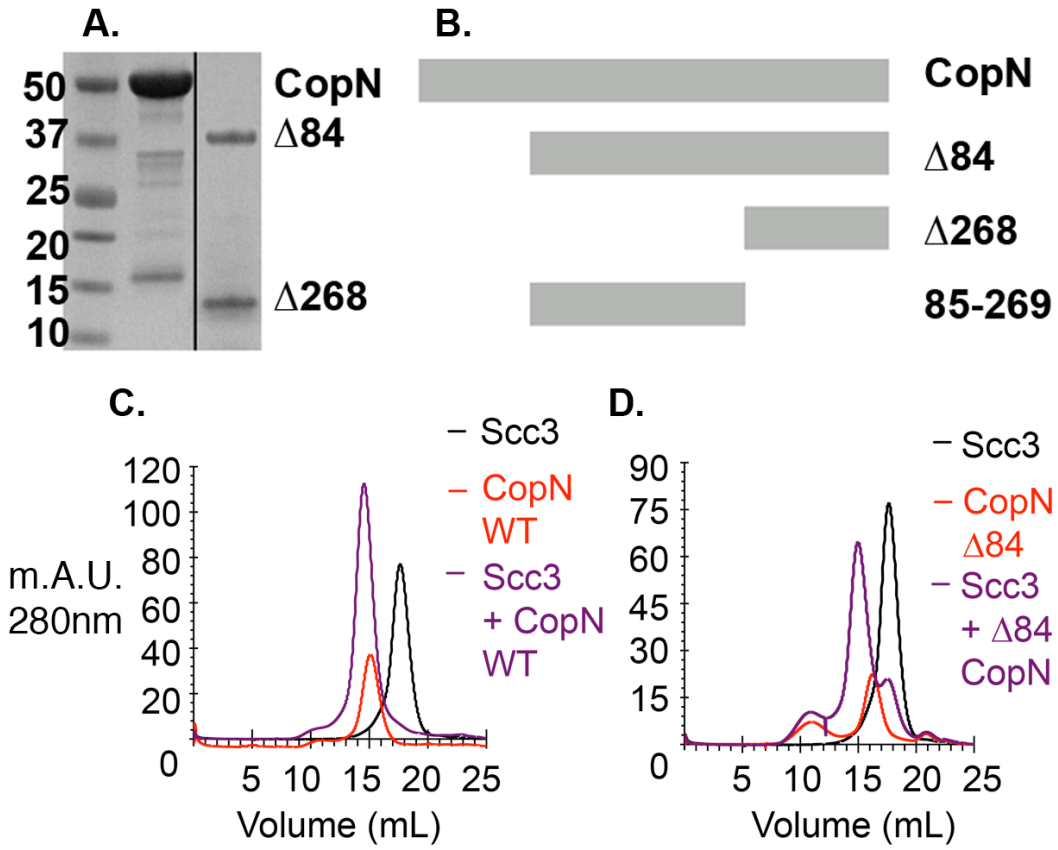

Figure 2-1: Domain structure of CopN as determined by limited proteolysis. **A**. SDS PAGE of limited proteolysis with trypsin shows two bands Δ84 and Δ268 that were unambiguously identified by mass spectrometry. **B.** The deduced domain structure of CopN. Based on limited proteolysis data and the MxiC structure (254), the first 84 residues are a flexible leader, residues 85-269 are a putative "gatekeeper" domain, and residues 269-399 are a putative regulatory domain. **C.** Size exclusion chromatography trace showing that Scc3 and CopN co-elute, resulting in a shift of Scc3 and CopN when the proteins are added together, relative to when they are added separately. **D.** Size exclusion chromatography trace showing Δ84 CopN interacts with Scc3 similarly to full length CopN.

CopN binds Scc3, a class II chaperone, using regions outside the unstructured amino terminus.

The amino-termini of type three secretion effectors are unstructured and function to promote secretion, with some binding cognate chaperones and becoming partially ordered upon binding (100,104,246,262). To determine if the amino-terminal region of CopN binds a chaperone, I first identified the relevant chaperone. The candidate chaperone, Scc3, which was shown to bind CopN in both yeast and bacterial 2-hybrid experiments (234,235), was cloned, expressed, and purified. Using purified components, I found the Scc3 promotes a shift of CopN, as well as an amino-terminal truncation of CopN (Δ84 CopN), to faster elution time on a size exclusion chromatography column, and that when added together the proteins co-elute at the faster time, indicating that Scc3 binds directly to CopN (figure 2-1, figure 2-2).

CopN binds directly to tubulin, but not to microtubules.

Over-expression of *C. pneumonia* CopN in eukaryotic cells results in both disruption of mitotic spindles, which are composed of MTs, and mitotic arrest (185). Such characteristics are consistent with the action of a MT destabilizing protein, motivating us to investigate the possibility that CopN binds tubulin or MTs. Using purified components I show that CopN binds directly to αβ tubulin. Using size exclusion chromatography to measure protein-protein interactions as a shift in retention time, the data show that CopN significantly retards the retention time for αβ tubulin (figure 2-3A, figure 2-4A,B), consistent with a model in which the disruption of mitotic spindles observed when CopN is expressed is mediated by direct tubulin binding. I next investigated whether additional homologs bound αβ tubulin. As shown in figure 2-3B and figure 2-4C, CopN from *C. psittaci B577 (C. abortus)*, but not from *C. trachomatis* (figure 2-3C, figure 2-4D), interacts with αβ tubulin by size exclusion chromatography.

To determine whether CopN bound to both MTs and tubulin, or if it was specific for unpolymerized tubulin, CopN was evaluated for ability to bind MTs using a MT pelleting assay. In this assay CopN was incubated with MTs, which were subsequently separated from free αβ tubulin by centrifugation. This assay is typically used to show binding to MTs, in which case the binding partner is pulled to the pellet with the MTs. As shown in figure 2-3D, CopN remains in the supernatant, indicating that it does not bind MTs. Although this experiment can't rule out that a small amount of CopN's binds to MTs, taken in its entirety, figure 2-3 shows that CopN has a clear preference for un-polymerized tubulin, indicating that it binds a surface of tubulin that is inaccessible or altered in MTs. With the assistance of Dr. Melanie Ohi, we further evaluated the possibility that CopN might induce bundling or some other alteration of MTs. Negative stain Electron Microscopy (EM) demonstrates that CopN does not alter MT structure (figure 2-5).

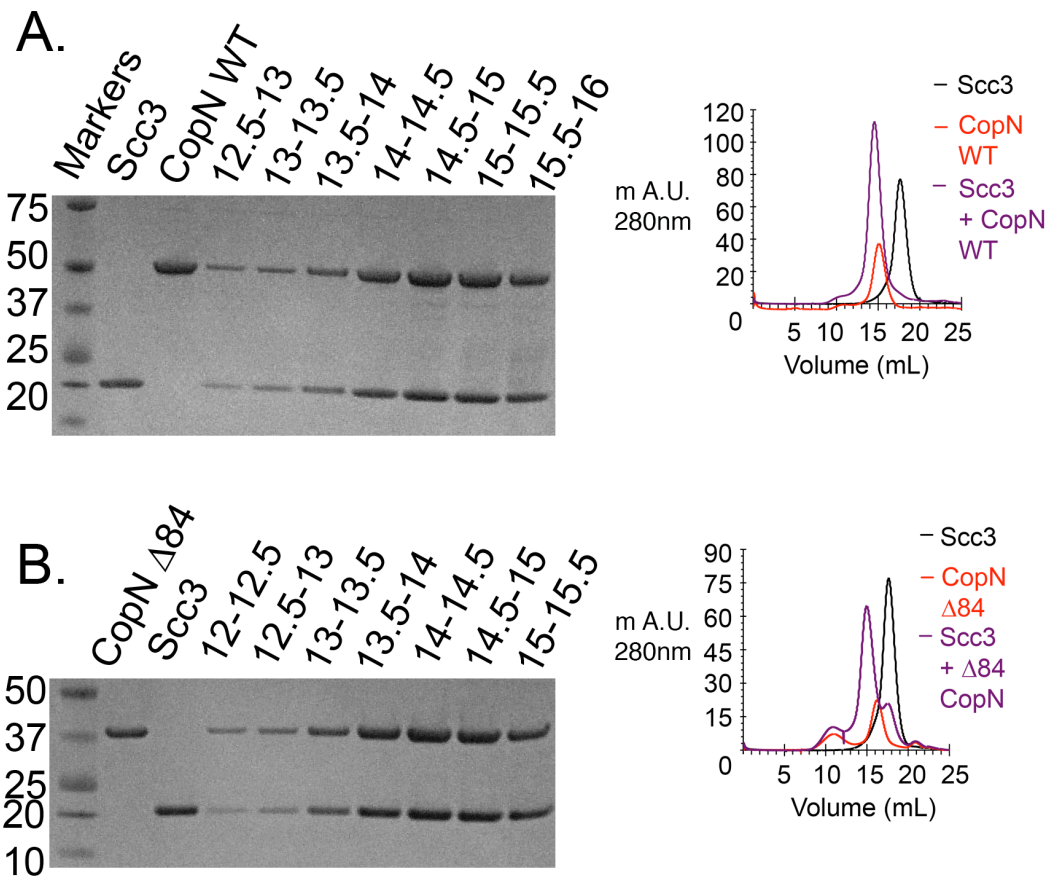

Figure 2-2: SDS-PAGE and size exclusion chromatography traces of CopN-Scc3 complexes. A. and B. SDS-PAGE shows that the peaks from the chromatographs contain the expected components. The shifted CopN + Scc3 peaks contain both CopN and Scc3.

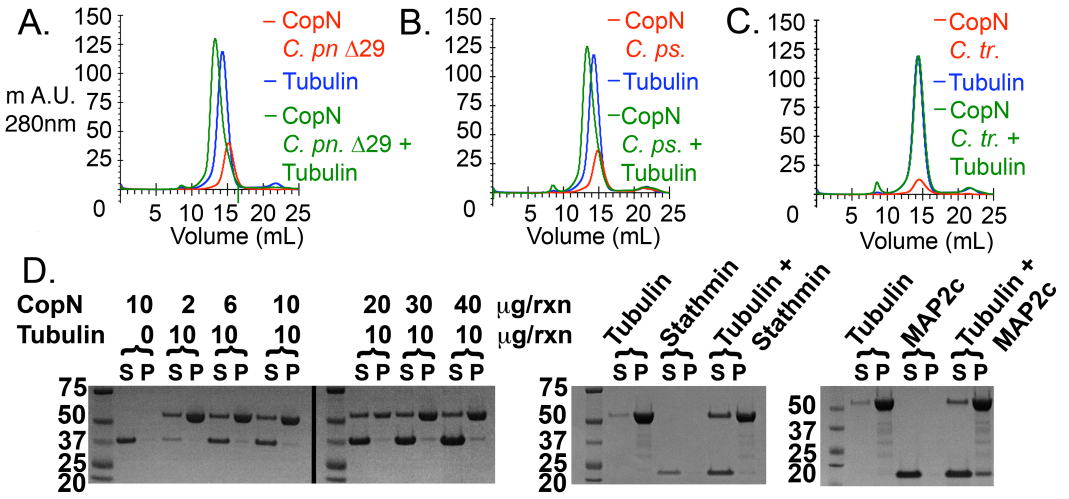

Figure 2-3: CopN binds tubulin, but not microtubules. A., B., and C. show size exclusion chromatography based binding assays, in which proteins are run individually and as a mixture on an analytical size exclusion chromatography column. In these traces, CopN is red, tubulin is blue, and the complex is green. In panels **A.** and **B.** CopN + Tubulin runs faster than either individual component, indicating that the purified proteins directly associate. Panel **C.** indicates that *C. trachomatis* CopN does not bind tubulin tightly enough to survive size exclusion chromatography. Panel **D**. shows a MT pelleting assay. In this assay, Taxol stabilized MT are prepared, mixed with *C. pneumoniae* CopN, stathmin, or MAP2c and fractionated between a soluble (S) tubulin containing fraction and an insoluble (P) MT containing fractions by centrifugation. CopN fails to co-pellet with MTs, indicating that it doesn't bind MTs. Taken together with panels **A. and B.,** these data indicate direct binding between CopN and tubulin, but not between CopN and MTs.

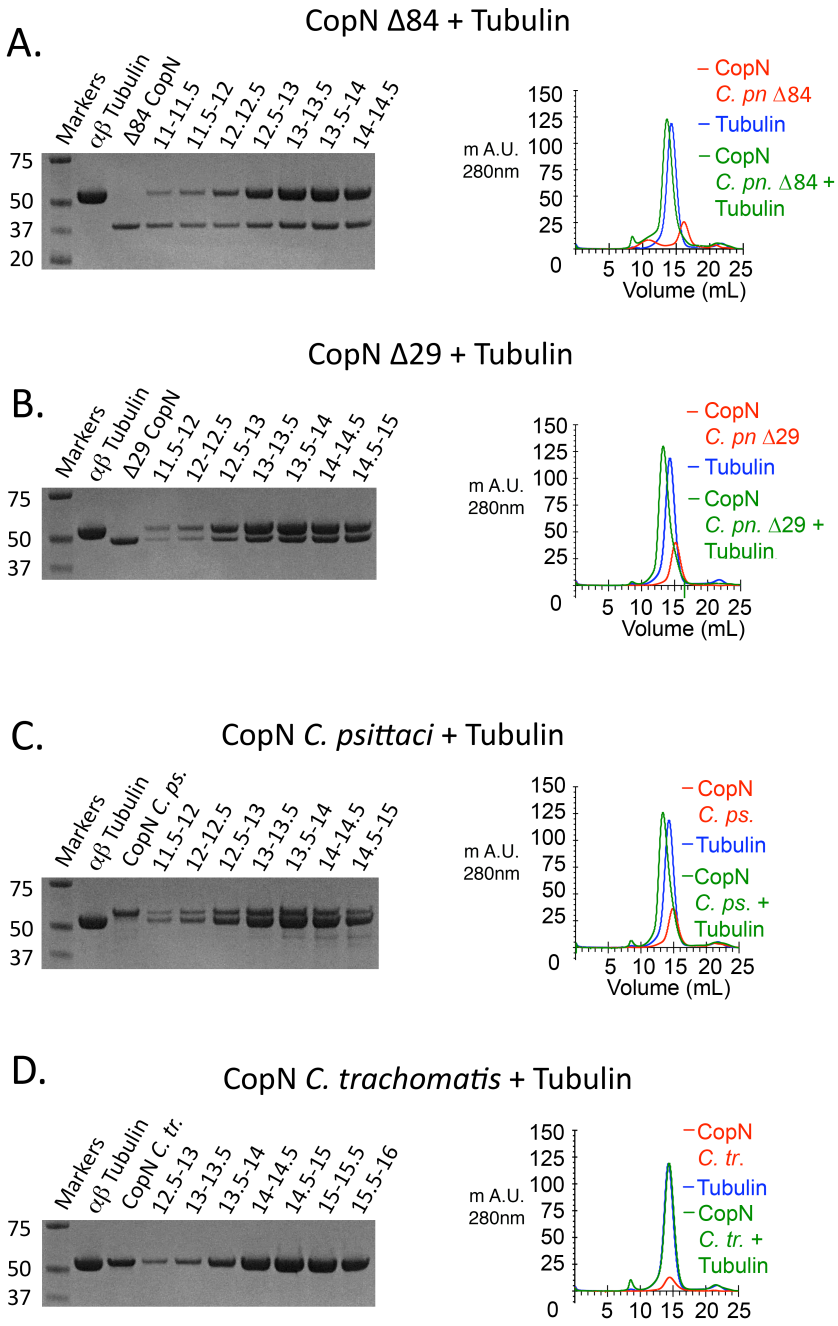

Figure 2-4: SDS-PAGE and size exclusion chromatography traces of CopN-tubulin complexes. A.-D. SDS-PAGE shows that in all cases where addition of CopN shifted the position of the CopN or tubulin peaks, the shifted peaks from the chromatographs contain both tubulin and CopN. *C. pneumoniae* Δ29 CopN, *C. pneumoniae* Δ84 CopN, and *C. psittaci* CopN form stable complexes with tubulin that survive size exclusion chromatography, CopN from *C. trachomatis* does not form a size exclusion chromatography resistant complex with tubulin.

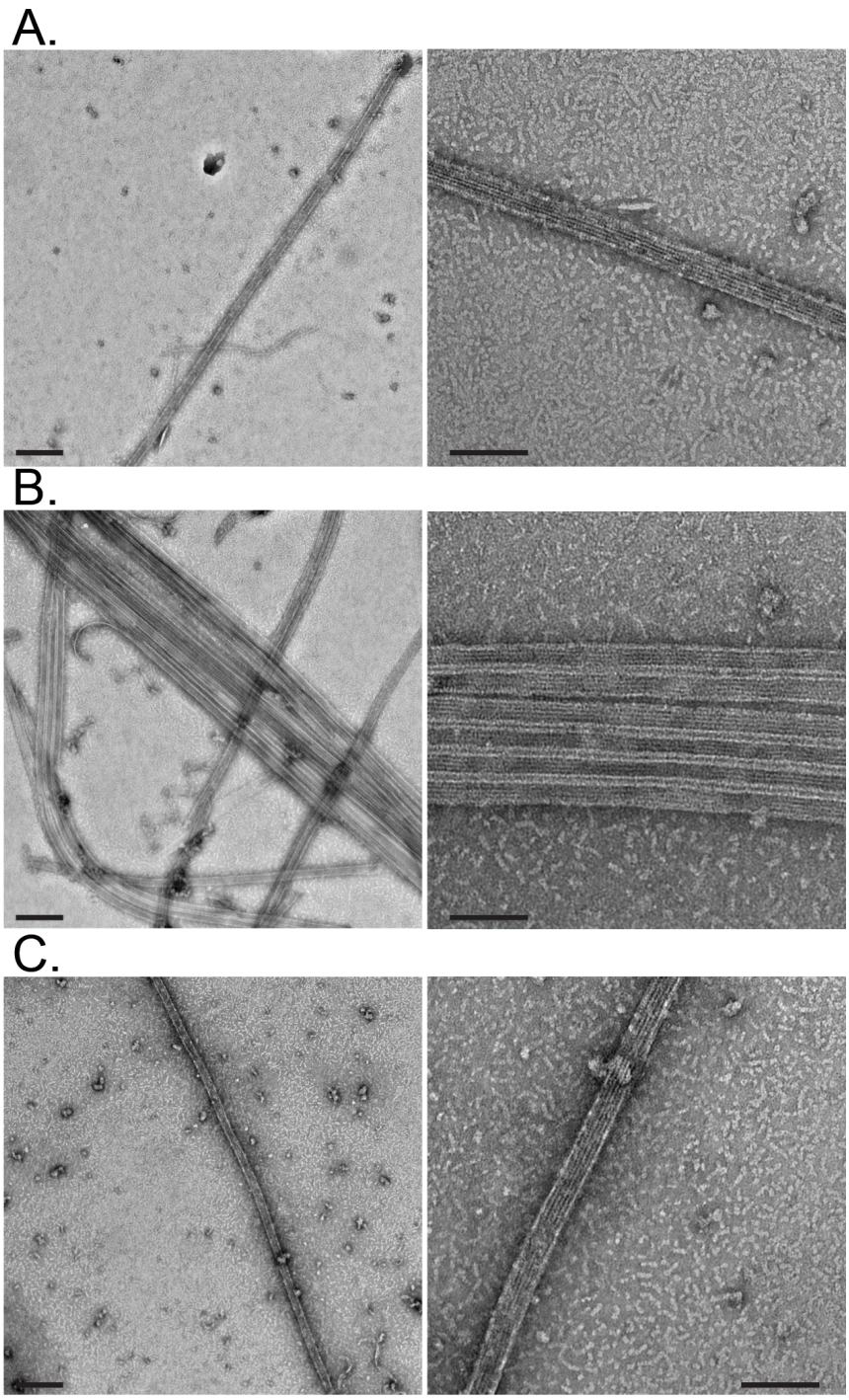

Figure 2-5: CopN does not induce microtubule bundling. Images of GMPCPP microtubules mixed with buffer, MAP2c MTBD, or CopNΔ84. Left panel, 11,000X magnification and scale bar, 200 nm. Right panel, 36,000X magnification and scale bar, 100nm. **(A)** Representative EM images of microtubules incubated with buffer. **(B)** Representative EM images of microtubules incubated with MAP2c MTBD, a known MT bundling protein. **(C)**. Representative EM images of microtubules incubated with *C. pneumoniae* Δ84 CopN.

CopN inhibits microtubule polymerization, but does not de-polymerize microtubules.

The direct interaction between CopN and αβ tubulin and the lack of a detectable interaction between CopN and MTs led us to hypothesize that CopN promotes MT instability by binding and sequestering αβ tubulin, thus preventing polymerization. That is, CopN might sequester αβ tubulin and effectively raise the critical concentration of assembly for tubulin. Stathmin, a eukaryotic tubulin binding protein, is known to use an analogous "sequestration" mechanism to prevent tubulin polymerization (225,236-239). To evaluate how tubulin binding by CopN alters MT polymerization, I optimized a standard, MT turbidity assay (222) for a 96 well plate. In this assay, tubulin is incubated at 37 ˚C and allowed to polymerize into MTs, which scatter light. Absorbance at 350nM is measured as an indicator of polymerization. Use of a 96 well format allowed us to directly compare all proteins in very uniform conditions. CopNs from *C. pneumonia* and *C. psittaci* strongly inhibit tubulin polymerization, whereas CopN from *C. trachomatis* shows weaker, but measurable inhibition (figure 2-6A). CopN from *C. pneumonia* was particularly effective at inhibiting MT formation, showing near complete inhibition at 25 *μ*M. Consistent with the observation that CopN binds free αβ tubulin but not MTs, I also observe that it inhibits αβ tubulin polymerization, but does not promote depolymerization of MTs. With the aid of Dr. Ryoma Ohi and Dr. Yaqing Du, I evaluated the ability of CopN to destabilize MTs by mixing CopN with preformed, rhodamine labeled MT, as described (256,258). As shown in figure 2-6B, no change in MT size is evident following incubation with CopN.

The similar capacities of both CopN and stathmin to bind free tubulin and inhibit polymerization motivated us to determine whether CopN is a distant prokaryotic stathmin homolog. Stathmins contain multiple copies of an ~35 amino acid tubulin binding repeat (TBR), each of which binds a single αβ tubulin (263). I was unable to identify regions of CopN with TBR-like sequence motifs, and chose to test experimentally, the idea that CopN might bind to a similar site on tubulin. I focused on the carboxy terminal gatekeeper

domain (Δ84 CopN) because longer constructs form dimers in size exclusion chromatography conditions, complicating the experiments. I evaluated Δ84 CopN's capacity to bind stathmin-tubulin complexes and form a super-shifted T2S-C complex (stathmin bound to 2 αβ tubulin dimers bound to one or more CopN's). As shown in figures 2-7 and figure 2-8, CopN does not interact with the T2S complex, consistent with a CopN-tubulin interface that physically overlaps with the stathmin-tubulin interface. I verified this result with a competition binding experiment and showed that CopN competes with biotinylated stathmin for binding to immobilized tubulin (figure 2-7).

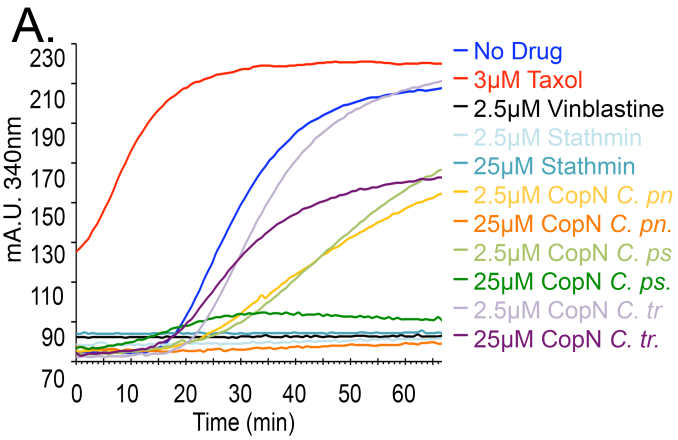

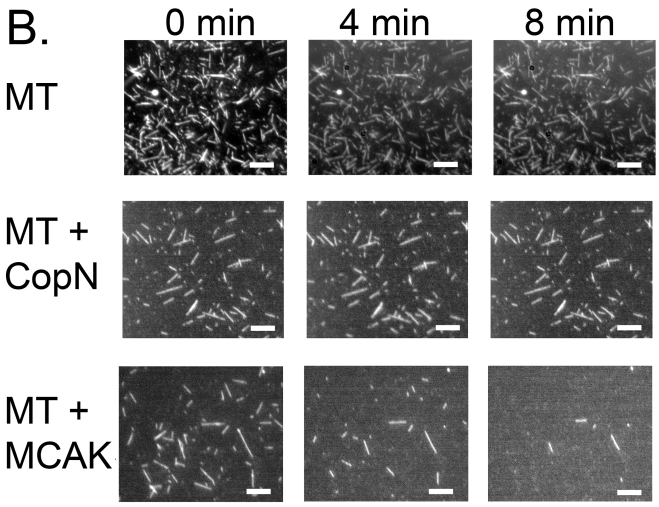

C.

	Control	MCAK	CopN
Depolymerization Rate (μm/min) n=32	0.031	1.17	0.028
SEM	0.037	0.063	0.0038

Figure 2-6: CopN inhibits tubulin polymerization, but doesn't depolymerize microtubules. A. Tubulin polymerization experiment. Curves represent extent of tubulin polymerization as monitored by light scattering. Controls of Taxol and Vinblastine indicate the dynamic range of the assay. The "No Drug" curve indicates the expected time course and extent of polymerization for tubulin alone under these conditions (6 *μ*M tubulin, 30% glycerol). All CopN's show some level of inhibition, with *C. pneumoniae* showing inhibition nearly as strong as Stathmin. **B.** MT disassembly assay showing that CopN is unable to disassemble preformed MTs. The top, middle, and bottom panels show 3 time points each for untreated, CopN (2.8mM), and MCAK (25nM) treated MTs. Scale bars are 6mm. **D.** Depolymerization rates calculated from measured MT lengths at t=0 and t=4 minutes for CopN, buffer, and MCAK (mitotic centromere associated kinesin, kinesin 13) a well known MT depolymerase (264).

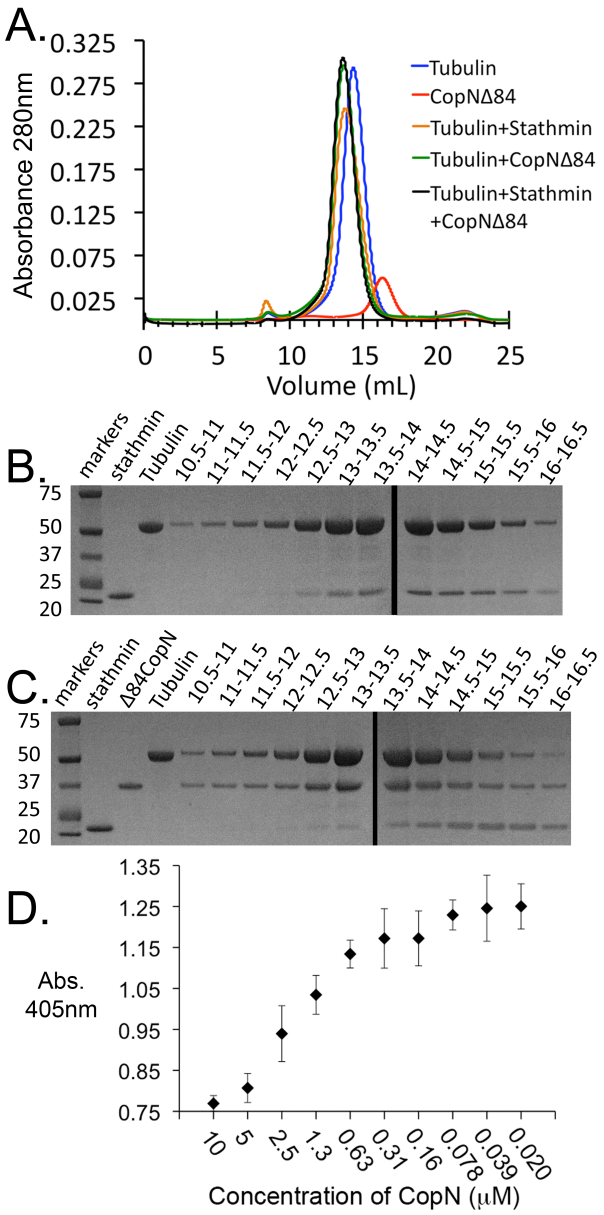

Figure 2-7: CopN is unable to bind to stathmin-tubulin complexes. A. Size exclusion chromatograph showing that Δ84 CopN is unable to shift a stathmin-tubulin complex. **B. and C.** SDS-PAGE on fractions from A. Panel A. shows SDS-PAGE from the stathmin-tubulin complex, which verifies that the peak for the stathmin-tubulin complex is located at ~13.5 mLs, and demonstrates that this peak contains both stathmin and tubulin. Panel **C.** shows SDS-PAGE from the stathmin-tubulin complex mixed with CopN, and indicates that, under these conditions, CopN displaces stathmin from the stathmin-tubulin complex. The CopN-tubulin peak is at ~13.5 mLs, but stathmin is centered at ~16 mLs. Stathmin is invisible in the chromatograph because it lacks tryptophans. **D.** A competition binding experiment in which mixtures containing a fixed (2mM) biotin-stathmin concentration and decreasing (from 10 to 0.020mM) unlabeled CopN were added to tubulin coated wells and biotin-stathmin binding was measured with alkaline phosphatase linked streptavidin.

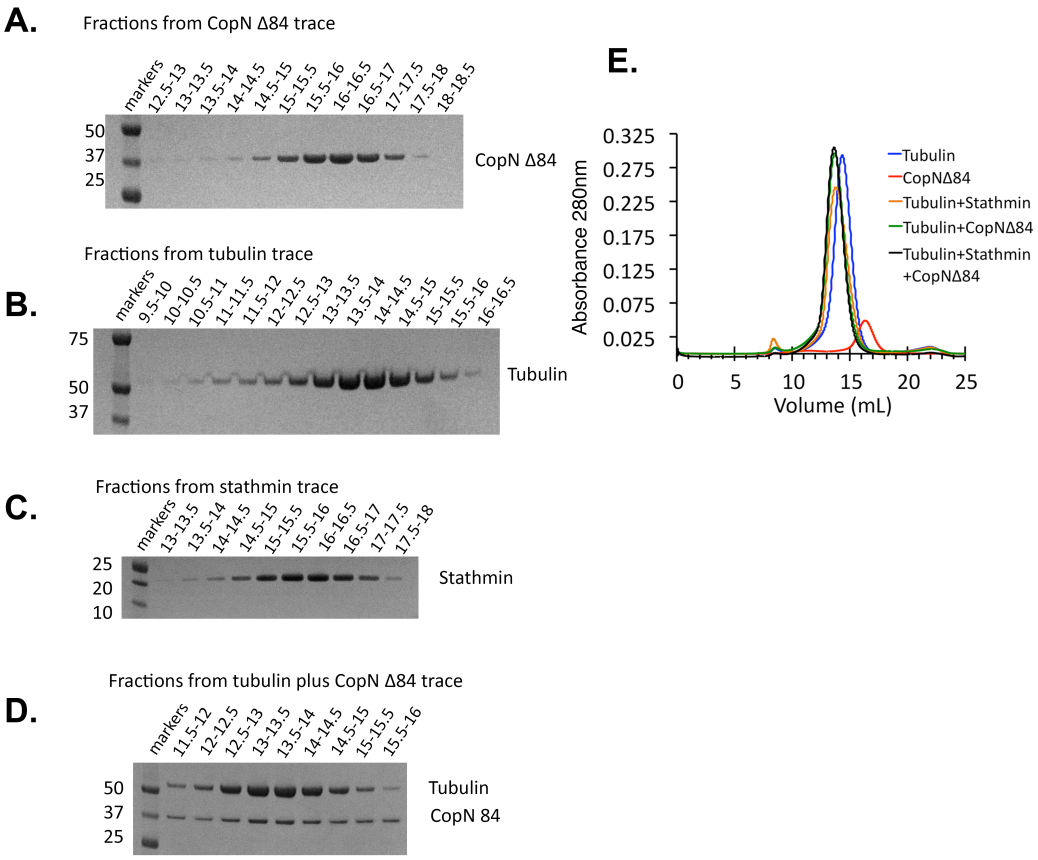

Figure 2-8: SDS-PAGE of controls from CopN-tubulin-stathmin super complex formation attempts. A.-D. SDS-PAGE of fractions from the CopN Δ84, tubulin, stathmin, and tubulin + CopN Δ84 size exclusion chromatography experiments described in the text and presented in figure 2-7. The chromatographs are shown in **E**.

Discussion

CopN is a multifunctional *Chlamydial* effector protein functioning both as the T3SS gatekeeper protein and as a secreted effector protein that causes mitotic arrest (133,185,196,235). Thus far, CopN is the only gatekeeper protein known to also function as an effector. As such, it is perhaps not surprising that CopN's chaperone use is also unusual.

T3SS chaperones are typically grouped by substrate function, with class I chaperones binding effectors, class II binding translocators, and class III binding components of the needle complex (245,265). The functional grouping into class I and class II chaperones corresponds with conserved structural characteristics. Class I chaperones are dimeric mixed α/β proteins composed of 5 beta strands and 3 alpha helices (245). Class II chaperones are monomeric all a helical tetricopeptide (TPR) proteins (266-268).

I show that CopN binds directly to Scc3 (figure 2-1), in agreement with results obtained from yeast and bacterial 2-hybrid experiments (234,235). Scc3 is similar to SycD from *Yersinia* and IpgC from *Shigella*, both of which are class II chaperones with a TPR fold (266-268). These biochemical studies demonstrate that this interaction is direct and robust, as it survives purification by size exclusion chromatography. Further, this interaction involves regions outside the flexible amino-terminus of CopN indicating that CopN's interaction with Scc3 is unique both in the structural details of the interaction and in that it binds a class II chaperone, which usually interact with translocators, rather than a class I or class III chaperone, which typically bind effectors and needle components, respectively (245).

CopN is both a putative component of the secretion complex and an effector, yet interacts with a chaperone typically reserved for translocators. It appears that gatekeeper

proteins do not have conserved chaperone uses, with YopN utilizing a class I chaperone (103) and CopN using a class II chaperone.

I have shown that CopN directly binds αβ tubulin and inhibits MT formation (figures 2-3 and 2-6). CopN does not bind or depolymerize existing MTs (figures 2-3 and 2-6), suggesting that its mechanism of action is through binding of αβ tubulin. Stathmin, a eukaryotic tubulin binding protein, also reduces MT assembly by binding free tubulin (225,236-239). CopN lacks the consensus TBR sequences that are conserved among highly divergent stathmins (263) and lacks any detectable sequence identity with stathmins. Although stathmin and CopN share no sequence identity, both inhibit MT assembly by binding free αβ tubulin, suggesting that *Chlamydia* have independently evolved an activity with similarity to stathmin.

MT formation is a non-equilibrium assembly process in which GTP hydrolysis by the b tubulin subunit (269) is coupled to polymerization (252). MTs are intrinsically dynamic, exhibiting two types of dynamic behavior; dynamic instability (270) and treadmilling (271). Dynamic instability refers to the observation that under identical conditions MTs alternate stochastically between polymerization and depolymerization (270). Treadmilling refers to the observation that MTs can simultaneously grow at one end and shrink at the other, a process that consumes GTP but results in no net change in MT length (271). These two processes ensure that MTs and free αβ tubulin readily interconvert, thus allowing proteins that target free αβ tubulin to influence polymerization. Polymerization is a bimolecular event in which two tubulin dimers or a tubulin dimer and a growing MT combine. As such, the rate of polymerization is influenced by the concentration of αβ tubulin, and proteins that reduce or increase the effective concentration of αβ tubulin affect polymerization rates. Within eukaryotes, a class of proteins, plus end binding proteins (+TIPS), enhances polymerization by binding MTs and free tubulin in a productive configuration (220,272,273). Stathmins, a much smaller group of proteins,

restricted to a single protein family with homologues throughout the kingdom of eukaryotes, bind tubulin in such a way as to block interfaces necessary for assembly. In so doing, stathmins lower the concentration of assembly-competent tubulin, reduce MT assembly, and destabilize MTs (222,225,236-242). *Chlamydia* have independently evolved CopN to exhibit a similar biochemical function.

Regulation of MT assembly is a mechanism to control cell division utilized by both stathmin and CopN (185,238,274). Stathmin regulates MT assembly in a cell cycle dependent manner, achieved by cell cycle dependent phosphorylation of stathmin, which reduces its inhibitory effect and allows cytokinesis to proceed (238,274). CopN also inhibits cell division (185), but two significant distinctions between these proteins, despite similar mechanisms, should be noted. While stathmin is highly abundant (238) and its activity is regulated, allowing cell division (274), no such regulation of CopN is known. Further, T3SS effectors are secreted in fairly small quantities –this has only been measured once, for SipA from *Salmonella,* where ~6,000 molecules per bacteria are secreted (275)– implying that similar biochemical functions are utilized in different ways to promote similar outcomes. CopN over-expression disrupts MTs and causes mitotic arrest (185), but it is unclear how many copies of CopN are required for this effect. It is known that during infection *Chlamydia* do not disrupt the host's cell-cycle until the infections are fairly dense (191), which can be ~1,000 bacteria per host cell (276-278). Thus, CopN could be present at very high levels in cells. Since αβ tubulin is present at millimolar concentrations (~25 million molecules) (279,280) in cells, CopN must either be abundant or targeted to the site of tubulin polymerization for αβ tubulin sequestration to significantly alter MT assembly. *Chlamydia* are indeed located at or near the MTOC (192,193,243), thus a mechanism involving tubulin sequestration at the site of tubulin polymerization seems likely. It remains to be determined if additional MT disrupting functions can be attributed to CopN. From this data I cannot rule out the possibility that CopN bound αβ

tubulin might also be sub-stoichiometrically incorporated into MTs causing additional changes in MT dynamics.

CHAPTER III

A GATEKEEPER CHAPERONE COMPLEX DIRECTS TRANSLOCATOR SECRETION DURING TYPE THREE SECRETION.

Introduction

Type Three Secretion Systems (T3SS) are conserved bacterial protein delivery machines used by many pathogenic Gram-negative bacteria to deliver a diverse group of protein molecules, termed effectors, into cells (245,281-283). The type three secretion (T3S) apparatus is a conserved molecular machine that forms a protein-conducting channel from the bacterial cytosol to the target cell cytosol. Major structural components of the T3SS include: a cytosolic-ring complex, which includes the ATPase that catalyzes protein unfolding and secretion; a basal-body, which forms a pore across both the inner and outer bacterial membranes; a needle complex, which extends from the basal-body to the host cell; and translocators, which form a pore in the target cell membrane, termed a translocon (110,284).

The T3S apparatus secretes a diverse group of effectors directly into host cells. The translocon through which effectors enter the target cell is an oligomeric pore formed by bacterial proteins termed translocators, that are themselves secretion substrates of the T3SS (245). Translocator secretion is regulated such that it occurs prior to effector secretion, ensuring that effector secretion occurs after a functional conduit from the bacterial cytoplasm to the target cell has been formed (285,286). Efficient secretion is dependent on the interaction of specialized chaperones with cytosolic T3SS components (265). Molecular structures have revealed two architectures for T3S chaperones: a mixed α/β homo or heterodimer and an all α-helical tetratricopeptide repeat (TPR) chaperone

(100,101,267,268,287). These chaperones, termed class I (α/β) and class II (TPR), are specific for effectors and translocators, respectively (265). The understanding of how the T3SS switches from translocator to effector secretion is limited, but in multiple systems this process is known to involve a conserved gatekeeper protein (127,128,131,133,181,182). Gatekeepers are encoded as one of two molecular architectures, either as two separate proteins (YopN-TyeA family), or as a gene fusion (MxiC family) (133). The importance of this architectural distinction is unknown, and a protein fusion resulting from ribosomal frameshifting has been reported without an evident functional change (288).

In *Chlamydia*, the gatekeeper, CopN, is known to directly bind Scc3, a translocator-specific chaperone (186,234,235,266,289). Translocator-specific chaperones (class II chaperones) bind directly to translocators, prevent their degradation and maintain the translocators in a secretion competent state (265,268). Structures from homologous class II chaperone/translocator pairs have revealed the chaperone to be a tetratricopeptide repeat (TPR) protein with a conserved binding groove that binds an amino terminal chaperone-binding motif on the translocator (267,268,287,290). In addition to binding translocators, Scc3 also binds CopN, and although the nature of this interaction is unknown, it does not involve the amino terminal chaperone-binding region of CopN, and Scc3 is not thought to be the secretion chaperone for CopN (186,234,235,289). It is not known if CopN and the *Chlamydial* translocators (CopB/B2) compete for the TPR binding groove on Scc3, if they can both bind simultaneously, or if different binding determinants are responsible for the Scc3-CopN interaction.

Complexes that include gatekeepers and translocator chaperones have been observed in immunopurified complexes from other systems, but only as components of large complexes that also include other components of the T3SS (127,132,181). Because such complexes are not readily accessible to structural study, I have focused structural studies on the gatekeeper-translocator chaperone complex from *Chlamydia*. I reason that

the CopN-Scc3 complex is likely to be involved in the ordered secretion of translocators prior to effectors, a conserved phenomenon termed the translocator-effector secretion hierarchy.

The origin of the translocator-effector secretion hierarchy is not fully understood, but has been proposed to arise from differential affinities and competition for binding sites either between chaperones and their effector or translocator cargo or between chaperone-effector/translocator complexes and cytosolic components of the T3SS (100,101,291-294). To assess the importance of gatekeeper-translocator chaperone interactions in diverse pathogens, and because adequate tools and reagents for functional analysis of CopN mutants are not available in *Chlamydia*, I have extended these structural analysis with functional studies of MxiC and IpgC, the gatekeeper and translocator-specific chaperone from *Shigella*.

Methods

Purification of His tagged proteins.

$CopN_{\Delta 84}$ and Scc3, from *C. pneumoniae* AR39, were amplified and cloned into pET28 with an amino-terminal hexa-histadine tag. $CopN_{\Delta 84}$ is an amino terminal 84 amino acid deletion of CopN. It was previously found to be the best behaved CopN variant from *C. pneumoniae* AR39 (186). All CopN variants were made in pET28 using PCR based mutagenesis and verified by sequencing. CopN truncation mutants were designed from described limited proteolysis mass spectrometry analysis (186). Proteins were expressed in BL21 *(DE3)* bacteria grown in Luria Broth at 37 ˚C. Bacteria at an optical density (at 600 nm) of ~0.6 were induced at 20˚C with 0.1mM isopropyl β-D-thiogalactopyranoside, and grown for ~12 hours. Cultures were harvested by centrifugation and lysed with a French

Press in phosphate buffered saline with ~1 μg/mL chicken egg white lysozyme, ~1 μg/mL bovine pancreatic deoxyribonuclease I, 10 μg/mL leupeptin, 1 μM PMSF, 0.7 μg/mL pepstatin. The lysate was clarified by centrifugation and proteins were purified by Co-NTA affinity using Talon resin. Eluted proteins were further purified by size exclusion chromatography, superdex 200, before being snap-frozen in liquid nitrogen and stored at -80 ˚C until needed.

Expression and purification of GST-CopB.

The Scc3 binding region of CopB, residues 158-178 based on sequence homology with IpaB from *Shigella* (268), was expressed as a GST fusion protein from PGEX-4T. Proteins were expressed and purified as for His tagged proteins with minor modifications; proteins were expressed from BL21 bacteria and purified with Glutathione Sepharose 4B (GE Healthcare).

Size exclusion chromatography assays.

Chaperone, and translocator peptide binding assays were performed by size exclusion chromatography, using a 24mL Superdex 200 10/300 GL (GE Healthcare), equilibrated in 10mM Tris-HCl pH 7.5, 150mM NaCl, run at 0.5 mL/min, and maintained at 4˚C. Equivalent molar concentrations, determined from calculated extinction coefficients, of proteins were applied to the size exclusion chromatography column. Protein complexes were incubated for 15 minutes prior to analysis.

Crystallization and preparation of heavy atom derivatives.

Scc3-CopN$_{\Delta 84}$ crystals were grown via vapor diffusion from a reservoir containing 0.2 M Na/K tartrate and 18-22% PEG 3350. Crystals were obtained from a 1:1 mixture of reservoir and 15mg/mL Scc3-CopN$_{\Delta 84}$. $KAu(CN)_2$ derivatives were prepared by adding

100mM $KAu(CN)_2$ to the crystal drop to a final concentration of 2mM $KAu(CN)_2$. After two days of incubation derivative crystals were harvested. Native and derivative crystals were cryoprotected with 15% glycerol and flash cooled.

Data collection, structure determination, and analysis.

Diffraction data were collected from single crystals on stations D and F at LS-CAT beam line at the Advanced Photon Source. Data were indexed, integrated and scaled with HKL2000 (295). Three gold atoms were located and refined using Phenix (296). The initial figure of merit for these sites was 0.46, which improved to 0.70 following density modification. The model was traced with a combination of automated and manual building in Phenix and COOT (296,297). Multiple rounds of refinement were done using Phenix. Refinement included simulated annealing, coordinate, individual B-factor, and TLS refinement as implemented in Phenix (296). Non-crystallographic symmetry constraints were included in all rounds of positional refinement. Data collection and refinement statistics are given in Table 3-1. Figures were prepared using Pymol, ClustalW, ESPript, the DALI server, the PISA server, and the Consurf server (298-302).

Sequence alignments.

Sequences used in the Consurf alignments of CopN homologs were chosen to represent the sequence diversity within genera shown in Figure 3-2 and included five *Chlamydial* sequences (NP_224529.1, NP_829326.1, YP_515466.1, 84785886, 332806765, YP_005809291.1), four *Shigella* sequences (YP_005712038, YP_313363.1, YP_001883209.1, YP_406185.1), three *Salmonella* sequences (1236849, 75349427, NP_461818.1), and three *Bordetella* sequences (NP_880900.1, WP_004568105.1, NP_884470.1). For the two-component gatekeepers, chimeric sequences were generated to agree with the spatial orientations in the YopN/TyeA structure (pdb accession code

1XL3). *Yersinia* YopN sequences used were NP_863522.1, NP_395173.1, and NP_052400.1. Because there is zero sequence diversity in TyeA from species evaluated here, I used YP_004210060.1 for all chimeras. An identical strategy was used for *Pseudomonas* and *Vibrio*. *Pseudomonas* sequences used were NP_250389.1, WP_003122865.1, and WP_010794024.1, WP_015648550.1, which were all matched with WP_009876220.1. *Vibrio* sequences used were NP_798046.1, YP_003285992.1, WP_005395115.1, WP_005377238.1, WP_005441804.1, WP_004745560.1, WP_005528936.1, which were all matched with WP_005395113.1.

Shigella secretion assay.

Secretion assays were performed essentially as described (131,303), with minor modifications. *Shigella* strain M90T was a gift from Marcia Goldberg. *Shigella* strain ΔmxiC as well as pUC19-mxiC have been previously described, and were gifts from Ariel Blocker (131). The pmxiC-RDR was made by standard molecular biology methods and used to transform *Shigella* strain ΔmxiC. Strains were grown on tryptic soy broth (TSB) plates containing 100μg/mL congo red, with appropriate antibiotics. Colonies were selected and grown overnight in liquid TSB broth at 37 °C and harvested by centrifugation. Pellets were resuspended in 5 mLs of fresh liquid medium. A fraction, ~1:25 final dilution, of the resuspended cultures was added to 50 mL TSB cultures and grown to an optical density of 1.0 (600 nm). Cultures were harvested by centrifugation, washed with warm media, and resuspended to a final OD_{600} of 5.0 in PBS + 100 mg/mL Congo Red at 37 °C for 10 min and 30 min. Samples were analyzed by SDS-Page using both coomassie and silver staining, as well as western blotting. Western blotting was done with an α-MxiC antibody primary, which was a gift from Ariel Blocker, and goat anti-rabbit secondary antibody (LI-COR Biosciences). Blots were developed with an Odyssey fluorescent scanner. Protein bands were identified from Mass Spectrometry of trypsin-digested bands

excised from coomassie-stained gels and was performed by the Vanderbilt University Proteomics Core.

Results

Structure of Scc3-CopN complex.

I determined the crystal structure of the Scc3-$CopN_{\Delta 84}$ complex and refined the structure to 2.4 Å (PDB ID 4NRH). The amino terminal 84 residues of CopN were not included in the construct used for crystallization because they are unstructured and dispensable for biochemical function (186). Data collection and structure refinement statistics are given in supplemental Table 3-1, and representative electron density is shown in Figure 3-1. Two nearly identical Scc3-$CopN_{\Delta 84}$ complexes (RMS deviation 0.34 Å for all $CopN_{\Delta 84}$ mainchain atoms and 0.49 Å for all Scc3 mainchain atoms) are present in the asymmetric unit. $CopN_{\Delta 84}$ forms a long cylindrical structure composed of three 4 or 5-helix X-bundle domains (Figure 3-2). $CopN_{\Delta 84}$ is structurally similar to other gatekeeper proteins, both MxiC from *Shigella* and the YopN-TyeA complex from *Yersinia*. The most substantial differences among family members relate to the position of the carboxy-terminal domain or subunit (Figure 3-2 and (103,254). In the Scc3-$CopN_{\Delta 84}$ complex, this domain is translated ~9.5 Å and rotated ~50˚ relative to the YopN-TyeA complex (Figure 3-2). Similarly, Scc3 is structurally similar to other translocator chaperones. The striking result from the Scc3-$CopN_{\Delta 84}$ is the unexpected assembly of the complex and the role of the Scc3 amino terminus in binding $CopN_{\Delta 84}$.

T3SS chaperones bind the amino terminus of effectors and translocators, and class II chaperones (those specific for translocators) use a conserved peptide-in-groove binding mode, utilizing the TPR binding groove, in which translocators bind in the concave

face of the chaperone (100,101,265,267,268,287,290). The structure reveals that Scc3 does not engage $CopN_{\Delta 84}$ using this conserved binding groove. Instead, an amino terminal extension, referred to here as a gatekeeper-binding region (GBR), forms a relatively flat surface, adjacent to the convex side of the TPR and binds across the interdomain interface of the last two cross-helix bundle domains of $CopN_{\Delta 84}$ (Figure 3-2). The interface formed by this interaction results from burial of 980 $Å^2$ of surface area. The Scc3 side of the interface is formed exclusively by residues from the GBR, consistent with separate functions of translocator and gatekeeper binding for the TPR and GBR regions of Scc3. Despite minimal sequence conservation, the GBR is a conserved feature of other translocator chaperones (Figure 3-3, Figure 3-1). In the homologs from *Shigella* and *Pseudomonas* it both mediates homo-dimerization and inhibits translocator binding (268,291,304). In the homologs from *Yersinia* and *Pseudomonas* crystallization and structure determination required removal of the GBR (267,287,290).

Table 3-1 Data collection, phasing, and refinement statistics.

	$Au(CN)_2$	Native
Data collection		
Space group	$P2_1$	$P2_1$
Cell dimensions		
a, *b*, *c* (Å)	62.88, 97.06, 94.36	61.57, 96.18, 94.47
α, β, γ (°)	90.0, 91.87, 90.0	90.0, 92.27, 90.0
Wavelength	1.00798	0.97872
Resolution (Å)	2.8 (2.85-2.80)	2.2 (2.28-2.2) 2.4 (2.49-2.40)
R_{sym}	8.8% (55%)	6.2 (55.4) 5.7 (34.0)
$I / \sigma I$	22.5 (3.25)	21.1 (2.4) 28.4 (4.46)
Completeness (%)	100 (99.7)	89.7 (55.4) 98.0 (82.2)
Redundancy	10.9 (9.6)	7.3 (4.5) 7.7(6.3)
Refinement		
Resolution (Å)		50-2.2 (2.25-2.2)
No. reflections		50,339 (1,807)
R_{work} / R_{free}		18.5/22.2
No. atoms		
Protein		7,302
Ligand/ion		2 Na^+
Water		414
B-factors		
Protein		49.8
Ligand/ion		51.1
Water		48.6
R.m.s deviations		
Bond lengths (Å)		0.006
Bond angles (°)		0.9

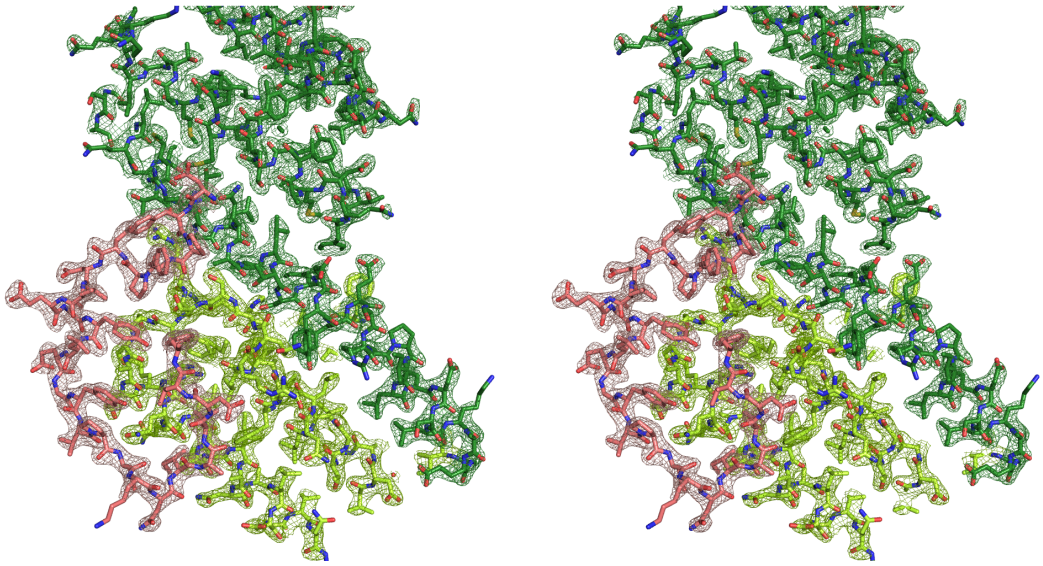

Figure 3-1. A Wall-eyed stereo-view of the Scc3-CopN$_{\Delta 84}$ structure. 2mlFol-DlFcl electron density, displayed at 1.5σ is overlaid on the structure. The map was calculated in Phenix (296). The GBR is shown in salmon and CopN is shown in green. The YopN-like domain is shown in dark green and the TyeA like domain is shown in light green.

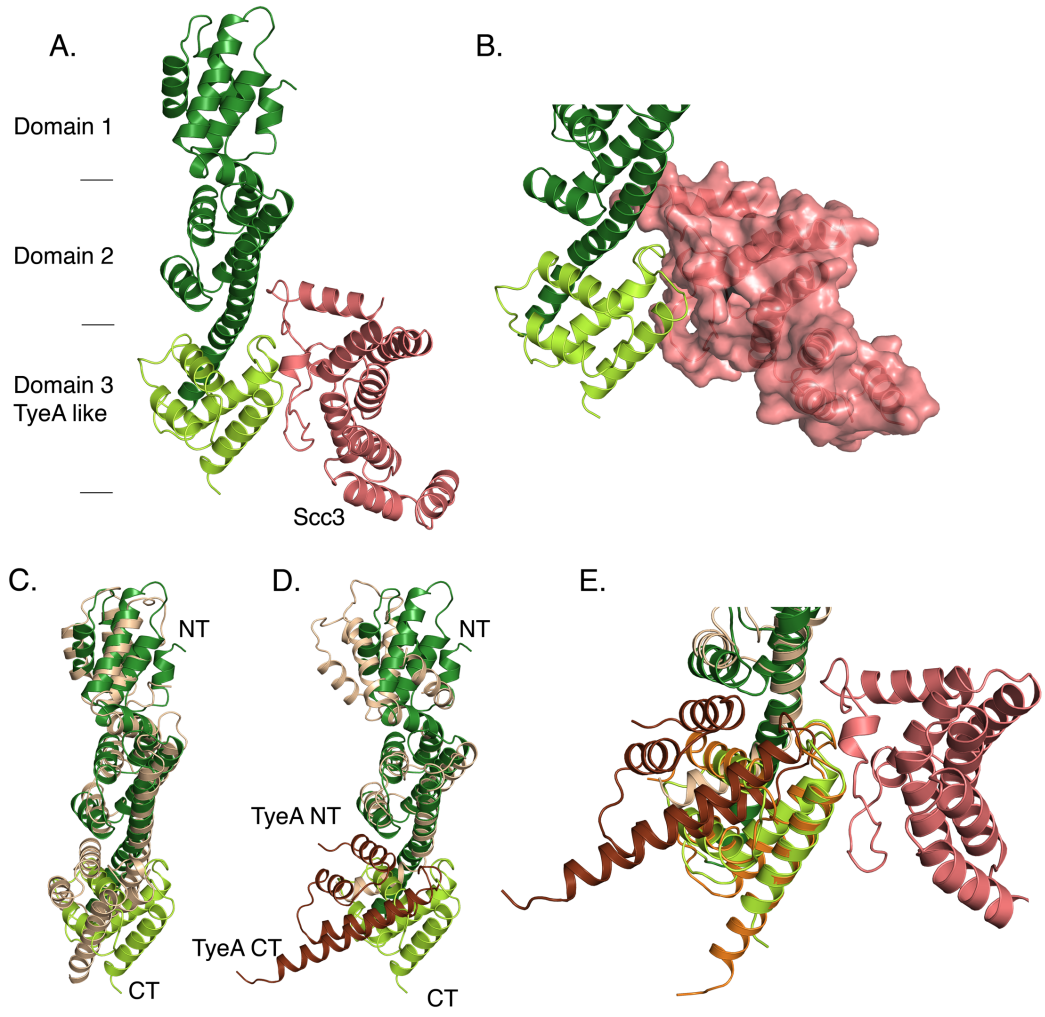

Figure 3-2. Crystal Structure of Scc3-CopN$_{\Delta 84}$. CopN is colored green, with the YopN homology region in dark green and the TyeA homology region in light green. **A.** A ribbon diagram of the Scc3-CopN$_{\Delta 84}$ structure. Approximate domain boundaries are indicated. Scc3, salmon, binds across the domain 2-domain 3 domain interface. **B.** A close-up of the Scc3-CopN$_{\Delta 84}$ interface, oriented as in **A**, with Scc3 shown as a molecular surface. Scc3 forms a relatively flat surface that bridges domains 2 and 3 of CopN$_{\Delta 84}$. **C., D.** Comparisons of CopN and homologs. **C.** Comparison between MxiC and CopN. MxiC is colored tan and shown with thin helices. **D.** Comparison between CopN and the YopN/TyeA complex. YopN is tan and TyeA is brown. YopN and TyeA are and shown with thin helices. **E.** Overlay of TyeA in orientation shown in **D**. and when aligned as a rigid body to the carboxy terminal 91 residues of CopN (rmsd = 0.4 Å).

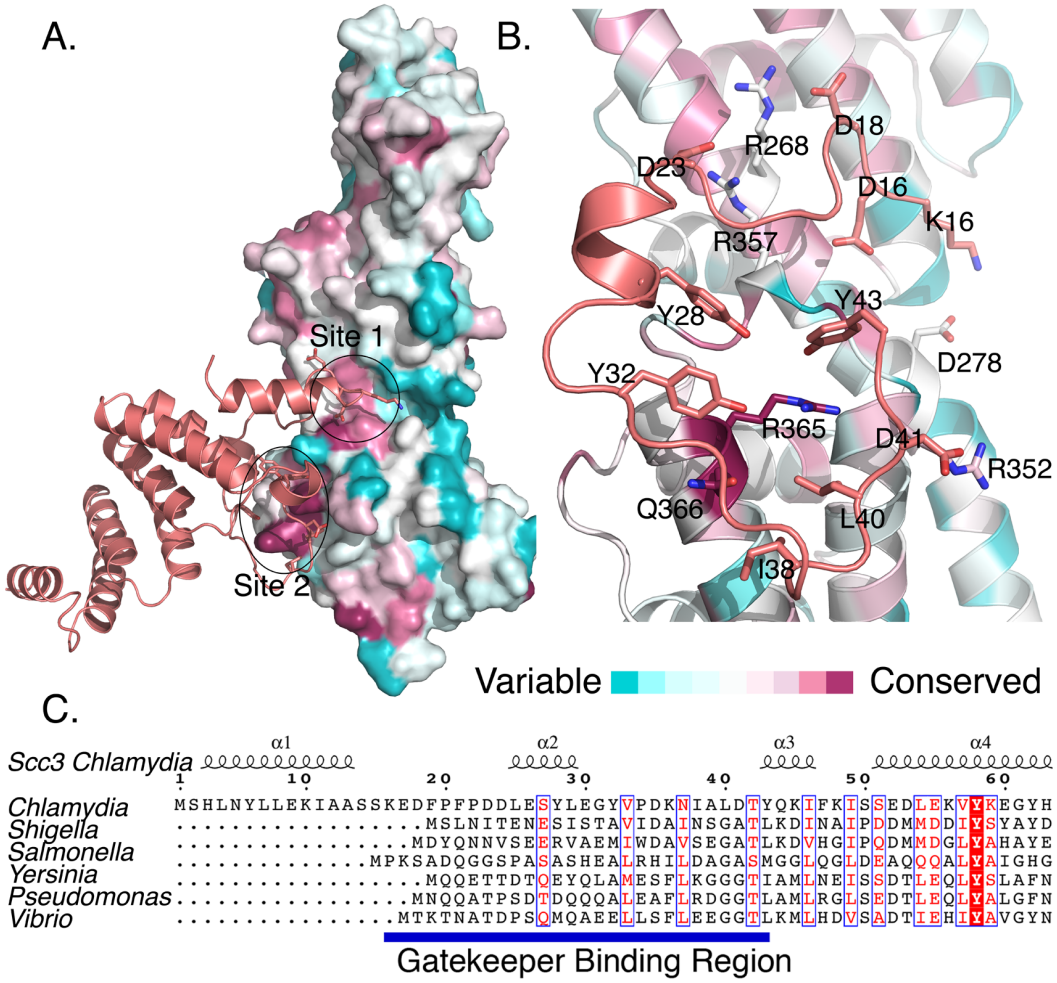

Figure 3-3. A., B. Sequence conservation displayed on the CopN$_{\Delta 84}$ structure (Part 1). Residues are colored by conservation (pink is conserved, blue is variable). **A.** Scc3 interacts with two conserved regions, site 1 and site 2, on CopN. **B.** An expanded view of the CopN-Scc3 interface. For clarity only the GBR region is shown. The interface is primarily composed of hydrophobic residues from Scc3 that surround a conserved arginine (R365) on CopN. **C.** Sequence conservation within GBR's is minimal. Scc3 homologs from multiple species are aligned based on conservation throughout their sequences, revealing that the GBR region is present, but not highly conserved in homologs. Sequences used are from *C. pneumonia, S flexneri, S. enterica, B. pertussis, Y. enterocolitica, P. aeruginosa, V. parahaemolyticus.* Multiple sequences from each genera used in **C**. were used in **A.** and **B**. (see methods).

The Scc3-CopN interface is conserved in other bacteria.

Scc3 engages $CopN_{\Delta 84}$ with residues from the GBR, which bind a contiguous surface on $CopN_{\Delta 84}$. This surface is formed by two distant patches of sequence conservation, region 1 and region 2, and spans the second and third domains of $CopN_{\Delta 84}$, requiring these two domains to be appropriately oriented (Figures 3-1, 3-3, 3-4). In the YopN-TyeA family, the third domain is encoded as a separate protein, such that in these homologs one would predict the interdomain interface recognized by the Scc3 homolog to be a dimer.

Residues 16-23 of Scc3 interact principally with region1 of $CopN_{\Delta 84}$, whereas residues 24-43 form a much larger interface in which Scc3 projects a ring of hydrophobic side chains toward $CopN_{\Delta 84}$ to surround a highly conserved arginine on $CopN_{\Delta 84}$ (Figures 3-3, 3-4). This interaction includes three tyrosines, one of which, Y43 is oriented to allow a π-cation interaction. Peripheral to this ring of hydrophobic residues are a collection of inter-molecular salt bridges (Figure 3-3). The circumscribed arginine is conserved across diverse species, including species with two polypeptide gatekeepers (this residue is an arginine in homologs from *Shigella*, *Vibrio*, *Pseudomonas*, *Bordetella*, and *Yersinia* and glutamine in *Salmonella*) (Figure 3-3). Residues on the CopN side of this interface are better conserved than those on the GBR, despite the fact that they span two proteins in the *Yersinia* architecture and are on the same protein in the architecture presented here (Figure 3-3, 3-5).

To assess the importance of the two binding regions, I disrupted each interaction by mutagenesis. I made an amino terminal 24 amino acid deletion to Scc3 ($Scc3_{\Delta 24}$), which eliminates the GBR-region one interaction. I also mutated the central arginine and two adjacent residues (G369R, A362R, and R365D) in region 2 of $CopN_{\Delta 84}$ ($CopN_{\Delta 84}$-RRD). G369, A362, and R365 are buried by Scc3 and likely solvent exposed in unliganded $CopN_{\Delta 84}$. I introduced charged residues at these sites with the expectation that the solvent

exposed charges would not disturb CopN, but would disrupt the $CopN_{\Delta 84}$-Scc3 complex $CopN_{\Delta 84}$-RRD is stable, as judged by an expression and purification profile similar to $CopN_{\Delta 84}$. As judged by the inability of $Scc3_{\Delta 24}$ to bind $CopN_{\Delta 84}$ and the inability of $CopN_{\Delta 84}$-RRD to bind Scc3 (Figure 3-6), both regions are important for Scc3-$CopN_{\Delta 84}$ complex formation.

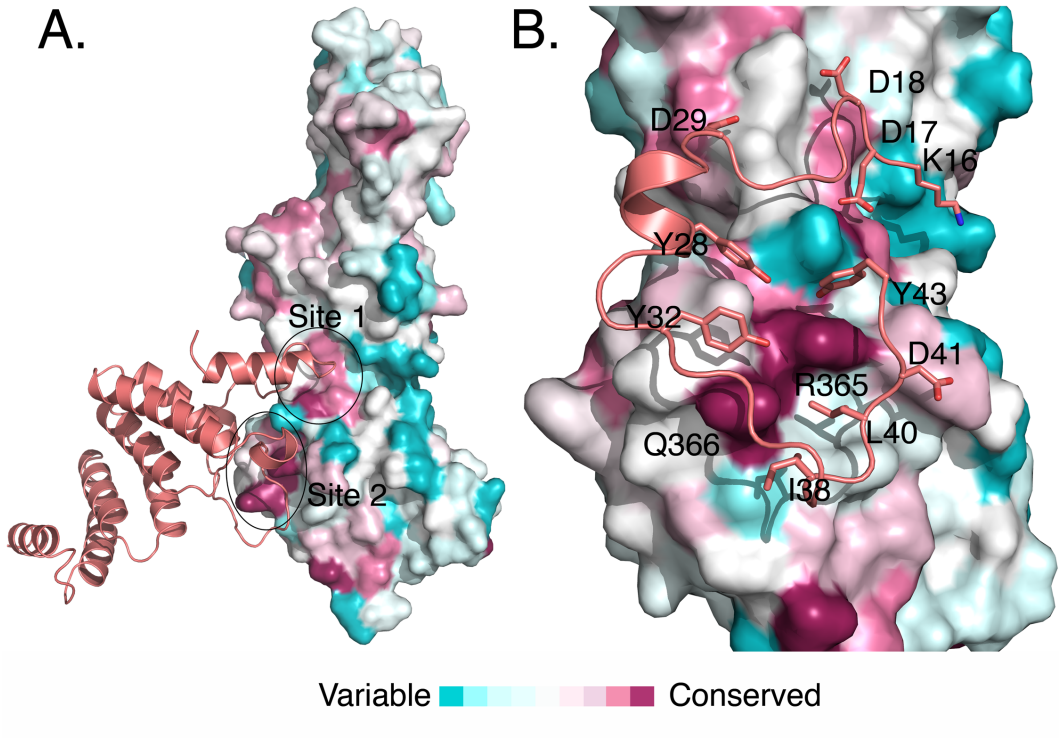

Figure 3-4. Sequence conservation displayed on the CopN$_{\Delta 84}$ structure (Part 2). Residues are colored by conservation (pink is conserved, blue is variable). **A.** Scc3 interacts with two conserved regions, site 1 and site 2, on CopN$_{\Delta 84}$. **B.** An expanded view of the CopN-Scc3 interface showing a surface representation of CopN. For clarity only the GBR region is shown. The interface is primarily composed of hydrophobic residues from Scc3 that surround a conserved arginine (R365) on CopN.

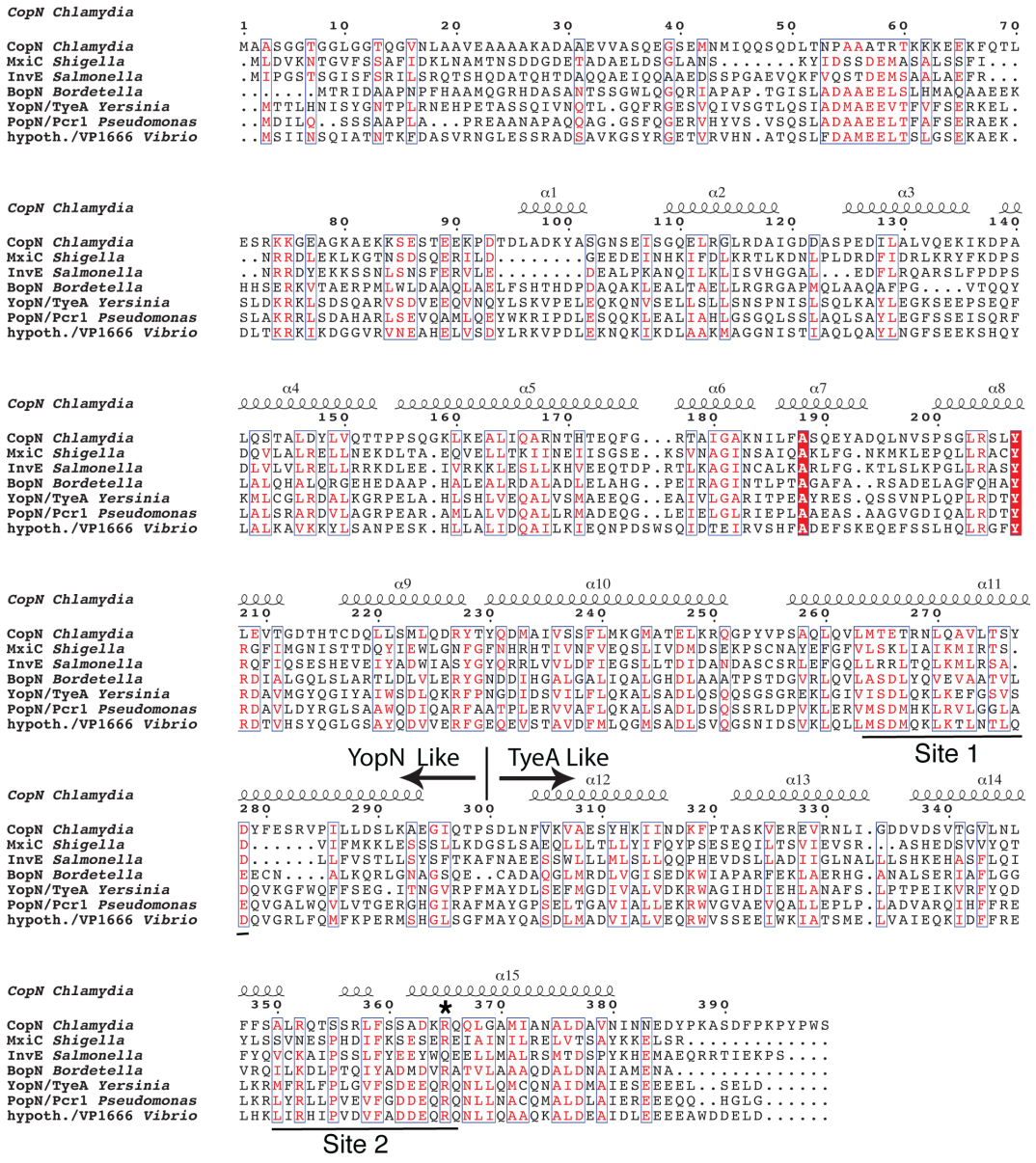

Figure 3-5. A gatekeeper sequence alignment reveals that although sequence identity is limited, the chaperone binding regions are conserved. Representative sequences from six genera of pathogenic bacteria are shown along with the secondary structural elements observed in the CopN structure. As described in the methods, chimeric sequences were generated for the two-component gatekeepers by combining YopN and TyeA fragments. The YopN-TyeA domain boundary, the Scc3 interacting sites, and the highly conserved arginine are labeled. Strictly conserved residues are white on a red background. Residues conserved in 5 of the 7 sequences are red on a white background. Residues conserved in fewer that 5 sequences are black.

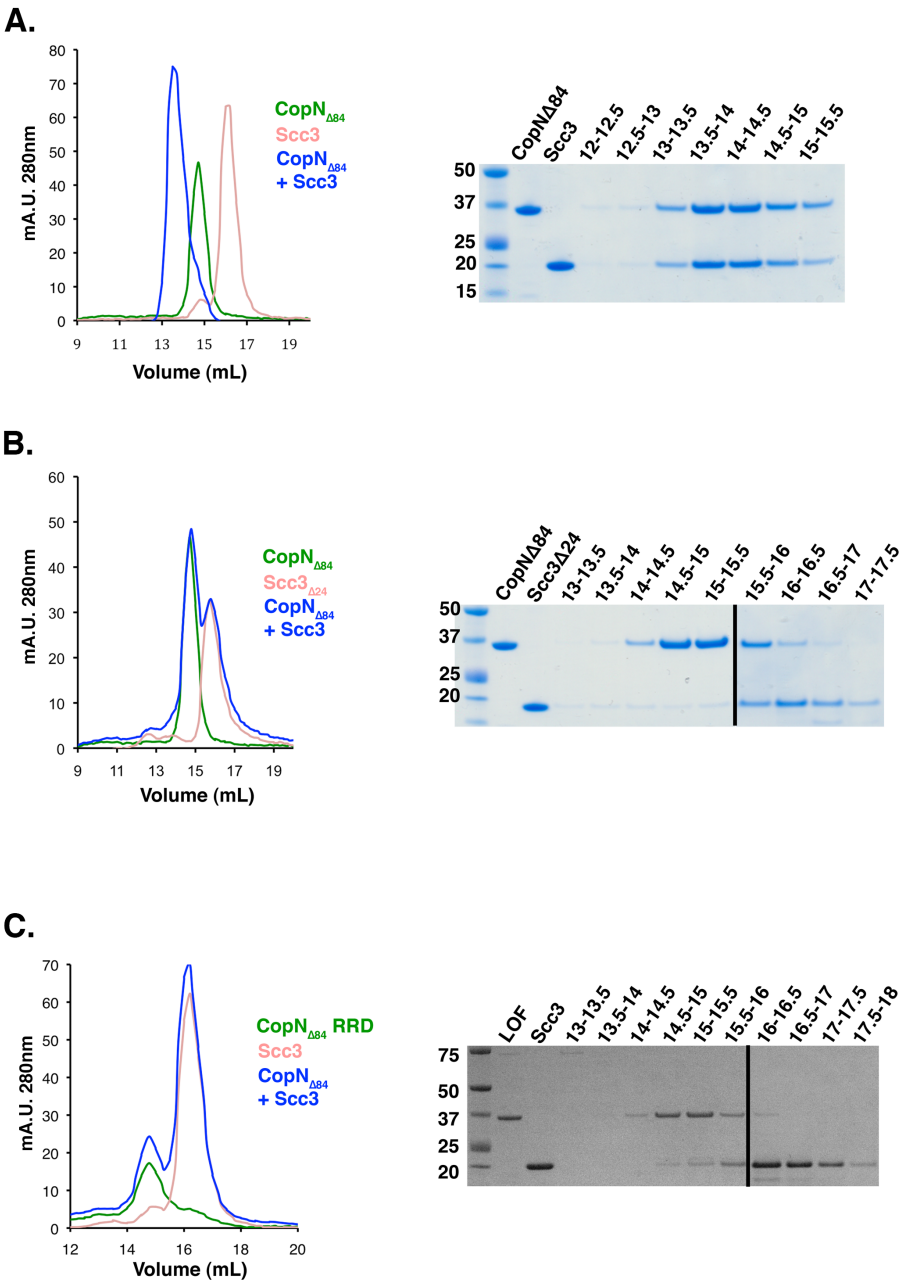

Figure 3-6. CopN-Scc3 binding experiments indicate that both site 1 and site 2 are needed for complex formation. Analytical size exclusion chromatography was used to determine the importance of the two sites of interaction in the CopN-Scc3 complex. **A.** CopNΔ84 binds directly to Scc3 as judged by the shift to a single, faster migrating, peak when both components are present. Both the change in retention time and the presence of both components in the eluted peak, shown in the gel to the right, indicate complex formation. **B.** Deletion of the amino terminal 24 amino acids of Scc3 (Scc3$_{\Delta24}$) disrupts CopN binding as judged the lack of co-migration on the size exclusion chromatography column. **C.** Mutation of site 2 on CopN disrupts Scc3 binding as judged by lack of co-migration on the size exclusion chromatography column. CopN$_{\Delta84}$RRD is mutated at three residues in site 1 (G369R, A362R, and R365D). R365 is the central arginine in site 2.

The translocator-binding site in Scc3 is available in the Scc3-CopN complex.

TPR family proteins are often unfolded when not bound to appropriate ligands and are considered to be somewhat flexible proteins (305,306). Scc3, by contrast appears stable with an appropriately organized binding cleft in the absence of ligand. Structural comparison with other class II chaperones, for which structures have been determined in complex with translocator-derived peptides, indicates that $CopN_{\Delta 84}$ binding causes no significant reorganization of the translocator-binding site (Figure 3-7). The Scc3-$CopN_{\Delta 84}$ binding mode leaves the translocator-binding site on Scc3 unperturbed and available to bind translocators (Figure 3-7). In support of this observation, the purified Scc3-$CopN_{\Delta 84}$ complex is able to directly bind a translocator-derived peptide (presented as residues 158-177 from CopB fused to GST) and form a $CopN_{\Delta 84}$-Scc3-$CopB_{158\text{-}177}$ complex as judged by size exclusion chromatography (Figure 3-7).

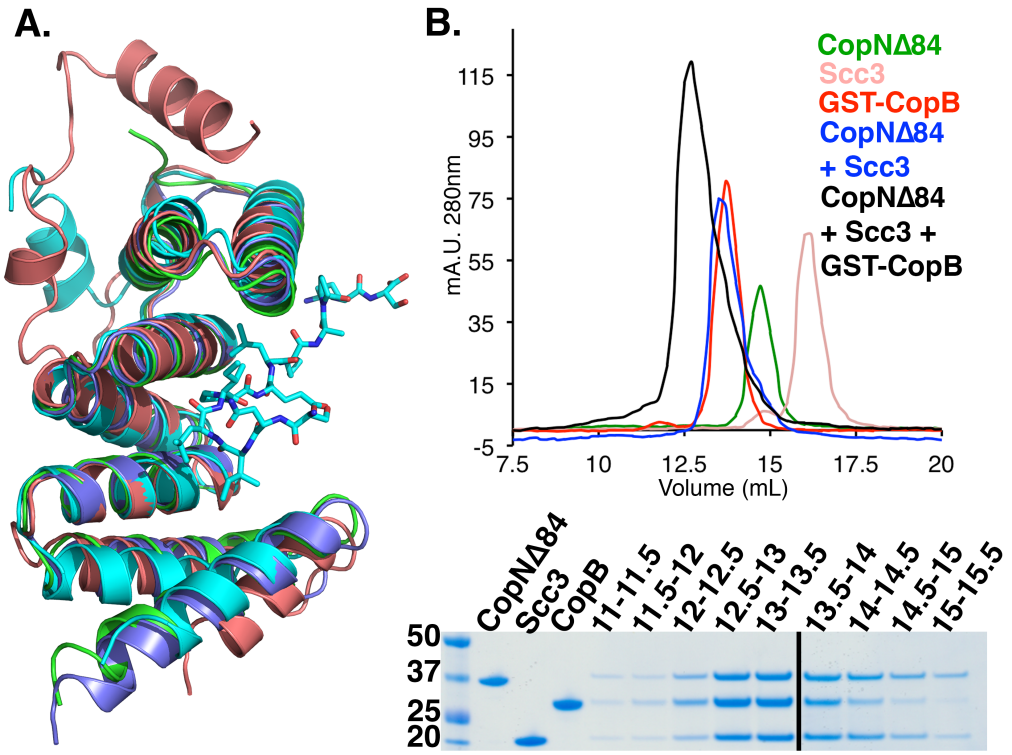

Figure 3-7. The Scc3-CopN$_{\Delta 84}$ complex binds directly to translocators. **A**. An overlay of class II T3S chaperones. All structures except the Scc3 structure were determined bound to translocator peptides. For clarity, only the IpaB peptide from *Shigella* is shown. Scc3 is shown in salmon, IpgC (*Shigella*) in teal, PcrH (*Pseudomonas*) in green, and SycD (*Yersinia*) in blue. The peptide-binding site is conserved and open in Scc3. **B.** CopN-Scc3 complex directly binds to the CopB translocator. Top: size exclusion chromatography traces reveal that the ternary complex is tight enough to survive size exclusion chromatography. Bottom: SDS PAGE confirming complex formation.

Disruption of the Scc3-CopN interface alters secretion in Shigella.

To determine the importance of the gatekeeper-chaperone interaction during T3S, I disrupted the homologous gatekeeper-translocator chaperone interface in *Shigella. Shigella,* unlike *Chlamydia,* are genetically tractable allowing disruption of the endogenous mxiC gene (the copN homolog) and rescue with a plasmid expressing mutant or wild-type MxiC. This is a well-established strategy that has been used to study other MxiC mutants (131,132). The CopN and Scc3 homologs in *Shigella*, MxiC and IpgC, form a complex that includes the T3SS ATPase (132). The Scc3-CopN$_{\Delta 84}$ structure was disrupted by mutation of G369R, A362R, and R365D on CopN (Figure 3-6), supporting the idea that the homologous mutations would disrupt IpgC-MxiC interface. I expressed the E331R/R334D/I338R MxiC mutant (MxiC-RDR) from a plasmid in a previously described mxiC null *Shigella* strain (131) and compared secretion profiles following Congo Red induction. MxiC-RDR is deficient in secretion of the translocators IpaB, IpaC, and IpaD, but efficiently secretes IpaA, an effector, and secretes elevated levels of the effectors OspC1-3 and IpgB (Figure 3-8). IpaA is not secreted efficiently if wild type MxiC is present, but is secreted earlier and in greater quantities ΔMxiC or MxiC-RDR strains (Figure 3-8). The secretion profile of MxiC-RDR closely mimics that of the ΔMxiC strain (Figure 3-8) highlighting the importance of gatekeeper-translocator chaperone complexes in translocator secretion. Similar to CopN, MxiC is both the gatekeeper and a T3S substrate (130,131,196). To verify that the mutations to MxiC did not destabilize MxiC, or otherwise prevent recognition and secretion of MxiC by the T3SS, I evaluated the secretion of MxiC-RDR (Figure 3-8). MxiC-RDR is secreted in a similar manner to MxiC, indicating that the mutations do not disrupt its ability to interact with the T3SS, yet is unable to direct translocators for secretion, and is unable to prevent inappropriately early secretion of IpaA, OspC1-3, and IpgB.

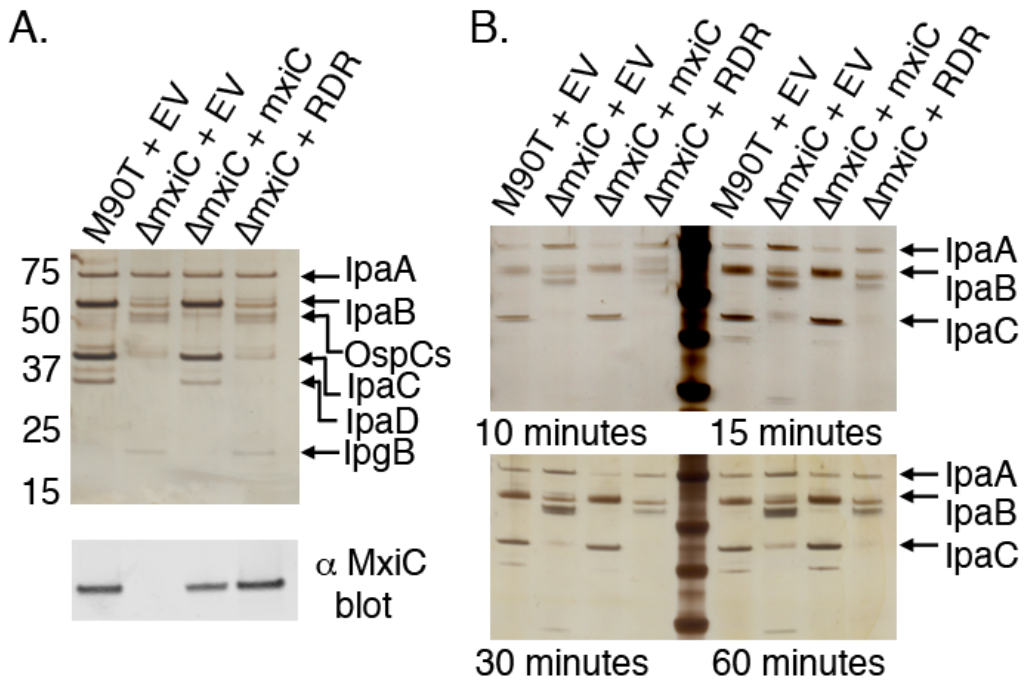

Figure 3-8. The gatekeeper-chaperone complex is needed for efficient translocator secretion. A. T3S was induced from wild type and mxiC mutant *Shigella* strains. M90T is a wild type strain. ΔmxiC is M90T derived, with mxiC deleted (131). EV: empty vector. Strains were complemented with mxiC, mxiC mutant (RDR), or empty vector (EV). Proteins were visualized by silver staining and identified by MS. IpaA, OspCs, and IpgB are effectors. IpaB, IpaC, and IpaD are translocators. Bottom: anti-MxiC blot of the same samples indicates that MxiC and MxiC-RDR are secreted normally. **B.** A secretion time course. The experiment shown in **A.** was repeated and samples taken a 10, 15, 30, and 60 minutes post induction. IpaA, an effector, is not secreted efficiently until ~30 minutes in the presence of MxiC, but in the absence of MxiC or in the presence of only MxiC-RDR it is secreted at ~10 minutes post induction.

Discussion

In this study I have presented the structure of $CopN_{\Delta 84}$ bound to Scc3. This structure provides the first description of a novel interaction for translocator-chaperones, which involves an amino-terminal extension, termed the GBR, binding across the YopN-TyeA-like domain interface in $CopN_{\Delta 84}$. The translocator-chaperone-gatekeeper interaction involves a conserved arginine from the gatekeeper and the amino terminal GBR from the chaperone. Despite the high conservation of the gatekeeper arginine, there is limited sequence conservation within the GBR. Despite this lack of sequence conservation within the chaperone, the presence of a GBR in class II chaperones appears to be conserved (Figure 3-3). Scc3's GBR is ~20 amino acids longer than others, implying that the extensive interactions made to the YopN-like domain are likely unique to the Scc3-$CopN_{\Delta 84}$ complex. Although the unique α1 helix of Scc3 (amino acids 2-15) does not contact CopN, α1 does orient the α1- α2 loop, which contacts CopN. In organisms with shorter GBRs, other T3S apparatus components likely contribute to organizing this interface. This appears to be the case in *Salmonella*, where the gatekeeper interacts with the translocator-chaperone when it is bound to either translocator, but not to the empty chaperone (127). In *Shigella* and *Pseudomonas*, the translocator-chaperones are known to homodimerize using the amino terminus, and translocator binding is necessary to disrupt this dimer (291,304). Although the monomeric chaperone is able to bind translocators, the data suggest a role for the chaperone amino terminus distinct from the role in homodimerization, namely a role in gatekeeper binding. Consistent with previous reports (291,304), I suggest that disruption of chaperone homodimers, by translocator binding, likely occurs prior to chaperone-gatekeeper complex formation.

The binding mode observed in this structure leaves the canonical translocator-binding groove free and available to bind translocators. The Scc3-$CopN_{\Delta 84}$ complex binds

directly to CopB (Figure 3-7), a *Chlamydial* translocator, thus establishing a physical link between the gatekeeper and a translocator. By physically linking gatekeepers and translocators, the temporal order of secretion events (gatekeepers, followed by translocators, and then effectors) is assured. The unusual CopN-Scc3 interface and relatively small buried-surface area (980 $Å^2$) are consistent with the physiological role of this complex, in that the gatekeeper-translocator chaperone must assemble and disassemble each cycle of translocator secretion.

In *Chlamydia* the CopN-Scc3 interaction can be formed with purified proteins, suggestion that it is stronger than in homologous systems, likely because the GBR is longer and complex formation is not prevented by chaperone homodimerization. The precise advantage this affords *Chlamydia* is unclear, but T3S activation may represent an early "committed step" for *Chlamydia* infection. As obligate intracellular pathogens, the need for *Chlamydia* to enter their host subsequent to T3S activation seems absolute. *Chlamydia* are dependent on their hosts for ATP (189) and therefore a T3S event that doesn't result in entry is likely fatal for the bacterium. Consistent with this idea, *Chlamydia* also express a second translocator chaperone, Scc2, which is expressed during late stages of infection, after invasion, and does not bind CopN (234,235).

Mutations shown to disrupt the CopN-Scc3 complex were evaluated in the MxiC-IpgC complex. The highly conserved central arginine and two additional charged residues, located at positions homologous to the sites mutated in CopN, were mutated (E331R/R334D/I338R) on a MxiC expressing plasmid and used to complement a mxiC deletion strain. This mutant MxiC (MxiC-RDR) was expressed and secreted normally, indicating that the mutations did not significantly disrupt MxiC. Strains harboring MxiC-RDR, however, mimicked deletion strains and were both deficient in translocator secretion and secreted elevated levels of effectors, resulting in significant effector secretion at early time points, prior to translocator secretion. These results support the conclusion that a key

function of MxiC during secretion is to scaffold translocators and that the MxiC-IpgC complex is needed for this function. This arrangement, in which assembly of a gatekeeper-chaperone-translocator complex is needed to both promote translocator secretion and to prevent effector secretion indicates that the relevant "plug" that prevents premature effector secretion is the gatekeeper-chaperone-translocator complex. Consistent with this interpretation, disruption of IpaB (a *Shigella* translocator) or MxiC (the gatekeeper) both cause constitutive effector secretion (131).

Collectively, these results support a new mechanism for the translocator-effector hierarchy, outlined in Figure 3-9. I suggest that the translocators are recruited to the T3S pore as a molecular complex including the gatekeeper, translocator-chaperone, and translocator. The entire complex is needed both to promote translocator secretion and to prevent effector secretion. A triggering event from the tip of the T3S needle is known to induce gatekeeper release (131), which through the molecular complex described above is directly linked to translocator secretion. Secretion of the gatekeeper and translocator then allows effector secretion through a gatekeeper independent mechanism, similar to the efficient effector secretion seen in gatekeeper mutants.

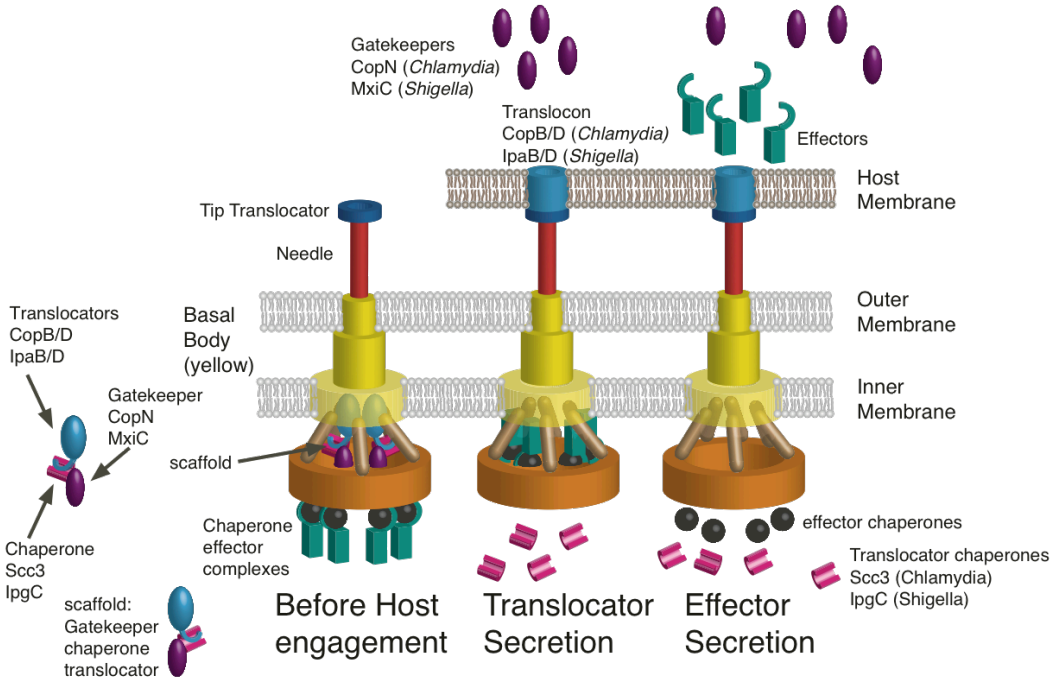

Figure 3-9. A minimal cartoon model for three steps of T3S, highlighting a role for the gatekeeper-chaperone complex in translocator secretion. Before host engagement gatekeeper-chaperone-translocator complexes are bound to the apparatus and prevent secretion of effectors. Upon binding of the apparatus to target membranes the, gatekeeper and pore forming translocators are secreted. The pore forming translocators assemble within the target membrane to form the translocon. After translocator and gatekeeper secretion, the apparatus is able to efficiently secrete effectors, which are secreted through the translocon directly into the host cytosol.

CHAPTER IV

CHLAMYDIA PNEUMONIAE GATEKEEPER PROTEIN, COPN, SEQUESTERS αβ-TUBULIN USING A CONSERVED BASIC FACE.

Introduction

Chlamydiae species are obligate intracellular bacteria that utilize a biphasic life cycle consisting of metabolically inactive elementary bodies (EBs) and metabolically active reticulate bodies (RBs) (191). Infection involves attachment and cellular uptake of EBs and subsequent differentiation into RBs. The RBs remain in endosome-derived membrane vacuoles termed 'inclusions,' which migrate to the microtubule-organizing center (MTOC) in a dynein and microtubule (MT) dependent process (192,193,243). After multiple rounds of bacterial cell division an unknown cue causes the RBs to re-differentiate into infectious EBs and spread to neighboring cells (191). As with many other gram-negative bacteria, *Chlamydia* use a type three secretion system (T3SS) and T3SS effectors to subvert host defenses and reprogram cell processes (188,196,244). A prominent target of these effectors is the host's MT cytoskeleton (185,192,193,243). Alteration of the host MT cytoskeleton is required for proper localization of inclusions to the MTOC and association of inclusions with centromeres (307). Additionally, *Chlamydia* infection disrupts the cell cycle, resulting in delayed cytokinesis and failure to properly segregate sister chromosomes (185,192,253). One effector known to target the MT cytoskeleton is CopN, which is known to bind tubulin, inhibit MT formation, prevent metaphase plate formation, destroy microtubule networks, and cause mitotic arrest (185,186,196). CopN is also a T3SS gatekeeper protein that directs the switch between translocator and effector

secretion (196) (and Archuleta, submitted), raising the question of how effector function is encoded in the presence of other functional constraints.

Type Three Secretion Systems (T3SS) are conserved bacterial protein delivery machines used by many pathogenic Gram-negative bacteria to deliver a diverse group of protein molecules, termed effectors, into cells (245,281-283). The type three secretion (T3S) apparatus is a conserved molecular machine that forms a protein-conducting channel from the bacterial cytosol to the target cell cytosol (Figure 4-1). Major structural components of the T3SS include: a cytosolic-ring complex that includes the ATPase that catalyzes protein unfolding and secretion; a basal-body that forms a pore across both the inner and outer bacterial membranes; a needle complex that extends from the basal-body to the host cell; and a translocon pore formed in the target cell membrane (110,284,286,308).

T3S is regulated in numerous ways, including regulation at the levels of transcription, assembly, and activation (265,285,309,310). A regulatory failsafe, which is conserved across species, involves the gatekeeper proteins, which block the secretion pore until T3S is activated (127,133,181,182). External cues initiate secretion, at which time gatekeepers are secreted and the T3SS becomes active (103,130-132,181,311,312). The exact mechanism by which an external signal is received by the gatekeeper is unknown, but it is known to involve a conformational change in the “Tip translocator” (a translocator that resides at the extracellular tip of the T3S needle), which is transmitted through the inner-rod components of the needle (131,313-316). I have recently shown that the *Chlamydial* gatekeeper, CopN, is also a molecular scaffold that recruits proteins to the T3SS (submitted). These discrete molecular functions are encoded in a ~400 amino acid protein. Gatekeepers interact with translocator chaperones, the C-ring of the T3S, and inner-rod components from the T3S needle (127,130-132,186,234,235). Despite the conservation needed to maintain these functions, gatekeepers have acquired additional

effector functions (184-186). The best studied of these is the microtubule destabilizing function of CopN from *Chlamydia pneumoniae*.

CopN is both the T3SS gatekeeper and a secreted effector protein that causes cell-cycle arrest, binds αβ tubulin, and inhibits microtubule formation (133,185,196,235)(Archuleta, submitted). I have suggested that CopN disrupts microtubules by sequestering αβ tubulin, a mechanism it shares with stathmin, a eukaryotic tubulin binding protein (225,236-239). Unlike stathmin, CopN is a folded protein with a defined and well-ordered tertiary structure (Archuleta, submitted). Further, CopN lacks identifiable tubulin-binding sequences, which are conserved among even highly divergent stathmins, and lacks any detectable sequence identity with stathmins (186,263). CopN and stathmin lack sequence identity or structural similarity, yet both inhibit MT assembly by sequestering free αβ tubulin. Further, CopN and stathmin bind overlapping sites on tubulin as evidenced by competition between the two for tubulin binding sites (186). These data suggest that *Chlamydia* have encoded stathmin-like functions on a structurally unrelated protein.

Methods

Purification of His tagged proteins.

$CopN_{\Delta 84}$ and Scc3, from *C. pneumoniae* AR39, were amplified and cloned into pET28 with an amino-terminal hexa-histadine tag. $CopN_{\Delta 84}$ is an amino terminal 84 amino acid deletion of CopN (186). All CopN variants were made in pET28 using PCR based mutagenesis and verified by sequencing. Proteins were expressed in BL21 *(DE3)* bacteria grown in Luria Broth at 37 ˚C. Bacteria at an optical density (at 600 nm) of ~0.6 were induced at 20˚C with 0.1mM isopropyl β-D-thiogalactopyranoside, and grown for ~12

hours. Cultures were harvested by centrifugation and lysed with a French Press in phosphate buffered saline with ~1 μg/mL chicken egg white lysozyme, ~1 μg/mL bovine pancreatic deoxyribonuclease I, 10 μg/mL leupeptin, 1μM PMSF, 0.7 μg/mL pepstatin. The lysate was clarified by centrifugation and proteins were purified by Co-NTA affinity using Talon resin. TOG1 domain construct 1-272 was overexpressed in E. coli and purified by Ni-affinity and size exclusion chromatography as described previously (317). All eluted proteins were further purified by size exclusion chromatography, superdex 200, before being snap-frozen in liquid nitrogen and stored at -80 ˚C until needed.

Tubulin purification.

Fresh bovine brains were obtained from a local slaughterhouse (C and F Meat Company, College Grove, TN) and tubulin was prepared as described (255), with the only modifications being that 600g of bovine brains rather than 1 Kg of porcine brains were used (buffer volumes were adjusted accordingly) and that the rotors used were a JA-10, Ti-45, and Ti-70.1 rather than SLA 1500, Ti-45, and TLA 100.4 (rotor velocities were adjusted to achieve appropriate g forces). Tubulin was snap-frozen in BRB80 buffer (80mM PIPES, 1mM $MgCl_2$, 1mM EGTA, pH 6.8) in liquid nitrogen and stored at -80 C until needed.

Size exclusion chromatography assays.

CopN homologs, Scc3, Tubulin, and TOG1 binding assays were performed by size exclusion chromatography, using a 24mL Superdex 200 10/300 GL (GE Healthcare), equilibrated in 10mM Tris-HCl pH 7.5, 150mM NaCl, run at 0.5 mL/min, and maintained at 4˚C. Equivalent molar concentrations, determined from calculated extinction coefficients, of proteins were applied to the size exclusion chromatography column. Protein complexes were incubated for 15 minutes prior to analysis.

Tubulin turbidity assays.

Turbidity assays were performed in triplicate in a BioTek Synergy 4 plate reader in 96 well plates. Each assay well included 150μg of tubulin, 3mM GTP, 80mM PIPES, 2mM $MgCl_2$, 0.5mM EGTA, and 30% glycerol in 300μL total volume. Plates were setup on ice, mixed, and transferred to an incubated plate reader maintained at 37˚C, absorbance at 340nm was measured at 45sec intervals, and the plates were shaken for 5sec before each measurement. Data presented are the average of three replicate wells.

Microtubule assembly assays.

To assay Microtubule assembly in the absence or presence of CopNΔ84, we used microtubule 'spindown experiments'. Yeast αβ tubulin (3μM) was polymerized without or with CopNΔ84 (9μM) in assembly buffer (100mM PIPES pH 6.9, 2mM MgSO4, 1mM EGTA, 10% glycerol, 1mM GTP) for 40 minutes at 30˚C. The Assembly reactions were cross-linked by diluting 10-fold into assembly buffer containing 1% glutaraldehyde and incubating 3 minutes at 30 ˚C. Cross-linking was then quenched by 5-fold dilution into assembly buffer containing 25mM Tris pH 6.8. 50μL of the quenched, cross-linked reactions was applied to the top of a glycerol cushion (20% glycerol in BRB80) and spun through the cushion at 22,579xg for 45 minutes at 20˚C (rotor JS13.1) onto poly-lysine coated coverslips. Coverslips were fixed using cold (20˚C) methanol for 3 minutes, blocked with 1mg/ml BSA and stained using FITC-DM1α (Sigma Aldrich). Fluorescence Imaging was performed using an Olympus IX81 Inverted microscope with a 60X objective.

Molecular Modeling.

The molecular models shown in Figure 4-1 were constructed using the program Modeller (318) as implemented in Chimera (319) with the *C. pneumoniae* CopN structure serving as a template for the *C. trachomatis* and *C. psittaci* sequences.

Results

CopN contains a large, conserved, basic face.

The recent crystal structure of CopN bound to Scc3, a chaperone for T3S translocators, has aided efforts to identify the tubulin-binding site on CopN. As described in Chapter III, residues 85-399 of CopN form an elongated helical-cross-bundle structure that is similar to other T3S gatekeepers without any evident tubulin binding appendages. Previous work has indicated that CopN residues 1-84 are not required for tubulin binding, indicating that tubulin binding is encoded by residues resolved in the recently reported structure (186). I have analyzed the CopN structure (pdb code 4NRH) and identified an electro-positive, or basic, surface that I show below includes the binding site for tubulin (Figure 4-1).

Although the amino acid composition of CopN is not remarkable (9.7% Arg+Lys and 13.6% Asp+Glu for the construct used in crystallization), the distribution of charged residues results in one face of CopN being largely basic, while another face is largely acidic (Figure 4-1). Because tubulin is known to use an acidic patch to bind both stathmin and tog domains (239,317), I reasoned that the large basic patch might be functionally important and assessed its conservation within other *Chlamydial* CopN proteins. Using a combination of molecular modeling and sequence alignments, I found that the basic region is indeed conserved, Figure 4-2. CopN from *C. trachomatis* is less effective than CopN from either *C. pneumoniae* or *C. psittaci* (186), at inhibiting tubulin polymerization (186) and consistent with this observation the basic patch on CopN from *C. trachomatis* is less basic, with three basic residues replaced by polar, non-basic, residues (K242N, R250S, R268S). Two of these residues (K242 and R250) map to the center of the basic region, while the third (R268) is adjacent to the Scc3 binding site, Figures 4-1 and 4-2.

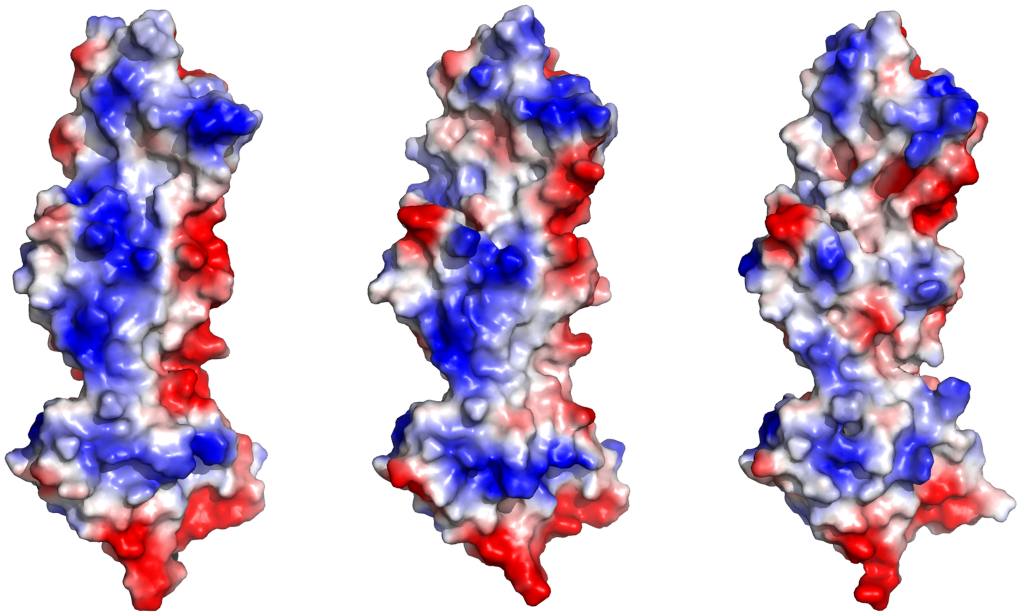

***C. pneumoniae* CopN** ***C. psittaci* CopN** ***C. trachomatis* CopN**

Figure 4-1. The basic face of CopN is conserved between *C. pneumoniae* and *C. psittaci*. The above electrostatic calculated from the structure *of C. pneuomoniae* CopN and models of CopNs from and *C. psittaci and C. trachomatis*. The models were produced using the *C. pneuomoniae* CopN structure and the program Modeller. These electrostatic renderings of each of the CopN homologs show a conserved basic face.

Tubulin binds CopN's basic face.

The CopN-Scc3 structure shows the Scc3 binding site to be distal to these mutations, toward the carboxy-terminal end of CopN (Figure 4-2 A). Scc3, however, binds within the basic face of CopN (Figure 4-2 A,B). I reasoned that tubulin and Scc3 may bind overlapping sites on CopN and assessed competition between Scc3 and tubulin for a binding site on CopN by size exclusion chromatography. As shown in Figure 4-2 C, Scc3 and tubulin both bind CopN and shift the retention time toward a larger complex, a ternary complex, however, cannot be formed, consistent with a shared binding site on CopN for Scc3 and tubulin. Because CopN potently inhibits tubulin polymerization as assayed by light scattering (186) (and Chapter II), I evaluated Scc3 for its ability to restore tubulin polymerization. I added stochiometric quantities of Scc3 to a tubulin polymerization experiment, and as expected from the size exclusion chromatography data, Scc3 restores tubulin polymerization (Figure 4-2 D), likely by binding CopN and preventing CopN from binding tubulin.

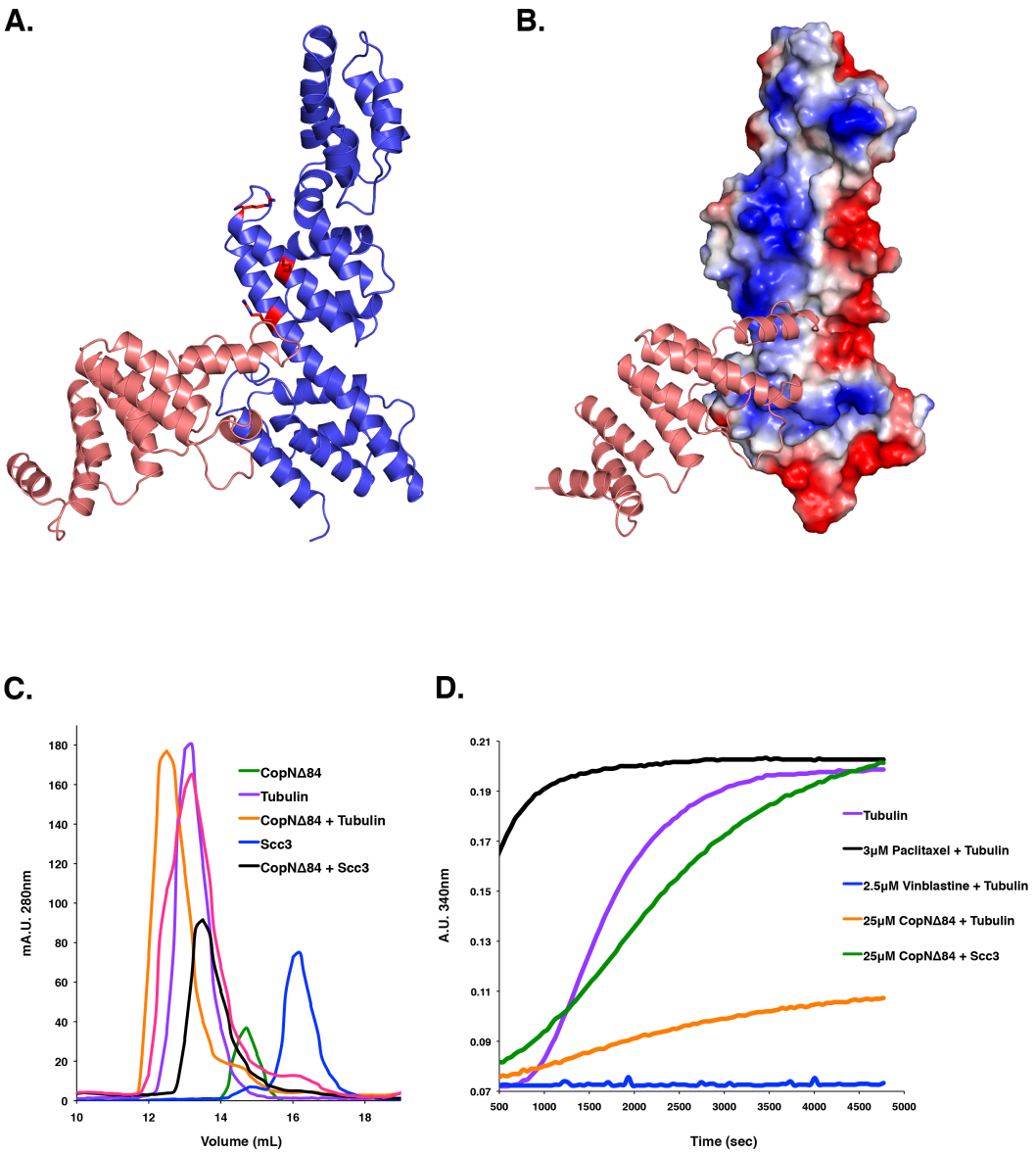

Figure 4-2. Tubulin and Scc3 compete for binding on CopN's basic face. A. A ribbon diagram of the Scc3-CopN$_{\Delta 84}$, CopN in blue and Scc3 in salmon, structure with residues K242, R250, and R268 highlighted in red. This diagram notes Scc3 binding below the highlighted basic residues. **B.** Scc3 binds the distal basic end of CopN. **C.** Tubulin and Scc3 compete for binding to CopN. The size exclusion chromatography traces reveal that the no ternary complex forms when Scc3, tubulin, and CopN are run together, suggesting tubulin and Scc3 compete for binding to CopN. **D.** Tubulin polymerization experiment. Curves represent extent of tubulin polymerization as monitored by light scattering. Controls of Taxol and Vinblastine indicate the dynamic range of the assay. The "Tubulin" curve indicates the expected time course and extent of polymerization for tubulin alone under these conditions (6 μM tubulin, 30% glycerol). CopN inhibits tubulin polymerization, however, addition of Scc3 recovers the tubulin polymerization.

CopN competes with Tog1 for a binding site on tubulin.

Tubulin contains a compatible acidic face, Figure 4-3 B, that I reasoned might bind the basic face of CopN. Using a similar competition binding strategy to that above, I have shown that while CopN and Tog1 from Stu2p both bind tubulin, as assessed by size exclusion chromatography, a ternary complex cannot be formed (Figure 4-3 A). Indicating that they bind overlapping sites, or binding of one induces a conformational change that precludes binding of the other. Complementary binding experiments have already established that CopN and stathmin compete for a similar site on tubulin (186) (and Chapter II), and the stathmin-tubulin and Tog1-tubulin have been determined and both effectors do indeed target the same acidic face of tubulin (Figure 4-3 B). These data, therefore, support the hypothesis that a single acidic patch on tubulin is the binding site for CopN, tog domains, and stathmin.

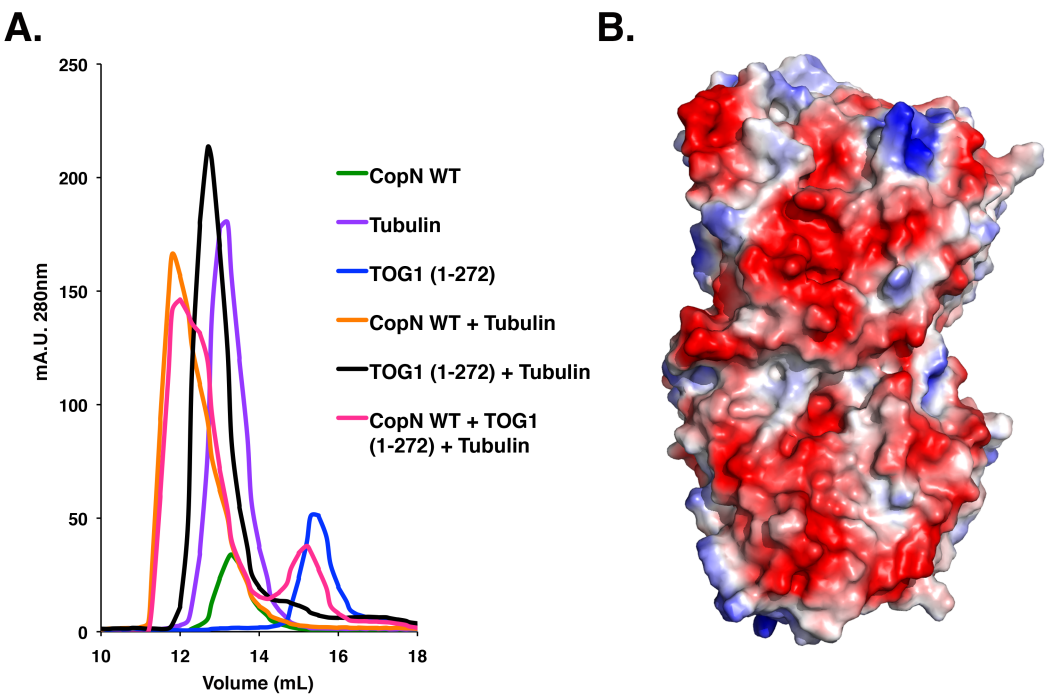

Figure 4-3. CopN competes with Tog1 for a binding site on tubulin's acidic face. A. CopN and TOG1 domain compete for binding to tubulin. The size exclusion chromatography traces reveal that the no ternary complex forms when TOG1, tubulin, and CopN are run together, suggesting TOG1 and CopN compete for binding to tubulin. **B.** An electrostatic rendering model of one αβ heterodimer of tubulin. The model reveals the acidic face of tubulin responsible to CopN and TOG1 binding (317).

Mutation of CopN's basic face disrupts function.

The above results lead us to suggest that the basic face on CopN binds the acidic patch on tubulin. As an alternative test of this hypothesis, I have evaluated mutations designed to disrupt the basic region, but to otherwise not destabilize CopN. Based on the crystal structure I designed K242E/K249E/R250E in which three conserved basic residues are replaced with glutamate. This protein, Δ84CopN-T is stable as judged by its size exclusion chromatography and by its ability to bind Scc3, but is unable to bind tubulin (Figure 4-5 A).

As a final test, I evaluated Δ84CopN-T for its ability to inhibit MT formation in an MT spindown assay. In this tubulin polymerization assay, fluorescently labeled tubulin was incubated with Δ84CopN-T or Δ84CopN and polymerization was initiated by dilution into 10% glycerol containing buffer. Samples were then cross-linked and spun onto microscope slides and MT were viewed in a fluorescent microscope. Under these conditions 9μM Δ84CopN completely abolished MT formation, while an equivalent concentration of Δ84CopN-T had no discernable effect (Figure 4-5 B). The above experiments were preformed by collaborators from the laboratory of Dr. Luke Rice.

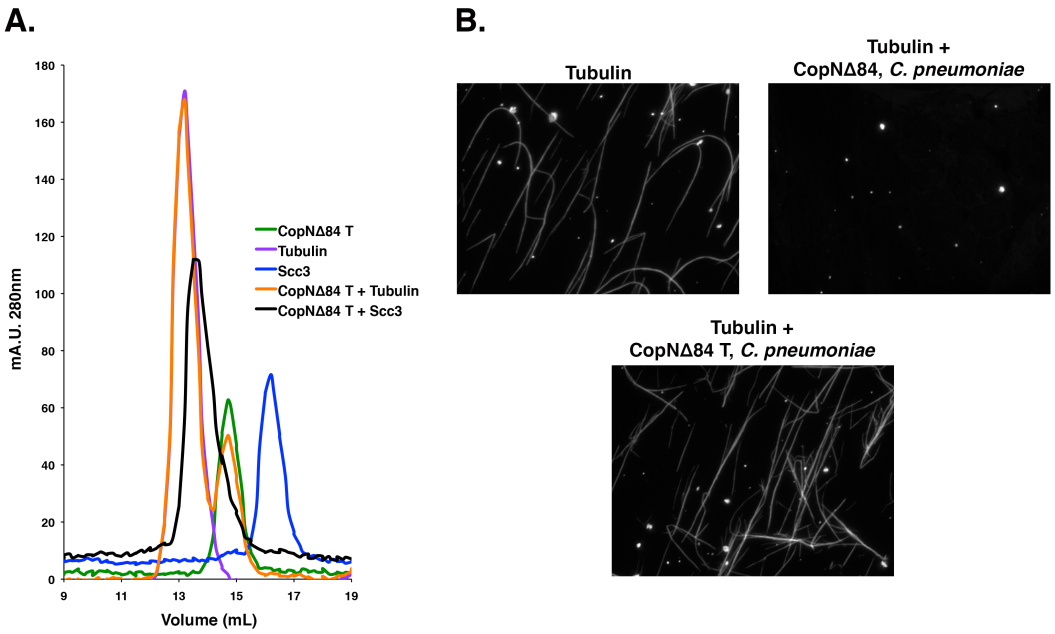

Figure 4-4. Mutation of CopN's basic face disrupts function. **A.** The CopN mutant, CopNΔ84 T, does not bind tubulin. The CopNΔ84T with mutations made at K242E, K249E, and R250E does not bind tubulin, but this tubulin-binding mutant retains the ability to bind Scc3. **B.** CopNΔ84 T has no effect on polymerized tubulin. The three panels show the effects of CopN on polymerized microtubules: the upper left panel is a tubulin alone control; the upper right panel contains tubulin and CopNΔ84 from C. pneumoniae; and the bottom panel contains tubulin and CopNΔ84 T from *C. pneumoniae*. As compared to the control, CopNΔ84 from C. pneumoniae causes disassembly of the microtubule network, upper right panel.

Discussion

CopN is a key component of the *Chlamydial* T3SS, functioning as a molecular scaffold that likely influences the secretion hierarchy (Chapter III), as a gatekeeper that regulates secretion (Chapter III), and as a secreted effector (Chapter II). Encoding these functions on a relatively small protein surface has been accomplished by evolving a tubulin binding site, which appears to be a unique feature of *Chlamydial* gatekeepers, adjacent to the translocator chaperone binding site, which appears to be common across multiple species (Chapter III). While Scc3 and Tubulin bind competitively to their respective binding sites, supporting the idea that the binding sites overlap, this is not likely physiologically important because Scc3 family chaperones are not secreted and tubulin is only present in the host. The ability of one surface to bind two different and unrelated proteins highlights the structural and functional diversity present even in small proteins.

Although CopN bears no structural similarities to other tubulin binding proteins, it appears to target a similar binding site on tubulin. CopN, Stathmin, Tog domains, and Kinesin all appear to bind the same acidic patch on tubulin (236,237,239,317,320). In this regard, CopN mimics cellular tubulin binding proteins. This mimicry is quite remarkable in that CopN disrupts MT assembly, Tog domains typically promote MT assembly, and Kinesin moves along assembled MTs (186,220,321). The different outcomes of binding to this site cannot currently be reconciled, but support the notion that tubulin assembly can be exquisitely regulated by effector proteins.

CHAPTER V

CONCLUSIONS AND FUTURE DIRECTIONS

Conclusions

Chlamydiae species are obligate intracellular pathogens that utilize a type a T3SS to deliver effector proteins and manipulate host cell processes. T3SSs are composed of conserved components; cytosolic components, a needle complex, which forms the conduit for secreted proteins, and translocators, which form the pore in the target cell. While the components that form the T3SS are conserved, the effectors are diverse. Despite T3SS machinery conservation, these proteins can acquire additional functions while maintaining their roles in the T3SS. One such multifunctional protein, CopN, is both T3SS effector and a regulator of secretion (133,185,196,235). CopN is a member of a family of T3SS regulators known as "gatekeeper" proteins that control effector secretion in other organisms. In its effector role, CopN binds free $\alpha\beta$ tubulin and inhibits microtubule polymerization.

Chapter II of this document describes that CopN directly binds αβ tubulin and inhibits tubulin polymerization into MTs. In this chapter, size exclusion chromatography analysis shows CopN binds directly to the class II chaperone, Scc3. Class II chaperones are monomeric all a helical tetricopeptide (TPR) proteins (266-268). Scc3 is similar to SycD from *Yersinia* and IpgC from *Shigella*, both of which are class II chaperones with a TPR fold that binds translocators (266-268). Previous studies show that expression of CopN in eukaryotic cells results in severe alterations in the MT network, including destruction of mitotic spindles (185). In Chapter II, I show that destruction of MTs is caused by CopN directly binding to αβ tubulin. CopN inhibits MT formation, but does not

bind or depolymerize existing MTs. These data suggest that its mechanism of action is through binding of αβ tubulin in a sequestration manner like that of the eukaryotic tubulin binding protein, stathmin (225,236-239).

In Chapter III, I presented the crystal structure of the Scc3-CopN$_{\Delta 84}$, which reveals a CopN-Scc3-translocator scaffold. Experiments in *Shigella* show that this scaffold is necessary for the ordered secretion of translocators before effectors. These data show CopN$_{\Delta 84}$ is structurally similar to other gatekeeper proteins, both MxiC from *Shigella* and the YopN-TyeA complex from *Yersinia*, and Scc3 is structurally similar to other translocator chaperones. The striking result from the Scc3-CopN$_{\Delta 84}$ is the unexpected assembly of the complex and the role of the Scc3 amino terminus in binding CopN$_{\Delta 84}$. The Scc3-CopN$_{\Delta 84}$ complex binds directly to the *Chlamydial* translocator, CopB, establishing a physical link between the gatekeeper and translocator. The mutations shown to disrupt the CopN-Scc3 complex were evaluated in the MxiC-IpgC complex in *Shigella*, and these data indicated that strains containing the mutations mimicked a deletion strain and were both deficient in translocator secretion and secreted elevated levels of effectors, resulting in significant effector secretion at early time points, prior to translocator secretion.

Finally in Chapter IV, I present data that indicates CopN basic face binds tubulin's acidic face. Structural studies of CopN revealed a basic face in which Scc3 binds to the distal end. This basic face is conserved between CopN homologs. In addition to sequence conservation, binding assays between Scc3 and tubulin show a ternary complex cannot be formed with CopN, Scc3, and tubulin. Also, turbidity assays reveal CopN no longer has an inhibitory effect on tubulin polymerization when Scc3 is added to the same experiment. Further mutagenesis to conserved residues on CopN show a loss of tubulin binding via size exclusion chromatography and MT spindown assays.

Future Directions

Determine a high-resolution crystallographic structure of the CopN-tubulin complex.

A crystallographic structure of the CopN + tubulin complex will give information regarding how CopN engages and sequesters tubulin. Previous studies show which residues are required for tubulin binding, however, it would be interesting to find other residues involved in tubulin sequestration. In my attempts to crystallize the CopN-tubulin complex has resulted in small unusable crystals for data collection (Figure 5-1). These crystals will either need to be optimized using CopNΔ84+bovine tubulin, or, a better strategy, using a CopNΔ84 + unpolymerizable yeast tubulin (317). In addition, this structure will aid in future studies done to move forward with a drug discovery screen. The structure will allow for us to see how a drug might disrupt the binding of CopN to tubulin.

Determine a high-resolution crystallographic structure of the CopN-Scc3-CopB complex.

Along with optimizing the co-crystals of CopN + tubulin, optimization of the CopN-Scc3-CopB complex crystals should also occur. The crystals that I have currently obtained diffract to ~ 3-3.5Å. Further optimization is required because although these crystals are improved in resolution relative to the initial crystals, diffraction is highly mosaic and anisotropic. These problems prevent data processing. In addition to determining the structure of the CopN-Scc3-CopB complex, we would like to determine potential therapeutics for inhibiting the interaction between the gatekeeper, CopN, and the translocator scaffold. These assays would be accomplished via a high throughput screening assay.

Determine the role and location of CopN during Chlamydial infection.

Finally, a long-term goal is to determine CopN's role in infection. This body of work identifies CopN as an effector that sequesters αβ tubulin in the eukaryotic cell, but it is still unclear why and when CopN achieves its purpose. For example, is CopN's purpose to shut down cell cycle regulation at a particular time during infection? Where is CopN localized in the eukaryotic host? These are difficult questions to answer given the evasive life cycle of *Chlamydia*, however, and will be answered require genetic tools.

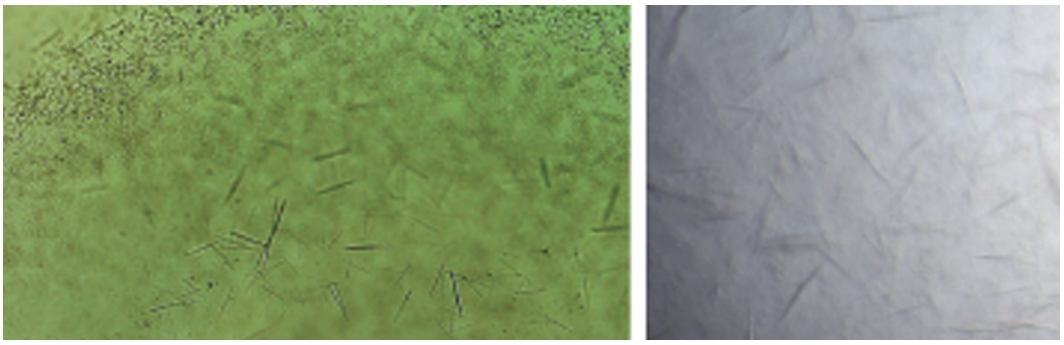

Figure 5-1. Crystallization of the CopN+tubulin complex. The above panels are examples of micro-crystals I was able to grow. These crystals are too small for data acquisition. These crystals must be grown larger in order to collect diffraction data.

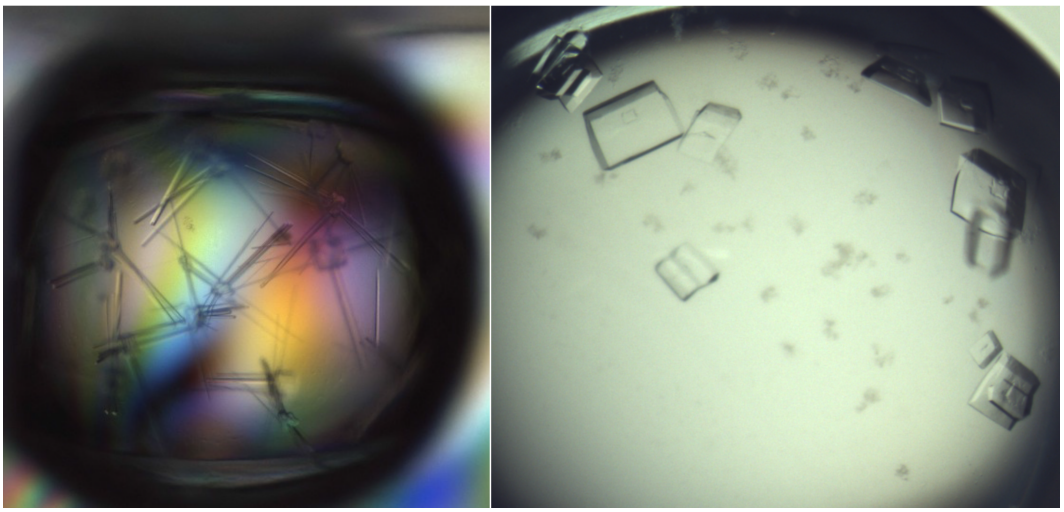

Figure 5-2. Crystallization of the tertiary complex between CopN+Scc3+CopB. The above panels are examples of current crystal form of the CopN+Scc3+CopB complex. These crystals require further optimization for better diffraction quality data. I have been able to able to optimize these crystals, which currently diffract to ~ 3-3.5Å. However, I am unable to index the diffraction data, suggesting the crystals are not single.

LIST OF PUBLICATIONS

Archuleta TL, Du Y, English CA, Lory S, Lesser C, Ohi MD, Ohi R, Spiller BW. The Chlamydia effector chlamydial outer protein N (CopN) sequesters tubulin and prevents microtubule assembly. J Biol Chem. 2011;286(39):33992-8. Epub 2011/08/16. doi: M111.258426 [pii] 10.1074/jbc.M111.258426. PubMed PMID: 21841198; PubMed Central PMCID: PMC3190796.

Archuleta TL, Spiller BW. A gatekeeper chaperone complex directs translocator secretion during type three secretion. Proc Natl Acad Sci U S A, Submitted.

Archuleta TL, Spiller BW. *Chlamydia pneumoniae* gatekeeper protein, CopN, sequesters αβ-tubulin using a conserved basic face. In preparation.

BIBLIOGRAPHY

1. Gram, C. (1884) Uber die isolirte Ffirbung der Schizomyceten in Schnitt-und Trockenpraparaten. *Fortschr. Med.*, **2**, 185-189.

2. Organization, W.H. (2008). World Health Organization, Vol. 2014.

3. Canton, R. and Bryan, J. (2012) Global antimicrobial resistance: from surveillance to stewardship. Part 1: surveillance and risk factors for resistance. *Expert review of anti-infective therapy*, **10**, 1269-1271.

4. Peleg, A.Y. and Hooper, D.C. (2010) Hospital-acquired infections due to gram-negative bacteria. *The New England journal of medicine*, **362**, 1804-1813.

5. U.S. Department of Health and Human Services: Center for Disease Control and Prevention. (September 16, 2013). Center for Disease Control and Prevention, 1600 Clifton Rd. Atlanta, GA 30333, USA, Vol. 2014.

6. Boucher, H.W., Talbot, G.H., Bradley, J.S., Edwards, J.E., Gilbert, D., Rice, L.B., Scheld, M., Spellberg, B. and Bartlett, J. (2009) Bad bugs, no drugs: no ESKAPE! An update from the Infectious Diseases Society of America. *Clin Infect Dis*, **48**, 1-12.

7. Hidron, A.I., Edwards, J.R., Patel, J., Horan, T.C., Sievert, D.M., Pollock, D.A., Fridkin, S.K., National Healthcare Safety Network, T. and Participating National Healthcare Safety Network, F. (2008) NHSN annual update: antimicrobial-resistant pathogens associated with healthcare-associated infections: annual summary of data reported to the National Healthcare Safety Network at the Centers for Disease Control and Prevention, 2006-2007. *Infection control and hospital epidemiology : the official journal of the Society of Hospital Epidemiologists of America*, **29**, 996-1011.

8. Gaynes, R., Edwards, J.R. and National Nosocomial Infections Surveillance, S. (2005) Overview of nosocomial infections caused by gram-negative bacilli. *Clin Infect Dis*, **41**, 848-854.

9. Roberts, R.R., Hota, B., Ahmad, I., Scott, R.D., 2nd, Foster, S.D., Abbasi, F., Schabowski, S., Kampe, L.M., Ciavarella, G.G., Supino, M. *et al.* (2009) Hospital and societal costs of antimicrobial-resistant infections in a Chicago teaching hospital: implications for antibiotic stewardship. *Clin Infect Dis*, **49**, 1175-1184.

10. Antibiotics, A.f.t.P.U.o. (September 2010). Alliance for the Prudent Use of Antibiotics, 200 Harrison Ave, Posner 3 (Business), Boston, MA, 02111, Vol. 2014.

11. Galan, J.E. (2009) Common themes in the design and function of bacterial effectors. *Cell host & microbe*, **5**, 571-579.

12. Dean, P. (2011) Functional domains and motifs of bacterial type III effector proteins and their roles in infection. *FEMS microbiology reviews*, **35**, 1100-1125.

13. Troisfontaines, P. and Cornelis, G.R. (2005) Type III secretion: more systems than you think. *Physiology*, **20**, 326-339.

14. Kostakioti, M., Newman, C.L., Thanassi, D.G. and Stathopoulos, C. (2005) Mechanisms of protein export across the bacterial outer membrane. *J Bacteriol*, **187**, 4306-4314.

15. Leo, J.C., Grin, I. and Linke, D. (2012) Type V secretion: mechanism(s) of autotransport through the bacterial outer membrane. *Philosophical transactions of the Royal Society of London. Series B, Biological sciences*, **367**, 1088-1101.

16. Silverman, J.M., Austin, L.S., Hsu, F., Hicks, K.G., Hood, R.D. and Mougous, J.D. (2011) Separate inputs modulate phosphorylation-dependent and -independent type VI secretion activation. *Mol Microbiol*, **82**, 1277-1290.

17. Abdallah, A.M., Gey van Pittius, N.C., Champion, P.A., Cox, J., Luirink, J., Vandenbroucke-Grauls, C.M., Appelmelk, B.J. and Bitter, W. (2007) Type VII secretion--mycobacteria show the way. *Nature reviews. Microbiology*, **5**, 883-891.

18. Fronzes, R., Christie, P.J. and Waksman, G. (2009) The structural biology of type IV secretion systems. *Nature reviews. Microbiology*, **7**, 703-714.

19. Douzi, B., Filloux, A. and Voulhoux, R. (2012) On the path to uncover the bacterial type II secretion system. *Philosophical transactions of the Royal Society of London. Series B, Biological sciences*, **367**, 1059-1072.

20. Christie, P.J., Whitaker, N. and Gonzalez-Rivera, C. (2014) Mechanism and structure of the bacterial type IV secretion systems. *Biochimica et biophysica acta*.

21. Henderson, I.R., Navarro-Garcia, F., Desvaux, M., Fernandez, R.C. and Ala'Aldeen, D. (2004) Type V protein secretion pathway: the autotransporter story. *Microbiol Mol Biol Rev*, **68**, 692-744.

22. Beckwith, J. (2013) The Sec-dependent pathway. *Res Microbiol*, **164**, 497-504.

23. Danese, P.N. and Silhavy, T.J. (1998) Targeting and assembly of periplasmic and outer-membrane proteins in Escherichia coli. *Annual review of genetics*, **32**, 59-94.

24. Wickner, W., Driessen, A.J. and Hartl, F.U. (1991) The enzymology of protein translocation across the Escherichia coli plasma membrane. *Annual review of biochemistry*, **60**, 101-124.

25. Osborne, A.R., Rapoport, T.A. and van den Berg, B. (2005) Protein translocation by the Sec61/SecY channel. *Annu Rev Cell Dev Biol*, **21**, 529-550.

26. de Keyzer, J., van der Does, C. and Driessen, A.J. (2003) The bacterial translocase: a dynamic protein channel complex. *Cellular and molecular life sciences : CMLS*, **60**, 2034-2052.

27. Driessen, A.J. (2001) SecB, a molecular chaperone with two faces. *Trends Microbiol*, **9**, 193-196.

28. Van den Berg, B., Clemons, W.M., Jr., Collinson, I., Modis, Y., Hartmann, E., Harrison, S.C. and Rapoport, T.A. (2004) X-ray structure of a protein-conducting channel. *Nature*, **427**, 36-44.

29. Berks, B.C. (1996) A common export pathway for proteins binding complex redox cofactors? *Mol Microbiol*, **22**, 393-404.

30. Santini, C.L., Ize, B., Chanal, A., Muller, M., Giordano, G. and Wu, L.F. (1998) A novel sec-independent periplasmic protein translocation pathway in Escherichia coli. *EMBO J*, **17**, 101-112.

31. Berks, B.C., Palmer, T. and Sargent, F. (2005) Protein targeting by the bacterial twin-arginine translocation (Tat) pathway. *Curr Opin Microbiol*, **8**, 174-181.

32. Weiner, J.H., Bilous, P.T., Shaw, G.M., Lubitz, S.P., Frost, L., Thomas, G.H., Cole, J.A. and Turner, R.J. (1998) A novel and ubiquitous system for membrane targeting and secretion of cofactor-containing proteins. *Cell*, **93**, 93-101.

33. Saltikov, C.W. and Newman, D.K. (2003) Genetic identification of a respiratory arsenate reductase. *Proc Natl Acad Sci U S A*, **100**, 10983-10988.

34. Seshadri, R., Adrian, L., Fouts, D.E., Eisen, J.A., Phillippy, A.M., Methe, B.A., Ward, N.L., Nelson, W.C., Deboy, R.T., Khouri, H.M. *et al.* (2005) Genome sequence of the PCE-dechlorinating bacterium Dehalococcoides ethenogenes. *Science*, **307**, 105-108.

35. John, M., Schmitz, R.P., Westermann, M., Richter, W. and Diekert, G. (2006) Growth substrate dependent localization of tetrachloroethene reductive dehalogenase in Sulfurospirillum multivorans. *Archives of microbiology*, **186**, 99-106.

36. Mackman, N., Nicaud, J.M., Gray, L. and Holland, I.B. (1985) Identification of polypeptides required for the export of haemolysin 2001 from E. coli. *Molecular & general genetics : MGG*, **201**, 529-536.

37. Linhartova, I., Bumba, L., Masin, J., Basler, M., Osicka, R., Kamanova, J., Prochazkova, K., Adkins, I., Hejnova-Holubova, J., Sadilkova, L. *et al.* (2010) RTX proteins: a highly diverse family secreted by a common mechanism. *FEMS microbiology reviews*, **34**, 1076-1112.

38. Kanonenberg, K., Schwarz, C.K. and Schmitt, L. (2013) Type I secretion systems - a story of appendices. *Res Microbiol*, **164**, 596-604.

39. Zaitseva, J., Jenewein, S., Jumpertz, T., Holland, I.B. and Schmitt, L. (2005) H662 is the linchpin of ATP hydrolysis in the nucleotide-binding domain of the ABC transporter HlyB. *EMBO J*, **24**, 1901-1910.

40. Holland, I.B., Schmitt, L. and Young, J. (2005) Type 1 protein secretion in bacteria, the ABC-transporter dependent pathway (review). *Molecular membrane biology*, **22**, 29-39.

41. Davidson, A.L., Dassa, E., Orelle, C. and Chen, J. (2008) Structure, function, and evolution of bacterial ATP-binding cassette systems. *Microbiol Mol Biol Rev*, **72**, 317-364, table of contents.

42. Jones, P.M., O'Mara, M.L. and George, A.M. (2009) ABC transporters: a riddle wrapped in a mystery inside an enigma. *Trends in biochemical sciences*, **34**, 520-531.

43. Hollenstein, K., Dawson, R.J. and Locher, K.P. (2007) Structure and mechanism of ABC transporter proteins. *Current opinion in structural biology*, **17**, 412-418.

44. Oswald, C., Holland, I.B. and Schmitt, L. (2006) The motor domains of ABC-transporters. What can structures tell us? *Naunyn-Schmiedeberg's archives of pharmacology*, **372**, 385-399.

45. Smith, P.C., Karpowich, N., Millen, L., Moody, J.E., Rosen, J., Thomas, P.J. and Hunt, J.F. (2002) ATP binding to the motor domain from an ABC transporter drives formation of a nucleotide sandwich dimer. *Mol Cell*, **10**, 139-149.

46. Chen, J., Lu, G., Lin, J., Davidson, A.L. and Quiocho, F.A. (2003) A tweezers-like motion of the ATP-binding cassette dimer in an ABC transport cycle. *Mol Cell*, **12**, 651-661.

47. Havarstein, L.S., Diep, D.B. and Nes, I.F. (1995) A family of bacteriocin ABC transporters carry out proteolytic processing of their substrates concomitant with export. *Mol Microbiol*, **16**, 229-240.

48. Wu, K.H. and Tai, P.C. (2004) Cys32 and His105 are the critical residues for the calcium-dependent cysteine proteolytic activity of CvaB, an ATP-binding cassette transporter. *J Biol Chem*, **279**, 901-909.

49. Duquesne, S., Destoumieux-Garzon, D., Peduzzi, J. and Rebuffat, S. (2007) Microcins, gene-encoded antibacterial peptides from enterobacteria. *Natural product reports*, **24**, 708-734.

50. Duquesne, S., Petit, V., Peduzzi, J. and Rebuffat, S. (2007) Structural and functional diversity of microcins, gene-encoded antibacterial peptides from enterobacteria. *Journal of molecular microbiology and biotechnology*, **13**, 200-209.

51. Ishii, S., Yano, T., Ebihara, A., Okamoto, A., Manzoku, M. and Hayashi, H. (2010) Crystal structure of the peptidase domain of Streptococcus ComA, a bifunctional ATP-binding cassette transporter involved in the quorum-sensing pathway. *J Biol Chem*, **285**, 10777-10785.

52. Lecher, J., Schwarz, C.K., Stoldt, M., Smits, S.H., Willbold, D. and Schmitt, L. (2012) An RTX transporter tethers its unfolded substrate during secretion via a unique N-terminal domain. *Structure*, **20**, 1778-1787.

53. Sandkvist, M., Michel, L.O., Hough, L.P., Morales, V.M., Bagdasarian, M., Koomey, M., DiRita, V.J. and Bagdasarian, M. (1997) General secretion pathway (eps) genes required for toxin secretion and outer membrane biogenesis in Vibrio cholerae. *J Bacteriol*, **179**, 6994-7003.

54. Lu, H.M., Mizushima, S. and Lory, S. (1993) A periplasmic intermediate in the extracellular secretion pathway of Pseudomonas aeruginosa exotoxin A. *J Bacteriol*, **175**, 7463-7467.

55. Zalewska-Piatek, B., Bury, K., Piatek, R., Bruzdziak, P. and Kur, J. (2008) Type II secretory pathway for surface secretion of DraD invasin from the uropathogenic Escherichia coli Dr+ strain. *J Bacteriol*, **190**, 5044-5056.

56. Horstman, A.L. and Kuehn, M.J. (2002) Bacterial surface association of heat-labile enterotoxin through lipopolysaccharide after secretion via the general secretory pathway. *J Biol Chem*, **277**, 32538-32545.

57. Shi, L., Deng, S., Marshall, M.J., Wang, Z., Kennedy, D.W., Dohnalkova, A.C., Mottaz, H.M., Hill, E.A., Gorby, Y.A., Beliaev, A.S. *et al.* (2008) Direct involvement of type II secretion system in extracellular translocation of Shewanella oneidensis outer membrane cytochromes MtrC and OmcA. *J Bacteriol*, **190**, 5512-5516.

58. Nguyen, B.D. and Valdivia, R.H. (2012) Virulence determinants in the obligate intracellular pathogen Chlamydia trachomatis revealed by forward genetic approaches. *Proc Natl Acad Sci U S A*, **109**, 1263-1268.

59. Pugsley, A.P. (1992) Translocation of a folded protein across the outer membrane in Escherichia coli. *Proc Natl Acad Sci U S A*, **89**, 12058-12062.

60. Jones, H.E., Holland, I.B. and Campbell, A.K. (2002) Direct measurement of free Ca(2+) shows different regulation of Ca(2+) between the periplasm and the cytosol of Escherichia coli. *Cell calcium*, **32**, 183-192.

61. Pauwels, K., Lustig, A., Wyns, L., Tommassen, J., Savvides, S.N. and Van Gelder, P. (2006) Structure of a membrane-based steric chaperone in complex with its lipase substrate. *Nature structural & molecular biology*, **13**, 374-375.

62. Mikami, B., Iwamoto, H., Malle, D., Yoon, H.J., Demirkan-Sarikaya, E., Mezaki, Y. and Katsuya, Y. (2006) Crystal structure of pullulanase: evidence for parallel binding of oligosaccharides in the active site. *J Mol Biol*, **359**, 690-707.

63. Creze, C., Castang, S., Derivery, E., Haser, R., Hugouvieux-Cotte-Pattat, N., Shevchik, V.E. and Gouet, P. (2008) The crystal structure of pectate lyase peli from soft rot pathogen Erwinia chrysanthemi in complex with its substrate. *J Biol Chem*, **283**, 18260-18268.

64. Filloux, A., Bally, M., Ball, G., Akrim, M., Tommassen, J. and Lazdunski, A. (1990) Protein secretion in gram-negative bacteria: transport across the outer membrane involves common mechanisms in different bacteria. *EMBO J*, **9**, 4323-4329.

65. Filloux, A., Michel, G. and Bally, M. (1998) GSP-dependent protein secretion in gram-negative bacteria: the Xcp system of Pseudomonas aeruginosa. *FEMS microbiology reviews*, **22**, 177-198.

66. Peabody, C.R., Chung, Y.J., Yen, M.R., Vidal-Ingigliardi, D., Pugsley, A.P. and Saier, M.H., Jr. (2003) Type II protein secretion and its relationship to bacterial type IV pili and archaeal flagella. *Microbiology*, **149**, 3051-3072.

67. Cianciotto, N.P. (2005) Type II secretion: a protein secretion system for all seasons. *Trends Microbiol*, **13**, 581-588.

68. Pugsley, A.P. (1993) The complete general secretory pathway in gram-negative bacteria. *Microbiological reviews*, **57**, 50-108.

69. Bleves, S., Lazdunski, A. and Filloux, A. (1996) Membrane topology of three Xcp proteins involved in exoprotein transport by Pseudomonas aeruginosa. *J Bacteriol*, **178**, 4297-4300.

70. Michel, G., Bleves, S., Ball, G., Lazdunski, A. and Filloux, A. (1998) Mutual stabilization of the XcpZ and XcpY components of the secretory apparatus in Pseudomonas aeruginosa. *Microbiology*, **144 (Pt 12)**, 3379-3386.

71. Py, B., Loiseau, L. and Barras, F. (2001) An inner membrane platform in the type II secretion machinery of Gram-negative bacteria. *EMBO Rep*, **2**, 244-248.

72. Arts, J., de Groot, A., Ball, G., Durand, E., El Khattabi, M., Filloux, A., Tommassen, J. and Koster, M. (2007) Interaction domains in the Pseudomonas aeruginosa type II secretory apparatus component XcpS (GspF). *Microbiology*, **153**, 1582-1592.

73. Johnson, T.L., Abendroth, J., Hol, W.G. and Sandkvist, M. (2006) Type II secretion: from structure to function. *FEMS Microbiol Lett*, **255**, 175-186.

74. Brok, R., Van Gelder, P., Winterhalter, M., Ziese, U., Koster, A.J., de Cock, H., Koster, M., Tommassen, J. and Bitter, W. (1999) The C-terminal domain of the Pseudomonas secretin XcpQ forms oligomeric rings with pore activity. *J Mol Biol*, **294**, 1169-1179.

75. Nouwen, N., Ranson, N., Saibil, H., Wolpensinger, B., Engel, A., Ghazi, A. and Pugsley, A.P. (1999) Secretin PulD: association with pilot PulS, structure, and ion-conducting channel formation. *Proc Natl Acad Sci U S A*, **96**, 8173-8177.

76. Reichow, S.L., Korotkov, K.V., Hol, W.G. and Gonen, T. (2010) Structure of the cholera toxin secretion channel in its closed state. *Nature structural & molecular biology*, **17**, 1226-1232.

77. Korotkov, K.V., Pardon, E., Steyaert, J. and Hol, W.G. (2009) Crystal structure of the N-terminal domain of the secretin GspD from ETEC determined with the assistance of a nanobody. *Structure*, **17**, 255-265.

78. Korotkov, K.V., Gonen, T. and Hol, W.G. (2011) Secretins: dynamic channels for protein transport across membranes. *Trends in biochemical sciences*, **36**, 433-443.

79. Bally, M., Filloux, A., Akrim, M., Ball, G., Lazdunski, A. and Tommassen, J. (1992) Protein secretion in Pseudomonas aeruginosa: characterization of seven xcp genes and processing of secretory apparatus components by prepilin peptidase. *Mol Microbiol*, **6**, 1121-1131.

80. Nunn, D. (1999) Bacterial type II protein export and pilus biogenesis: more than just homologies? *Trends in cell biology*, **9**, 402-408.

81. Nunn, D.N. and Lory, S. (1993) Cleavage, methylation, and localization of the Pseudomonas aeruginosa export proteins XcpT, -U, -V, and -W. *J Bacteriol*, **175**, 4375-4382.

82. Sauvonnet, N., Vignon, G., Pugsley, A.P. and Gounon, P. (2000) Pilus formation and protein secretion by the same machinery in Escherichia coli. *EMBO J*, **19**, 2221-2228.

83. Camberg, J.L. and Sandkvist, M. (2005) Molecular analysis of the Vibrio cholerae type II secretion ATPase EpsE. *J Bacteriol*, **187**, 249-256.

84. Patrick, M., Korotkov, K.V., Hol, W.G. and Sandkvist, M. (2011) Oligomerization of EpsE coordinates residues from multiple subunits to facilitate ATPase activity. *J Biol Chem*, **286**, 10378-10386.

85. Filloux, A. (2004) The underlying mechanisms of type II protein secretion. *Biochimica et biophysica acta*, **1694**, 163-179.

86. Hobbs, M. and Mattick, J.S. (1993) Common components in the assembly of type 4 fimbriae, DNA transfer systems, filamentous phage and protein-secretion apparatus: a general system for the formation of surface-associated protein complexes. *Mol Microbiol*, **10**, 233-243.

87. Shevchik, V.E., Robert-Baudouy, J. and Condemine, G. (1997) Specific interaction between OutD, an Erwinia chrysanthemi outer membrane protein of the general secretory pathway, and secreted proteins. *EMBO J*, **16**, 3007-3016.

88. Galan, J.E. and Curtiss, R., 3rd. (1989) Cloning and molecular characterization of genes whose products allow Salmonella typhimurium to penetrate tissue culture cells. *Proc Natl Acad Sci U S A*, **86**, 6383-6387.

89. Galan, J.E., Ginocchio, C. and Costeas, P. (1992) Molecular and functional characterization of the Salmonella invasion gene invA: homology of InvA to members of a new protein family. *J Bacteriol*, **174**, 4338-4349.

90. Salmond, G.P. and Reeves, P.J. (1993) Membrane traffic wardens and protein secretion in gram-negative bacteria. *Trends in biochemical sciences*, **18**, 7-12.

91. Altmeyer, R.M., McNern, J.K., Bossio, J.C., Rosenshine, I., Finlay, B.B. and Galan, J.E. (1993) Cloning and molecular characterization of a gene involved in Salmonella adherence and invasion of cultured epithelial cells. *Mol Microbiol*, **7**, 89-98.

92. Kaniga, K., Bossio, J.C. and Galan, J.E. (1994) The Salmonella typhimurium invasion genes invF and invG encode homologues of the AraC and PulD family of proteins. *Mol Microbiol*, **13**, 555-568.

93. Burkinshaw, B.J. and Strynadka, N.C. (2014) Assembly and structure of the T3SS. *Biochimica et biophysica acta*.

94. Pozidis, C., Chalkiadaki, A., Gomez-Serrano, A., Stahlberg, H., Brown, I., Tampakaki, A.P., Lustig, A., Sianidis, G., Politou, A.S., Engel, A. *et al.* (2003) Type

III protein translocase: HrcN is a peripheral ATPase that is activated by oligomerization. *J Biol Chem*, **278**, 25816-25824.

95. Akeda, Y. and Galan, J.E. (2004) Genetic analysis of the Salmonella enterica type III secretion-associated ATPase InvC defines discrete functional domains. *J Bacteriol*, **186**, 2402-2412.

96. Imada, K., Minamino, T., Tahara, A. and Namba, K. (2007) Structural similarity between the flagellar type III ATPase FliI and F1-ATPase subunits. *Proc Natl Acad Sci U S A*, **104**, 485-490.

97. Zarivach, R., Vuckovic, M., Deng, W., Finlay, B.B. and Strynadka, N.C. (2007) Structural analysis of a prototypical ATPase from the type III secretion system. *Nature structural & molecular biology*, **14**, 131-137.

98. Lorenzini, E., Singer, A., Singh, B., Lam, R., Skarina, T., Chirgadze, N.Y., Savchenko, A. and Gupta, R.S. (2010) Structure and protein-protein interaction studies on Chlamydia trachomatis protein CT670 (YscO Homolog). *J Bacteriol*, **192**, 2746-2756.

99. Ibuki, T., Imada, K., Minamino, T., Kato, T., Miyata, T. and Namba, K. (2011) Common architecture of the flagellar type III protein export apparatus and F- and V-type ATPases. *Nature structural & molecular biology*, **18**, 277-282.

100. Stebbins, C.E. and Galan, J.E. (2001) Maintenance of an unfolded polypeptide by a cognate chaperone in bacterial type III secretion. *Nature*, **414**, 77-81.

101. Birtalan, S.C., Phillips, R.M. and Ghosh, P. (2002) Three-dimensional secretion signals in chaperone-effector complexes of bacterial pathogens. *Mol Cell*, **9**, 971-980.

102. Phan, J., Tropea, J.E. and Waugh, D.S. (2004) Structure of the Yersinia pestis type III secretion chaperone SycH in complex with a stable fragment of YscM2. *Acta crystallographica. Section D, Biological crystallography*, **60**, 1591-1599.

103. Schubot, F.D., Jackson, M.W., Penrose, K.J., Cherry, S., Tropea, J.E., Plano, G.V. and Waugh, D.S. (2005) Three-dimensional structure of a macromolecular assembly that regulates type III secretion in Yersinia pestis. *J Mol Biol*, **346**, 1147-1161.

104. Lilic, M., Vujanac, M. and Stebbins, C.E. (2006) A common structural motif in the binding of virulence factors to bacterial secretion chaperones. *Mol Cell*, **21**, 653-664.

105. Vujanac, M. and Stebbins, C.E. (2013) Context-dependent protein folding of a virulence peptide in the bacterial and host environments: structure of an SycH-YopH chaperone-effector complex. *Acta crystallographica. Section D, Biological crystallography*, **69**, 546-554.

106. Radics, J., Konigsmaier, L. and Marlovits, T.C. (2014) Structure of a pathogenic type 3 secretion system in action. *Nature structural & molecular biology*, **21**, 82-87.

107. Dohlich, K., Zumsteg, A.B., Goosmann, C. and Kolbe, M. (2014) A substrate-fusion protein is trapped inside the Type III Secretion System channel in Shigella flexneri. *PLoS Pathog*, **10**, e1003881.

108. Kubori, T., Matsushima, Y., Nakamura, D., Uralil, J., Lara-Tejero, M., Sukhan, A., Galan, J.E. and Aizawa, S.I. (1998) Supramolecular structure of the Salmonella typhimurium type III protein secretion system. *Science*, **280**, 602-605.

109. Marlovits, T.C., Kubori, T., Sukhan, A., Thomas, D.R., Galan, J.E. and Unger, V.M. (2004) Structural insights into the assembly of the type III secretion needle complex. *Science*, **306**, 1040-1042.

110. Hodgkinson, J.L., Horsley, A., Stabat, D., Simon, M., Johnson, S., da Fonseca, P.C., Morris, E.P., Wall, J.S., Lea, S.M. and Blocker, A.J. (2009) Three-dimensional reconstruction of the Shigella T3SS transmembrane regions reveals 12-fold symmetry and novel features throughout. *Nature structural & molecular biology*, **16**, 477-485.

111. Schraidt, O. and Marlovits, T.C. (2011) Three-dimensional model of Salmonella's needle complex at subnanometer resolution. *Science*, **331**, 1192-1195.

112. Bergeron, J.R., Worrall, L.J., Sgourakis, N.G., DiMaio, F., Pfuetzner, R.A., Felise, H.B., Vuckovic, M., Yu, A.C., Miller, S.I., Baker, D. *et al.* (2013) A refined model of the prototypical Salmonella SPI-1 T3SS basal body reveals the molecular basis for its assembly. *PLoS Pathog*, **9**, e1003307.

113. Kawamoto, A., Morimoto, Y.V., Miyata, T., Minamino, T., Hughes, K.T., Kato, T. and Namba, K. (2013) Common and distinct structural features of Salmonella injectisome and flagellar basal body. *Scientific reports*, **3**, 3369.

114. Kudryashev, M., Stenta, M., Schmelz, S., Amstutz, M., Wiesand, U., Castano-Diez, D., Degiacomi, M.T., Munnich, S., Bleck, C.K., Kowal, J. *et al.* (2013) In situ structural analysis of the Yersinia enterocolitica injectisome. *eLife*, **2**, e00792.

115. Tamano, K., Aizawa, S., Katayama, E., Nonaka, T., Imajoh-Ohmi, S., Kuwae, A., Nagai, S. and Sasakawa, C. (2000) Supramolecular structure of the Shigella type III secretion machinery: the needle part is changeable in length and essential for delivery of effectors. *EMBO J*, **19**, 3876-3887.

116. Kubori, T., Sukhan, A., Aizawa, S.I. and Galan, J.E. (2000) Molecular characterization and assembly of the needle complex of the Salmonella typhimurium type III protein secretion system. *Proc Natl Acad Sci U S A*, **97**, 10225-10230.

117. Kimbrough, T.G. and Miller, S.I. (2000) Contribution of Salmonella typhimurium type III secretion components to needle complex formation. *Proc Natl Acad Sci U S A*, **97**, 11008-11013.

118. Hakansson, S., Schesser, K., Persson, C., Galyov, E.E., Rosqvist, R., Homble, F. and Wolf-Watz, H. (1996) The YopB protein of Yersinia pseudotuberculosis is essential for the translocation of Yop effector proteins across the target cell plasma

membrane and displays a contact-dependent membrane disrupting activity. *EMBO J*, **15**, 5812-5823.

119. Blocker, A., Gounon, P., Larquet, E., Niebuhr, K., Cabiaux, V., Parsot, C. and Sansonetti, P. (1999) The tripartite type III secreton of Shigella flexneri inserts IpaB and IpaC into host membranes. *The Journal of cell biology*, **147**, 683-693.

120. Schoehn, G., Di Guilmi, A.M., Lemaire, D., Attree, I., Weissenhorn, W. and Dessen, A. (2003) Oligomerization of type III secretion proteins PopB and PopD precedes pore formation in Pseudomonas. *EMBO J*, **22**, 4957-4967.

121. Creasey, E.A., Delahay, R.M., Daniell, S.J. and Frankel, G. (2003) Yeast two-hybrid system survey of interactions between LEE-encoded proteins of enteropathogenic Escherichia coli. *Microbiology*, **149**, 2093-2106.

122. Marlovits, T.C., Kubori, T., Lara-Tejero, M., Thomas, D., Unger, V.M. and Galan, J.E. (2006) Assembly of the inner rod determines needle length in the type III secretion injectisome. *Nature*, **441**, 637-640.

123. Wagner, S., Konigsmaier, L., Lara-Tejero, M., Lefebre, M., Marlovits, T.C. and Galan, J.E. (2010) Organization and coordinated assembly of the type III secretion export apparatus. *Proc Natl Acad Sci U S A*, **107**, 17745-17750.

124. Diepold, A., Amstutz, M., Abel, S., Sorg, I., Jenal, U. and Cornelis, G.R. (2010) Deciphering the assembly of the Yersinia type III secretion injectisome. *EMBO J*, **29**, 1928-1940.

125. Diepold, A., Wiesand, U. and Cornelis, G.R. (2011) The assembly of the export apparatus (YscR,S,T,U,V) of the Yersinia type III secretion apparatus occurs independently of other structural components and involves the formation of an YscV oligomer. *Mol Microbiol*, **82**, 502-514.

126. Kresse, A.U., Beltrametti, F., Muller, A., Ebel, F. and Guzman, C.A. (2000) Characterization of SepL of enterohemorrhagic Escherichia coli. *J Bacteriol*, **182**, 6490-6498.

127. Kubori, T. and Galan, J.E. (2002) Salmonella type III secretion-associated protein InvE controls translocation of effector proteins into host cells. *J Bacteriol*, **184**, 4699-4708.

128. O'Connell, C.B., Creasey, E.A., Knutton, S., Elliott, S., Crowther, L.J., Luo, W., Albert, M.J., Kaper, J.B., Frankel, G. and Donnenberg, M.S. (2004) SepL, a protein required for enteropathogenic Escherichia coli type III translocation, interacts with secretion component SepD. *Mol Microbiol*, **52**, 1613-1625.

129. Deng, W., Li, Y., Hardwidge, P.R., Frey, E.A., Pfuetzner, R.A., Lee, S., Gruenheid, S., Strynakda, N.C., Puente, J.L. and Finlay, B.B. (2005) Regulation of type III secretion hierarchy of translocators and effectors in attaching and effacing bacterial pathogens. *Infect Immun*, **73**, 2135-2146.

130. Botteaux, A., Sory, M.P., Biskri, L., Parsot, C. and Allaoui, A. (2009) MxiC is secreted by and controls the substrate specificity of the Shigella flexneri type III secretion apparatus. *Mol Microbiol*, **71**, 449-460.

131. Martinez-Argudo, I. and Blocker, A.J. (2010) The Shigella T3SS needle transmits a signal for MxiC release, which controls secretion of effectors. *Mol Microbiol*, **78**, 1365-1378.

132. Cherradi, Y., Schiavolin, L., Moussa, S., Meghraoui, A., Meksem, A., Biskri, L., Azarkan, M., Allaoui, A. and Botteaux, A. (2013) Interplay between predicted inner-rod and gatekeeper in controlling substrate specificity of the type III secretion system. *Mol Microbiol*, **87**, 1183-1199.

133. Pallen, M.J., Beatson, S.A. and Bailey, C.M. (2005) Bioinformatics analysis of the locus for enterocyte effacement provides novel insights into type-III secretion. *BMC Microbiol*, **5**, 9.

134. Sukhan, A., Kubori, T., Wilson, J. and Galan, J.E. (2001) Genetic analysis of assembly of the Salmonella enterica serovar Typhimurium type III secretion-associated needle complex. *J Bacteriol*, **183**, 1159-1167.

135. Cascales, E. and Christie, P.J. (2003) The versatile bacterial type IV secretion systems. *Nature reviews. Microbiology*, **1**, 137-149.

136. Alvarez-Martinez, C.E. and Christie, P.J. (2009) Biological diversity of prokaryotic type IV secretion systems. *Microbiol Mol Biol Rev*, **73**, 775-808.

137. Juhas, M., van der Meer, J.R., Gaillard, M., Harding, R.M., Hood, D.W. and Crook, D.W. (2009) Genomic islands: tools of bacterial horizontal gene transfer and evolution. *FEMS microbiology reviews*, **33**, 376-393.

138. Baron, C. (2005) From bioremediation to biowarfare: on the impact and mechanism of type IV secretion systems. *FEMS Microbiol Lett*, **253**, 163-170.

139. Nagai, H. and Kubori, T. (2011) Type IVB Secretion Systems of Legionella and Other Gram-Negative Bacteria. *Frontiers in microbiology*, **2**, 136.

140. Backert, S. and Clyne, M. (2011) Pathogenesis of Helicobacter pylori infection. *Helicobacter*, **16 Suppl 1**, 19-25.

141. Fischer, W. (2011) Assembly and molecular mode of action of the Helicobacter pylori Cag type IV secretion apparatus. *FEBS J*, **278**, 1203-1212.

142. Llosa, M., Roy, C. and Dehio, C. (2009) Bacterial type IV secretion systems in human disease. *Mol Microbiol*, **73**, 141-151.

143. Pena, A., Matilla, I., Martin-Benito, J., Valpuesta, J.M., Carrascosa, J.L., de la Cruz, F., Cabezon, E. and Arechaga, I. (2012) The hexameric structure of a conjugative VirB4 protein ATPase provides new insights for a functional and phylogenetic relationship with DNA translocases. *J Biol Chem*, **287**, 39925-39932.

144. Cascales, E. and Christie, P.J. (2004) Definition of a bacterial type IV secretion pathway for a DNA substrate. *Science*, **304**, 1170-1173.

145. Lang, S., Kirchberger, P.C., Gruber, C.J., Redzej, A., Raffl, S., Zellnig, G., Zangger, K. and Zechner, E.L. (2011) An activation domain of plasmid R1 TraI protein delineates stages of gene transfer initiation. *Mol Microbiol*, **82**, 1071-1085.

146. Jose, J., Jahnig, F. and Meyer, T.F. (1995) Common structural features of IgA1 protease-like outer membrane protein autotransporters. *Mol Microbiol*, **18**, 378-380.

147. Desvaux, M., Parham, N.J. and Henderson, I.R. (2004) Type V protein secretion: simplicity gone awry? *Current issues in molecular biology*, **6**, 111-124.

148. Sijbrandi, R., Urbanus, M.L., ten Hagen-Jongman, C.M., Bernstein, H.D., Oudega, B., Otto, B.R. and Luirink, J. (2003) Signal recognition particle (SRP)-mediated targeting and Sec-dependent translocation of an extracellular Escherichia coli protein. *J Biol Chem*, **278**, 4654-4659.

149. Ieva, R. and Bernstein, H.D. (2009) Interaction of an autotransporter passenger domain with BamA during its translocation across the bacterial outer membrane. *Proc Natl Acad Sci U S A*, **106**, 19120-19125.

150. Ruiz-Perez, F., Henderson, I.R., Leyton, D.L., Rossiter, A.E., Zhang, Y. and Nataro, J.P. (2009) Roles of periplasmic chaperone proteins in the biogenesis of serine protease autotransporters of Enterobacteriaceae. *J Bacteriol*, **191**, 6571-6583.

151. Ruiz-Perez, F., Henderson, I.R. and Nataro, J.P. (2010) Interaction of FkpA, a peptidyl-prolyl cis/trans isomerase with EspP autotransporter protein. *Gut microbes*, **1**, 339-344.

152. Sauri, A., Soprova, Z., Wickstrom, D., de Gier, J.W., Van der Schors, R.C., Smit, A.B., Jong, W.S. and Luirink, J. (2009) The Bam (Omp85) complex is involved in secretion of the autotransporter haemoglobin protease. *Microbiology*, **155**, 3982-3991.

153. Knowles, T.J., Scott-Tucker, A., Overduin, M. and Henderson, I.R. (2009) Membrane protein architects: the role of the BAM complex in outer membrane protein assembly. *Nature reviews. Microbiology*, **7**, 206-214.

154. Jacob-Dubuisson, F., Buisine, C., Willery, E., Renauld-Mongenie, G. and Locht, C. (1997) Lack of functional complementation between Bordetella pertussis filamentous hemagglutinin and Proteus mirabilis HpmA hemolysin secretion machineries. *J Bacteriol*, **179**, 775-783.

155. Julio, S.M. and Cotter, P.A. (2005) Characterization of the filamentous hemagglutinin-like protein FhaS in Bordetella bronchiseptica. *Infect Immun*, **73**, 4960-4971.

156. Linke, D., Riess, T., Autenrieth, I.B., Lupas, A. and Kempf, V.A. (2006) Trimeric autotransporter adhesins: variable structure, common function. *Trends Microbiol*, **14**, 264-270.

157. Szczesny, P., Linke, D., Ursinus, A., Bar, K., Schwarz, H., Riess, T.M., Kempf, V.A., Lupas, A.N., Martin, J. and Zeth, K. (2008) Structure of the head of the Bartonella adhesin BadA. *PLoS Pathog*, **4**, e1000119.

158. Salacha, R., Kovacic, F., Brochier-Armanet, C., Wilhelm, S., Tommassen, J., Filloux, A., Voulhoux, R. and Bleves, S. (2010) The Pseudomonas aeruginosa patatin-like protein PlpD is the archetype of a novel Type V secretion system. *Environmental microbiology*, **12**, 1498-1512.

159. Oberhettinger, P., Schutz, M., Leo, J.C., Heinz, N., Berger, J., Autenrieth, I.B. and Linke, D. (2012) Intimin and invasin export their C-terminus to the bacterial cell surface using an inverse mechanism compared to classical autotransport. *PloS one*, **7**, e47069.

160. Pukatzki, S., Ma, A.T., Sturtevant, D., Krastins, B., Sarracino, D., Nelson, W.C., Heidelberg, J.F. and Mekalanos, J.J. (2006) Identification of a conserved bacterial protein secretion system in Vibrio cholerae using the Dictyostelium host model system. *Proc Natl Acad Sci U S A*, **103**, 1528-1533.

161. Hood, R.D., Singh, P., Hsu, F., Guvener, T., Carl, M.A., Trinidad, R.R., Silverman, J.M., Ohlson, B.B., Hicks, K.G., Plemel, R.L. *et al.* (2010) A type VI secretion system of Pseudomonas aeruginosa targets a toxin to bacteria. *Cell host & microbe*, **7**, 25-37.

162. MacIntyre, D.L., Miyata, S.T., Kitaoka, M. and Pukatzki, S. (2010) The Vibrio cholerae type VI secretion system displays antimicrobial properties. *Proc Natl Acad Sci U S A*, **107**, 19520-19524.

163. Russell, A.B., Hood, R.D., Bui, N.K., LeRoux, M., Vollmer, W. and Mougous, J.D. (2011) Type VI secretion delivers bacteriolytic effectors to target cells. *Nature*, **475**, 343-347.

164. Pukatzki, S., Ma, A.T., Revel, A.T., Sturtevant, D. and Mekalanos, J.J. (2007) Type VI secretion system translocates a phage tail spike-like protein into target cells where it cross-links actin. *Proc Natl Acad Sci U S A*, **104**, 15508-15513.

165. Leiman, P.G., Basler, M., Ramagopal, U.A., Bonanno, J.B., Sauder, J.M., Pukatzki, S., Burley, S.K., Almo, S.C. and Mekalanos, J.J. (2009) Type VI secretion apparatus and phage tail-associated protein complexes share a common evolutionary origin. *Proc Natl Acad Sci U S A*, **106**, 4154-4159.

166. Pell, L.G., Kanelis, V., Donaldson, L.W., Howell, P.L. and Davidson, A.R. (2009) The phage lambda major tail protein structure reveals a common evolution for long-tailed phages and the type VI bacterial secretion system. *Proc Natl Acad Sci U S A*, **106**, 4160-4165.

167. Das, S., Chakrabortty, A., Banerjee, R. and Chaudhuri, K. (2002) Involvement of in vivo induced icmF gene of Vibrio cholerae in motility, adherence to epithelial cells,

and conjugation frequency. *Biochemical and biophysical research communications*, **295**, 922-928.

168. Enos-Berlage, J.L., Guvener, Z.T., Keenan, C.E. and McCarter, L.L. (2005) Genetic determinants of biofilm development of opaque and translucent Vibrio parahaemolyticus. *Mol Microbiol*, **55**, 1160-1182.

169. Aschtgen, M.S., Bernard, C.S., De Bentzmann, S., Lloubes, R. and Cascales, E. (2008) SciN is an outer membrane lipoprotein required for type VI secretion in enteroaggregative Escherichia coli. *J Bacteriol*, **190**, 7523-7531.

170. Weber, B., Hasic, M., Chen, C., Wai, S.N. and Milton, D.L. (2009) Type VI secretion modulates quorum sensing and stress response in Vibrio anguillarum. *Environmental microbiology*, **11**, 3018-3028.

171. Bingle, L.E., Bailey, C.M. and Pallen, M.J. (2008) Type VI secretion: a beginner's guide. *Curr Opin Microbiol*, **11**, 3-8.

172. Cascales, E. (2008) The type VI secretion toolkit. *EMBO Rep,* **9**, 735-741.

173. Leiman, P.G., Arisaka, F., van Raaij, M.J., Kostyuchenko, V.A., Aksyuk, A.A., Kanamaru, S. and Rossmann, M.G. (2010) Morphogenesis of the T4 tail and tail fibers. *Virology journal*, **7**, 355.

174. Basler, M., Pilhofer, M., Henderson, G.P., Jensen, G.J. and Mekalanos, J.J. (2012) Type VI secretion requires a dynamic contractile phage tail-like structure. *Nature,* **483**, 182-186.

175. Aschtgen, M.S., Thomas, M.S. and Cascales, E. (2010) Anchoring the type VI secretion system to the peptidoglycan: TssL, TagL, TagP... what else? *Virulence*, **1**, 535-540.

176. Gey Van Pittius, N.C., Gamieldien, J., Hide, W., Brown, G.D., Siezen, R.J. and Beyers, A.D. (2001) The ESAT-6 gene cluster of Mycobacterium tuberculosis and other high G+C Gram-positive bacteria. *Genome biology*, **2**, RESEARCH0044.

177. Sampson, S.L. (2011) Mycobacterial PE/PPE proteins at the host-pathogen interface. *Clinical & developmental immunology*, **2011**, 497203.

178. Houben, E.N., Bestebroer, J., Ummels, R., Wilson, L., Piersma, S.R., Jimenez, C.R., Ottenhoff, T.H., Luirink, J. and Bitter, W. (2012) Composition of the type VII secretion system membrane complex. *Mol Microbiol*, **86**, 472-484.

179. Mahfoud, M., Sukumaran, S., Hulsmann, P., Grieger, K. and Niederweis, M. (2006) Topology of the porin MspA in the outer membrane of Mycobacterium smegmatis. *J Biol Chem*, **281**, 5908-5915.

180. Chandran, V., Fronzes, R., Duquerroy, S., Cronin, N., Navaza, J. and Waksman, G. (2009) Structure of the outer membrane complex of a type IV secretion system. *Nature*, **462**, 1011-1015.

181. Iriarte, M., Sory, M.P., Boland, A., Boyd, A.P., Mills, S.D., Lambermont, I. and Cornelis, G.R. (1998) TyeA, a protein involved in control of Yop release and in translocation of Yersinia Yop effectors. *EMBO J*, **17**, 1907-1918.

182. Joseph, S.S. and Plano, G.V. (2007) Identification of TyeA residues required to interact with YopN and to regulate Yop secretion. *Advances in experimental medicine and biology*, **603**, 235-245.

183. Kwuan, L., Adams, W. and Auerbuch, V. (2013) Impact of host membrane pore formation by the Yersinia pseudotuberculosis type III secretion system on the macrophage innate immune response. *Infect Immun*, **81**, 905-914.

184. Crabill, E., Karpisek, A. and Alfano, J.R. (2012) The Pseudomonas syringae HrpJ protein controls the secretion of type III translocator proteins and has a virulence role inside plant cells. *Mol Microbiol*, **85**, 225-238.

185. Huang, J., Lesser, C.F. and Lory, S. (2008) The essential role of the CopN protein in Chlamydia pneumoniae intracellular growth. *Nature*, **456**, 112-115.

186. Archuleta, T.L., Du, Y., English, C.A., Lory, S., Lesser, C., Ohi, M.D., Ohi, R. and Spiller, B.W. (2011) The Chlamydia effector chlamydial outer protein N (CopN) sequesters tubulin and prevents microtubule assembly. *J Biol Chem*, **286**, 33992-33998.

187. Engel, J. (2004) Tarp and Arp: How Chlamydia induces its own entry. *Proc Natl Acad Sci U S A*, **101**, 9947-9948.

188. Valdivia, R.H. (2008) Chlamydia effector proteins and new insights into chlamydial cellular microbiology. *Curr Opin Microbiol*, **11**, 53-59.

189. Saka, H.A. and Valdivia, R.H. (2010) Acquisition of nutrients by Chlamydiae: unique challenges of living in an intracellular compartment. *Curr Opin Microbiol*, **13**, 4-10.

190. Ho, T.D. and Starnbach, M.N. (2005) The Salmonella enterica serovar typhimurium-encoded type III secretion systems can translocate Chlamydia trachomatis proteins into the cytosol of host cells. *Infect Immun*, **73**, 905-911.

191. Moulder, J.W. (1991) Interaction of chlamydiae and host cells in vitro. *Microbiological reviews*, **55**, 143-190.

192. Grieshaber, S.S., Grieshaber, N.A., Miller, N. and Hackstadt, T. (2006) Chlamydia trachomatis causes centrosomal defects resulting in chromosomal segregation abnormalities. *Traffic*, **7**, 940-949.

193. Grieshaber, S.S., Grieshaber, N.A. and Hackstadt, T. (2003) Chlamydia trachomatis uses host cell dynein to traffic to the microtubule-organizing center in a p50 dynamitin-independent process. *J Cell Sci*, **116**, 3793-3802.

194. Clifton, D.R., Fields, K.A., Grieshaber, S.S., Dooley, C.A., Fischer, E.R., Mead, D.J., Carabeo, R.A. and Hackstadt, T. (2004) A chlamydial type III translocated

protein is tyrosine-phosphorylated at the site of entry and associated with recruitment of actin. *Proc Natl Acad Sci U S A*, **101**, 10166-10171.

195. Betts, H.J., Wolf, K. and Fields, K.A. (2009) Effector protein modulation of host cells: examples in the Chlamydia spp. arsenal. *Curr Opin Microbiol*, **12**, 81-87.

196. Fields, K.A. and Hackstadt, T. (2000) Evidence for the secretion of Chlamydia trachomatis CopN by a type III secretion mechanism. *Mol Microbiol*, **38**, 1048-1060.

197. Kern, J.M., Maass, V. and Maass, M. (2009) Molecular pathogenesis of chronic Chlamydia pneumoniae infection: a brief overview. *Clin Microbiol Infect*, **15**, 36-41.

198. Matsumoto, A. (1981) Isolation and electron microscopic observations of intracytoplasmic inclusions containing Chlamydia psittaci. *J Bacteriol*, **145**, 605-612.

199. Matsumoto, A. (1982) Electron microscopic observations of surface projections on Chlamydia psittaci reticulate bodies. *J Bacteriol*, **150**, 358-364.

200. Mueller, C.A., Broz, P. and Cornelis, G.R. (2008) The type III secretion system tip complex and translocon. *Mol Microbiol*, **68**, 1085-1095.

201. Cocchiaro, J.L. and Valdivia, R.H. (2009) New insights into Chlamydia intracellular survival mechanisms. *Cell Microbiol*, **11**, 1571-1578.

202. Scidmore, M.A., Fischer, E.R. and Hackstadt, T. (2003) Restricted fusion of Chlamydia trachomatis vesicles with endocytic compartments during the initial stages of infection. *Infect Immun*, **71**, 973-984.

203. Scidmore, M.A. and Hackstadt, T. (2001) Mammalian 14-3-3beta associates with the Chlamydia trachomatis inclusion membrane via its interaction with IncG. *Mol Microbiol*, **39**, 1638-1650.

204. Hackstadt, T., Rockey, D.D., Heinzen, R.A. and Scidmore, M.A. (1996) Chlamydia trachomatis interrupts an exocytic pathway to acquire endogenously synthesized sphingomyelin in transit from the Golgi apparatus to the plasma membrane. *EMBO J*, **15**, 964-977.

205. Johnson, K.A., Tan, M. and Sutterlin, C. (2009) Centrosome abnormalities during a Chlamydia trachomatis infection are caused by dysregulation of the normal duplication pathway. *Cell Microbiol*, **11**, 1064-1073.

206. Howard, J. and Hyman, A.A. (2003) Dynamics and mechanics of the microtubule plus end. *Nature*, **422**, 753-758.

207. Bowne-Anderson, H., Zanic, M., Kauer, M. and Howard, J. (2013) Microtubule dynamic instability: a new model with coupled GTP hydrolysis and multistep catastrophe. *BioEssays : news and reviews in molecular, cellular and developmental biology*, **35**, 452-461.

208. Conde, C. and Caceres, A. (2009) Microtubule assembly, organization and dynamics in axons and dendrites. *Nature reviews. Neuroscience*, **10**, 319-332.

209. Gould, R.R. and Borisy, G.G. (1977) The pericentriolar material in Chinese hamster ovary cells nucleates microtubule formation. *The Journal of cell biology*, **73**, 601-615.

210. Vinh, D.B., Kern, J.W., Hancock, W.O., Howard, J. and Davis, T.N. (2002) Reconstitution and characterization of budding yeast gamma-tubulin complex. *Molecular biology of the cell*, **13**, 1144-1157.

211. Seetapun, D., Castle, B.T., McIntyre, A.J., Tran, P.T. and Odde, D.J. (2012) Estimating the microtubule GTP cap size in vivo. *Current biology : CB*, **22**, 1681-1687.

212. Walker, R.A., Pryer, N.K. and Salmon, E.D. (1991) Dilution of individual microtubules observed in real time in vitro: evidence that cap size is small and independent of elongation rate. *The Journal of cell biology*, **114**, 73-81.

213. Inoue, S. and Salmon, E.D. (1995) Force generation by microtubule assembly/disassembly in mitosis and related movements. *Molecular biology of the cell*, **6**, 1619-1640.

214. Howard, J. (2001) *Mechanics of motor proteins and the cytoskeleton*. Sinauer Associates, Publishers, Sunderland, Mass.

215. Gustke, N., Trinczek, B., Biernat, J., Mandelkow, E.M. and Mandelkow, E. (1994) Domains of tau protein and interactions with microtubules. *Biochemistry*, **33**, 9511-9522.

216. Andersen, S.S. (2000) Spindle assembly and the art of regulating microtubule dynamics by MAPs and Stathmin/Op18. *Trends in cell biology*, **10**, 261-267.

217. Kinoshita, K., Noetzel, T.L., Arnal, I., Drechsel, D.N. and Hyman, A.A. (2006) Global and local control of microtubule destabilization promoted by a catastrophe kinesin MCAK/XKCM1. *Journal of muscle research and cell motility*, **27**, 107-114.

218. Schuyler, S.C. and Pellman, D. (2001) Microtubule "plus-end-tracking proteins": The end is just the beginning. *Cell*, **105**, 421-424.

219. Slep, K.C., Rogers, S.L., Elliott, S.L., Ohkura, H., Kolodziej, P.A. and Vale, R.D. (2005) Structural determinants for EB1-mediated recruitment of APC and spectraplakins to the microtubule plus end. *The Journal of cell biology*, **168**, 587-598.

220. Slep, K.C. and Vale, R.D. (2007) Structural basis of microtubule plus end tracking by XMAP215, CLIP-170, and EB1. *Mol Cell*, **27**, 976-991.

221. Al-Bassam, J., Larsen, N.A., Hyman, A.A. and Harrison, S.C. (2007) Crystal structure of a TOG domain: conserved features of XMAP215/Dis1-family TOG domains and implications for tubulin binding. *Structure*, **15**, 355-362.

222. Belmont, L.D. and Mitchison, T.J. (1996) Identification of a protein that interacts with tubulin dimers and increases the catastrophe rate of microtubules. *Cell*, **84**, 623-631.

223. Marklund, U., Larsson, N., Gradin, H.M., Brattsand, G. and Gullberg, M. (1996) Oncoprotein 18 is a phosphorylation-responsive regulator of microtubule dynamics. *EMBO J*, **15**, 5290-5298.

224. Jourdain, L., Curmi, P., Sobel, A., Pantaloni, D. and Carlier, M.F. (1997) Stathmin: a tubulin-sequestering protein which forms a ternary T2S complex with two tubulin molecules. *Biochemistry*, **36**, 10817-10821.

225. Curmi, P.A., Andersen, S.S., Lachkar, S., Gavet, O., Karsenti, E., Knossow, M. and Sobel, A. (1997) The stathmin/tubulin interaction in vitro. *J Biol Chem*, **272**, 25029-25036.

226. Steinmetz, M.O., Kammerer, R.A., Jahnke, W., Goldie, K.N., Lustig, A. and van Oostrum, J. (2000) Op18/stathmin caps a kinked protofilament-like tubulin tetramer. *EMBO J*, **19**, 572-580.

227. Sobel, A. (1991) Stathmin: a relay phosphoprotein for multiple signal transduction? *Trends in biochemical sciences*, **16**, 301-305.

228. Schubart, U.K., Xu, J., Fan, W., Cheng, G., Goldstein, H., Alpini, G., Shafritz, D.A., Amat, J.A., Farooq, M., Norton, W.T. *et al.* (1992) Widespread differentiation stage-specific expression of the gene encoding phosphoprotein p19 (metablastin) in mammalian cells. *Differentiation; research in biological diversity*, **51**, 21-32.

229. Larsson, N., Marklund, U., Gradin, H.M., Brattsand, G. and Gullberg, M. (1997) Control of microtubule dynamics by oncoprotein 18: dissection of the regulatory role of multisite phosphorylation during mitosis. *Molecular and cellular biology*, **17**, 5530-5539.

230. Horwitz, S.B., Shen, H.J., He, L., Dittmar, P., Neef, R., Chen, J. and Schubart, U.K. (1997) The microtubule-destabilizing activity of metablastin (p19) is controlled by phosphorylation. *J Biol Chem*, **272**, 8129-8132.

231. Kuntziger, T., Gavet, O., Sobel, A. and Bornens, M. (2001) Differential effect of two stathmin/Op18 phosphorylation mutants on Xenopus embryo development. *J Biol Chem*, **276**, 22979-22984.

232. Curmi, P.A., Gavet, O., Charbaut, E., Ozon, S., Lachkar-Colmerauer, S., Manceau, V., Siavoshian, S., Maucuer, A. and Sobel, A. (1999) Stathmin and its phosphoprotein family: general properties, biochemical and functional interaction with tubulin. *Cell structure and function*, **24**, 345-357.

233. Wittmann, T., Bokoch, G.M. and Waterman-Storer, C.M. (2004) Regulation of microtubule destabilizing activity of Op18/stathmin downstream of Rac1. *J Biol Chem*, **279**, 6196-6203.

234. Spaeth, K.E., Chen, Y.S. and Valdivia, R.H. (2009) The Chlamydia type III secretion system C-ring engages a chaperone-effector protein complex. *PLoS Pathog*, **5**, e1000579.

235. Slepenkin, A., de la Maza, L.M. and Peterson, E.M. (2005) Interaction between components of the type III secretion system of Chlamydiaceae. *J Bacteriol*, **187**, 473-479.

236. Ravelli, R.B., Gigant, B., Curmi, P.A., Jourdain, I., Lachkar, S., Sobel, A. and Knossow, M. (2004) Insight into tubulin regulation from a complex with colchicine and a stathmin-like domain. *Nature*, **428**, 198-202.

237. Jourdain, I., Lachkar, S., Charbaut, E., Gigant, B., Knossow, M., Sobel, A. and Curmi, P.A. (2004) A synergistic relationship between three regions of stathmin family proteins is required for the formation of a stable complex with tubulin. *Biochem J*, **378**, 877-888.

238. Cassimeris, L. (2002) The oncoprotein 18/stathmin family of microtubule destabilizers. *Current opinion in cell biology*, **14**, 18-24.

239. Gigant, B., Curmi, P.A., Martin-Barbey, C., Charbaut, E., Lachkar, S., Lebeau, L., Siavoshian, S., Sobel, A. and Knossow, M. (2000) The 4 A X-ray structure of a tubulin:stathmin-like domain complex. *Cell*, **102**, 809-816.

240. Manna, T., Thrower, D.A., Honnappa, S., Steinmetz, M.O. and Wilson, L. (2009) Regulation of microtubule dynamic instability in vitro by differentially phosphorylated stathmin. *J Biol Chem*, **284**, 15640-15649.

241. Manna, T., Thrower, D., Miller, H.P., Curmi, P. and Wilson, L. (2006) Stathmin strongly increases the minus end catastrophe frequency and induces rapid treadmilling of bovine brain microtubules at steady state in vitro. *J Biol Chem*, **281**, 2071-2078.

242. Howell, B., Larsson, N., Gullberg, M. and Cassimeris, L. (1999) Dissociation of the tubulin-sequestering and microtubule catastrophe-promoting activities of oncoprotein 18/stathmin. *Molecular biology of the cell*, **10**, 105-118.

243. Mital, J., Miller, N.J., Fischer, E.R. and Hackstadt, T. (2010) Specific chlamydial inclusion membrane proteins associate with active Src family kinases in microdomains that interact with the host microtubule network. *Cell Microbiol*, **12**, 1235-1249.

244. Hsia, R.C., Pannekoek, Y., Ingerowski, E. and Bavoil, P.M. (1997) Type III secretion genes identify a putative virulence locus of Chlamydia. *Mol Microbiol*, **25**, 351-359.

245. Cornelis, G.R. (2006) The type III secretion injectisome. *Nature reviews. Microbiology*, **4**, 811-825.

246. Ghosh, P. (2004) Process of protein transport by the type III secretion system. *Microbiol Mol Biol Rev*, **68**, 771-795.

247. Dean, P. and Kenny, B. (2009) The effector repertoire of enteropathogenic E. coli: ganging up on the host cell. *Curr Opin Microbiol*, **12**, 101-109.

248. Schroeder, G.N. and Hilbi, H. (2008) Molecular pathogenesis of Shigella spp.: controlling host cell signaling, invasion, and death by type III secretion. *Clinical microbiology reviews*, **21**, 134-156.

249. Johnson, S., Deane, J.E. and Lea, S.M. (2005) The type III needle and the damage done. *Current opinion in structural biology*, **15**, 700-707.

250. Cossart, P. and Sansonetti, P.J. (2004) Bacterial invasion: the paradigms of enteroinvasive pathogens. *Science*, **304**, 242-248.

251. Yoshida, S. and Sasakawa, C. (2003) Exploiting host microtubule dynamics: a new aspect of bacterial invasion. *Trends Microbiol*, **11**, 139-143.

252. Desai, A. and Mitchison, T.J. (1997) Microtubule polymerization dynamics. *Annu Rev Cell Dev Biol*, **13**, 83-117.

253. Balsara, Z.R., Misaghi, S., Lafave, J.N. and Starnbach, M.N. (2006) Chlamydia trachomatis infection induces cleavage of the mitotic cyclin B1. *Infect Immun*, **74**, 5602-5608.

254. Deane, J.E., Roversi, P., King, C., Johnson, S. and Lea, S.M. (2008) Structures of the Shigella flexneri type 3 secretion system protein MxiC reveal conformational variability amongst homologues. *J Mol Biol*, **377**, 985-992.

255. Castoldi, M. and Popov, A.V. (2003) Purification of brain tubulin through two cycles of polymerization-depolymerization in a high-molarity buffer. *Protein expression and purification*, **32**, 83-88.

256. Du, Y., English, C.A. and Ohi, R. (2010) The kinesin-8 Kif18A dampens microtubule plus-end dynamics. *Current biology : CB*, **20**, 374-380.

257. Roger, B., Al-Bassam, J., Dehmelt, L., Milligan, R.A. and Halpain, S. (2004) MAP2c, but not tau, binds and bundles F-actin via its microtubule binding domain. *Current biology : CB*, **14**, 363-371.

258. Germane, K.L., Ohi, R., Goldberg, M.B. and Spiller, B.W. (2008) Structural and functional studies indicate that Shigella VirA is not a protease and does not directly destabilize microtubules. *Biochemistry*, **47**, 10241-10243.

259. Desai, A., Verma, S., Mitchison, T.J. and Walczak, C.E. (1999) Kin I kinesins are microtubule-destabilizing enzymes. *Cell*, **96**, 69-78.

260. Hyman, A., Drechsel, D., Kellogg, D., Salser, S., Sawin, K., Steffen, P., Wordeman, L. and Mitchison, T. (1991) Preparation of modified tubulins. *Methods in enzymology*, **196**, 478-485.

261. Ohi, M., Li, Y., Cheng, Y. and Walz, T. (2004) Negative Staining and Image Classification - Powerful Tools in Modern Electron Microscopy. *Biological procedures online*, **6**, 23-34.

262. Rodgers, L., Gamez, A., Riek, R. and Ghosh, P. (2008) The type III secretion chaperone SycE promotes a localized disorder-to-order transition in the natively unfolded effector YopE. *J Biol Chem*, **283**, 20857-20863.

263. Lachkar, S., Lebois, M., Steinmetz, M.O., Guichet, A., Lal, N., Curmi, P.A., Sobel, A. and Ozon, S. (2010) Drosophila stathmins bind tubulin heterodimers with high and variable stoichiometries. *J Biol Chem*, **285**, 11667-11680.

264. Howard, J. and Hyman, A.A. (2007) Microtubule polymerases and depolymerases. *Current opinion in cell biology*, **19**, 31-35.

265. Parsot, C., Hamiaux, C. and Page, A.L. (2003) The various and varying roles of specific chaperones in type III secretion systems. *Curr Opin Microbiol*, **6**, 7-14.

266. Fields, K.A., Fischer, E.R., Mead, D.J. and Hackstadt, T. (2005) Analysis of putative Chlamydia trachomatis chaperones Scc2 and Scc3 and their use in the identification of type III secretion substrates. *J Bacteriol*, **187**, 6466-6478.

267. Buttner, C.R., Sorg, I., Cornelis, G.R., Heinz, D.W. and Niemann, H.H. (2008) Structure of the Yersinia enterocolitica type III secretion translocator chaperone SycD. *J Mol Biol*, **375**, 997-1012.

268. Lunelli, M., Lokareddy, R.K., Zychlinsky, A. and Kolbe, M. (2009) IpaB-IpgC interaction defines binding motif for type III secretion translocator. *Proc Natl Acad Sci U S A*, **106**, 9661-9666.

269. Weisenberg, R.C., Deery, W.J. and Dickinson, P.J. (1976) Tubulin-nucleotide interactions during the polymerization and depolymerization of microtubules. *Biochemistry*, **15**, 4248-4254.

270. Mitchison, T. and Kirschner, M. (1984) Dynamic instability of microtubule growth. *Nature*, **312**, 237-242.

271. Margolis, R.L. and Wilson, L. (1978) Opposite end assembly and disassembly of microtubules at steady state in vitro. *Cell*, **13**, 1-8.

272. Slep, K.C. (2010) Structural and mechanistic insights into microtubule end-binding proteins. *Current opinion in cell biology*, **22**, 88-95.

273. Al-Bassam, J., van Breugel, M., Harrison, S.C. and Hyman, A. (2006) Stu2p binds tubulin and undergoes an open-to-closed conformational change. *The Journal of cell biology*, **172**, 1009-1022.

274. Steinmetz, M.O. (2007) Structure and thermodynamics of the tubulin-stathmin interaction. *J Struct Biol*, **158**, 137-147.

275. Schlumberger, M.C., Muller, A.J., Ehrbar, K., Winnen, B., Duss, I., Stecher, B. and Hardt, W.D. (2005) Real-time imaging of type III secretion: Salmonella SipA injection into host cells. *Proc Natl Acad Sci U S A*, **102**, 12548-12553.

276. Skilton, R.J., Cutcliffen, L.T., Barlow, D., Wang, Y., Salim, O., Lambden, P.R. and Clarke, I.N. (2009) Penicillin induced persistence in Chlamydia trachomatis: high quality time lapse video analysis of the developmental cycle. *PloS one*, **4**, e7723.

277. Campbell, L.A. and Kuo, C.C. (2009) Cultivation and laboratory maintenance of Chlamydia pneumoniae. *Curr Protoc Microbiol*, **Chapter 11**, Unit11B 11.

278. Mukhopadhyay, S., Clark, A.P., Sullivan, E.D., Miller, R.D. and Summersgill, J.T. (2004) Detailed protocol for purification of Chlamydia pneumoniae elementary bodies. *Journal of clinical microbiology*, **42**, 3288-3290.

279. Hiller, G. and Weber, K. (1978) Radioimmunoassay for tubulin: a quantitative comparison of the tubulin content of different established tissue culture cells and tissues. *Cell*, **14**, 795-804.

280. Bulinski, J.C., Morgan, J.L., Borisy, G.G. and Spooner, B.S. (1980) Comparison of methods for tubulin quantitation in HeLa cell and brain tissue extracts. *Analytical biochemistry*, **104**, 432-439.

281. Cornelis, G.R. (2002) Yersinia type III secretion: send in the effectors. *The Journal of cell biology*, **158**, 401-408.

282. Galan, J.E. and Wolf-Watz, H. (2006) Protein delivery into eukaryotic cells by type III secretion machines. *Nature*, **444**, 567-573.

283. Galan, J.E. and Cossart, P. (2005) Host-pathogen interactions: a diversity of themes, a variety of molecular machines. *Curr Opin Microbiol*, **8**, 1-3.

284. Abrusci, P., Vergara-Irigaray, M., Johnson, S., Beeby, M.D., Hendrixson, D.R., Roversi, P., Friede, M.E., Deane, J.E., Jensen, G.J., Tang, C.M. *et al.* (2013) Architecture of the major component of the type III secretion system export apparatus. *Nature structural & molecular biology*, **20**, 99-104.

285. Deane, J.E., Abrusci, P., Johnson, S. and Lea, S.M. (2010) Timing is everything: the regulation of type III secretion. *Cellular and molecular life sciences : CMLS*, **67**, 1065-1075.

286. Stamm, L.M. and Goldberg, M.B. (2011) Microbiology. Establishing the secretion hierarchy. *Science*, **331**, 1147-1148.

287. Job, V., Mattei, P.J., Lemaire, D., Attree, I. and Dessen, A. (2010) Structural basis of chaperone recognition of type III secretion system minor translocator proteins. *J Biol Chem*, **285**, 23224-23232.

288. Ferracci, F., Day, J.B., Ezelle, H.J. and Plano, G.V. (2004) Expression of a functional secreted YopN-TyeA hybrid protein in Yersinia pestis is the result of a +1 translational frameshift event. *J Bacteriol*, **186**, 5160-5166.

289. Silva-Herzog, E., Joseph, S.S., Avery, A.K., Coba, J.A., Wolf, K., Fields, K.A. and Plano, G.V. (2011) Scc1 (CP0432) and Scc4 (CP0033) function as a type III secretion chaperone for CopN of Chlamydia pneumoniae. *J Bacteriol*, **193**, 3490-3496.

290. Schreiner, M. and Niemann, H.H. (2012) Crystal structure of the Yersinia enterocolitica type III secretion chaperone SycD in complex with a peptide of the minor translocator YopD. *BMC structural biology*, **12**, 13.

291. Tomalka, A.G., Zmina, S.E., Stopford, C.M. and Rietsch, A. (2013) Dimerization of the Pseudomonas aeruginosa translocator chaperone PcrH is required for stability, not function. *J Bacteriol*, **195**, 4836-4843.

292. Lara-Tejero, M., Kato, J., Wagner, S., Liu, X. and Galan, J.E. (2011) A sorting platform determines the order of protein secretion in bacterial type III systems. *Science*, **331**, 1188-1191.

293. Winnen, B., Schlumberger, M.C., Sturm, A., Schupbach, K., Siebenmann, S., Jenny, P. and Hardt, W.D. (2008) Hierarchical effector protein transport by the Salmonella Typhimurium SPI-1 type III secretion system. *PloS one*, **3**, e2178.

294. Thomas, N.A., Deng, W., Baker, N., Puente, J. and Finlay, B.B. (2007) Hierarchical delivery of an essential host colonization factor in enteropathogenic Escherichia coli. *J Biol Chem*, **282**, 29634-29645.

295. Otwinowski, Z. and Minor, W. (1997) In Charles W. Carter, Jr. (ed.), *Methods in enzymology*. Academic Press, Vol. Volume 276, pp. 307-326.

296. Adams, P.D., Grosse-Kunstleve, R.W., Hung, L.W., Ioerger, T.R., McCoy, A.J., Moriarty, N.W., Read, R.J., Sacchettini, J.C., Sauter, N.K. and Terwilliger, T.C. (2002) PHENIX: building new software for automated crystallographic structure determination. *Acta crystallographica. Section D, Biological crystallography*, **58**, 1948-1954.

297. Emsley, P. and Cowtan, K. (2004) Coot: model-building tools for molecular graphics. *Acta crystallographica. Section D, Biological crystallography*, **60**, 2126-2132.

298. DeLano, W.L. (2002), DeLano Scientific, San Carlos, CA, USA., Vol. 2013.

299. Panchenko, A.R. and Bryant, S.H. (2002) A comparison of position-specific score matrices based on sequence and structure alignments. *Protein science : a publication of the Protein Society*, **11**, 361-370.

300. Gouet, P., Robert, X. and Courcelle, E. (2003) ESPript/ENDscript: Extracting and rendering sequence and 3D information from atomic structures of proteins. *Nucleic acids research*, **31**, 3320-3323.

301. Holm, L. and Sander, C. (1995) Dali: a network tool for protein structure comparison. *Trends in biochemical sciences*, **20**, 478-480.

302. Ashkenazy, H., Erez, E., Martz, E., Pupko, T. and Ben-Tal, N. (2010) ConSurf 2010: calculating evolutionary conservation in sequence and structure of proteins and nucleic acids. *Nucleic acids research*, **38**, W529-533.

303. Demers, B., Sansonetti, P.J. and Parsot, C. (1998) Induction of type III secretion in Shigella flexneri is associated with differential control of transcription of genes encoding secreted proteins. *EMBO J*, **17**, 2894-2903.

304. Adam, P.R., Patil, M.K., Dickenson, N.E., Choudhari, S., Barta, M., Geisbrecht, B.V., Picking, W.L. and Picking, W.D. (2012) Binding affects the tertiary and quaternary structures of the Shigella translocator protein IpaB and its chaperone IpgC. *Biochemistry*, **51**, 4062-4071.

305. Cliff, M.J., Williams, M.A., Brooke-Smith, J., Barford, D. and Ladbury, J.E. (2005) Molecular recognition via coupled folding and binding in a TPR domain. *J Mol Biol*, **346**, 717-732.

306. LeNoue-Newton, M., Watkins, G.R., Zou, P., Germane, K.L., McCorvey, L.R., Wadzinski, B.E. and Spiller, B.W. (2011) The E3 ubiquitin ligase- and protein phosphatase 2A (PP2A)-binding domains of the Alpha4 protein are both required for Alpha4 to inhibit PP2A degradation. *J Biol Chem*, **286**, 17665-17671.

307. Scidmore, M.A. (2011) Recent advances in Chlamydia subversion of host cytoskeletal and membrane trafficking pathways. *Microbes Infect*, **13**, 527-535.

308. Sorg, J.A., Blaylock, B. and Schneewind, O. (2006) Secretion signal recognition by YscN, the Yersinia type III secretion ATPase. *Proc Natl Acad Sci U S A*, **103**, 16490-16495.

309. Parsot, C., Ageron, E., Penno, C., Mavris, M., Jamoussi, K., d'Hauteville, H., Sansonetti, P. and Demers, B. (2005) A secreted anti-activator, OspD1, and its chaperone, Spa15, are involved in the control of transcription by the type III secretion apparatus activity in Shigella flexneri. *Mol Microbiol*, **56**, 1627-1635.

310. Brutinel, E.D. and Yahr, T.L. (2008) Control of gene expression by type III secretory activity. *Curr Opin Microbiol*, **11**, 128-133.

311. Ferracci, F., Schubot, F.D., Waugh, D.S. and Plano, G.V. (2005) Selection and characterization of Yersinia pestis YopN mutants that constitutively block Yop secretion. *Mol Microbiol*, **57**, 970-987.

312. Forsberg, A., Viitanen, A.M., Skurnik, M. and Wolf-Watz, H. (1991) The surface-located YopN protein is involved in calcium signal transduction in Yersinia pseudotuberculosis. *Mol Microbiol*, **5**, 977-986.

313. Mueller, C.A., Broz, P., Muller, S.A., Ringler, P., Erne-Brand, F., Sorg, I., Kuhn, M., Engel, A. and Cornelis, G.R. (2005) The V-antigen of Yersinia forms a distinct structure at the tip of injectisome needles. *Science*, **310**, 674-676.

314. Sani, M., Botteaux, A., Parsot, C., Sansonetti, P., Boekema, E.J. and Allaoui, A. (2007) IpaD is localized at the tip of the Shigella flexneri type III secretion apparatus. *Biochimica et biophysica acta*, **1770**, 307-311.

315. Veenendaal, A.K., Hodgkinson, J.L., Schwarzer, L., Stabat, D., Zenk, S.F. and Blocker, A.J. (2007) The type III secretion system needle tip complex mediates host cell sensing and translocon insertion. *Mol Microbiol*, **63**, 1719-1730.

316. Lara-Tejero, M. and Galan, J.E. (2009) Salmonella enterica serovar typhimurium pathogenicity island 1-encoded type III secretion system translocases mediate intimate attachment to nonphagocytic cells. *Infect Immun*, **77**, 2635-2642.

317. Ayaz, P., Ye, X., Huddleston, P., Brautigam, C.A. and Rice, L.M. (2012) A TOG:alphabeta-tubulin complex structure reveals conformation-based mechanisms for a microtubule polymerase. *Science*, **337**, 857-860.

318. Sali, A. (1989-2014). Andrej Sali, University of California San Francisco, San Francisco, CA 94158-2330, USA, Vol. 2014, pp. Program for Comparative Protein Structure Modeling by Satisfaction of Spacial Restraints.

319. Pettersen, E.F., Goddard, T.D., Huang, C.C., Couch, G.S., Greenblatt, D.M., Meng, E.C. and Ferrin, T.E. (2004) UCSF Chimera--a visualization system for exploratory research and analysis. *Journal of computational chemistry*, **25**, 1605-1612.

320. Gigant, B., Wang, W., Dreier, B., Jiang, Q., Pecqueur, L., Pluckthun, A., Wang, C. and Knossow, M. (2013) Structure of a kinesin-tubulin complex and implications for kinesin motility. *Nature structural & molecular biology*, **20**, 1001-1007.

321. Vale, R.D., Reese, T.S. and Sheetz, M.P. (1985) Identification of a novel force-generating protein, kinesin, involved in microtubule-based motility. *Cell*, **42**, 39-50.